



1987

Molecular Properties of Cetiedil and Its Interactions with Human Erythrocytes

Chakravarthy Narasimhan
Loyola University Chicago

Follow this and additional works at: https://ecommons.luc.edu/luc_diss

 Part of the [Chemistry Commons](#)

Recommended Citation

Narasimhan, Chakravarthy, "Molecular Properties of Cetiedil and Its Interactions with Human Erythrocytes" (1987). *Dissertations*. 2513.
https://ecommons.luc.edu/luc_diss/2513

This Dissertation is brought to you for free and open access by the Theses and Dissertations at Loyola eCommons. It has been accepted for inclusion in Dissertations by an authorized administrator of Loyola eCommons. For more information, please contact ecommons@luc.edu.



This work is licensed under a [Creative Commons Attribution-NonCommercial-No Derivative Works 3.0 License](#).
Copyright © 1987 Chakravarthy Narasimhan

1/1²

**MOLECULAR PROPERTIES OF CETIEDIL
AND
ITS INTERACTIONS WITH HUMAN ERYTHROCYTES**

45

by
CHAKRAVARTHY NARASIMHAN

**A Dissertation Submitted to the Faculty of the Graduate School
of Loyola University of Chicago in Partial Fulfillment
of the Requirements for the Degree of
Doctor of Philosophy
January
1987**

ACKNOWLEDGEMENTS

The author gratefully acknowledges Dr. Leslie Wo-Mei Fung for suggesting this project and her guidance throughout the course of this work. The author would also like to thank Drs. Michael E. Johnson, Duarte Mota de Freitas, Kenneth W. Olsen and Albert J. Rotermund for their excellent suggestions and their time spent in reviewing this dissertation. The author also gratefully acknowledges Dr. Fung for providing financial support through her research grants, the Chemistry Department of Loyola University for the Teaching Assistantship and the Schmitt Dissertation Fellowship Committee for awarding the Fellowship. The author sincerely thanks Dr. Michael E. Johnson and the Research Resources Center (RRC) Faculty of the University of Illinois at Chicago for allowing the use of their NMR facility at the RRC. The author would also like to thank McNeil Pharmaceuticals, Pa., for their generous supply of cetiedil citrate throughout this project, Dr.M. Westerman of Mount Sinai Hospital of Chicago and Drs. M.E. Johnson and L. Kar of the University of Illinois at Chicago for providing with sickle cells, and the American Red Cross Blood Bank, Chicago Chapter, for normal Blood. The constant support and encouragement of the fellow graduate students are also deeply appreciated.

VITA

The author, Chakravarthy Narasimhan, is the son of P.S. Chakravarthy and Kamala Chakravarthy. He was born March 27, 1956, in Cuddalore, India.

His elementary and high school education were obtained from St. Joseph's Secondary School, Cuddalore, India.

In June, 1973, Mr. Narasimhan entered Madras University, and obtained Pre-University Education Certificate in April, 1974. He continued his studies in chemistry at Madras University and received Bachelor of Science degree in Chemistry in May, 1977 and Master of Science in Chemistry in May, 1979. The thesis for his Master's degree was, "Deamination Studies on Gelatin". During the periods of June, 1979 to July 1980, Mr. Narasimhan worked as a Lab Analyst Trainee in the Madras Fertilizers Ltd., taught junior college Chemistry, and worked as a cashier in the Indian Overseas Bank in India.

In August, 1980, Mr. Narasimhan entered Illinois Institute of Technology to further pursue the study of chemistry, with emphasis in biophysical chemistry. He received the degree of Master of Science in Chemistry, in December, 1982. While at IIT, he worked with Dr. C. Allen Bush on his thesis, "Identification, Fractionation and Characterization of Carboxyl Reduced Chondroitin Oligosaccharides".

In January, 1983, Mr. Narasimhan entered Loyola University of Chicago. He was granted graduate research assistantship during January, 1983 to August 1985. In September, 1985, he was awarded Arthur J. Schmidt Dissertation Fellowship enabling him to complete the Doctor of Philosophy degree in 1986, under the supervision of Dr. Leslie Wo-Mei Fung.

Mr. Narasimhan has been a member of the American Chemical society and the Biophysical Society since 1983.

TABLE OF CONTENTS

	Page
ACKNOWLEDGEMENTS	ii
VITA	iii
LIST OF TABLES	iv
LIST OF FIGURES	v
 Chapter	
I. INTRODUCTION	1
Sickle Cell Anemia	1
Antisickling Agents	2
Cetiedil	4
Clinical Investigations on the Effects of Cetiedil on Human Erythrocytes	4
The Effects of Cetiedil on Sickle Cell Morphology	5
Current Understanding of the Antisickling Mechanism of Cetiedil	5
Some Biophysical Methods Used in the Study of Small Molecule Interaction with Membrane Components ..	6
Spin Label Electron Paramagnetic Resonance (EPR)	7
Nuclear Magnetic Resonance Spectroscopy (NMR) ...	8
Ultraviolet (UV) Difference Spectroscopy	9
II. STATEMENT OF THE PROBLEM	12
Specific Aims of the Project	12
The Optical and Structural Properties of Cetiedil in Solution	12
The Partitioning Properties of Cetiedil between the Membranous Lipids and Aqueous Phases	12
The Binding Properties of Cetiedil to Membrane Proteins and Lipids	12
The Effect of Cetiedil on Water Transport across Red Cell Membranes	13
Significance of the Project	13
III. MATERIALS AND METHODS	15
Sample Preparation	15
Buffers	15
Cetiedil Solution	15
Red Blood Cells Preparation	16
Spin Labeled Membrane Samples	16
Preparation of Homogeneous Phospholipid Vesicles	18

Chapter	Page
Cetiedil-Membrane Samples	20
Cetiedil-RBC Samples for NMR Studies	21
Experimental Measurements	22
Cetiedil Extinction Coefficient Measurements	22
Critical Micelle Concentration Determination ...	22
pH Measurements	23
UV Difference Spectroscopic Measurements	23
NMR Absorption Spectra Measurement	24
¹³ C NMR	24
¹ H NMR	26
EPR Experiments	26
Water Exchange Time Measurements	29
Cell Volume Measurements	29
Determination of Hemoglobin	
Concentration	29
Cell Volume	29
Spin-Spin Relaxation Time	30
Measurement of Changes in the Intracellular	
Water Content	30
Data Analysis	32
UV Difference Spectral Data Analysis	32
EPR Data Analysis	34
5-Doxyl Streatate Labeled Samples	34
Mal-6 Labeled Samples	34
Water Exchange Time Data Analysis	35
IV. RESULTS AND DISCUSSION	38
Molecular Properties of Cetiedil	38
pH Effects	38
Extinction Coefficient of Cetiedil	41
Cetiedil Micelles	44
Solvent Effects on the Conformation of Cetiedil	
Molecules in Solution	44
Binding Properties of Cetiedil to Membrane	57
Membrane Effects on Cetiedil Conformation	57
Cetiedil-Membrane Interaction	66
Cetiedil Partitioning between the Membranous Lipid	
and Buffer Phases	67
Absorption Spectral Changes Induced by Membrane	
Lipids	67
Partition Coefficient of Cetiedil in Membrane	
Lipid	72
Effect of Cetiedil on Lipid Spin Label Mobility	77
Effect of Cetiedil on Membrane Proteins	78
Effect of Cetiedil on Water Transport across Red Cell	
Membranes	87
V. CONCLUSIONS	95
BIBLIOGRAPHY	99

Chapter

Page

APPENDIX I

.....

111

43

LIST OF TABLES

Table	Page
1. Spectral Parameters for NMR Experiments	27
2. Spectral Parameters for EPR Experiments	28
3. Experimental Parameters for ^1H of Water Relaxation Time Measurements	31
4. Carbon Chemical Shifts (δ) of Cetiedil in Different Solvents	52
5. Proton Chemical Shifts (ppm) of Cetiedil in 5 mM Phosphate Buffer with 150 mM NaCl with a Final pH of 6.3	60
6. Chemical Shift Differences of Cetiedil in Buffer and Membrane compared to D_2O	65
7. Equilibrium Binding Parameters in 5 mM Phosphate Buffer with 150 mM NaCl at pH 6.3	85
8. Effect of Cetiedil on the Hematocrit Values of RBC	88
9A. Effect of Cetiedil on the Water Exchange Time across RBC	90
9B. t and p Values of Student t -test of Paired Samples on Data Given in Table 9A	90
10. Effect of Cetiedil on the Cellular Water Content	94

LIST OF FIGURES

Figure	Page
1. SDS Gel (5.0 % Polyacrylamide) Electrophoresis of Human Erythrocyte Membranes (A) and Simplified Membranes (B)	19
2. pH Profile of Cetiedil in Blood Serum (plus) and in PBS (triangle)	40
3. Plot of A_{233} <u>versus</u> Concentration of Cetiedil in 5 mM Phosphate Buffer with 150 mM NaCl	43
4. Critical Micelle Concentration Plot of Cetiedil	46
5. Plot of Absorbance <u>versus</u> Concentration to Check the Linearity of the Instrument	48
6. 90 MHz ^{13}C NMR Spectrum of Cetiedil Citrate in D_2O at 23 °C	50
7. 200 MHz ^1H NMR Spectra of the Aliphatic Region of Cetiedil Citrate at Different Concentrations	56
8. 50 MHz ^{13}C NMR Spectra of Cetiedil Citrate in the Presence of Membranes at 23 °C	59
9. Linewidth Correlation Diagram of Cetiedil Carbons	63
10. The Relationship between the Total and the Free Cetiedil Concentration in a Membrane Sample (1.33 mg/mL) in 5 mM Phosphate Buffer with 150 mM NaCl	69
11. Plot of λ_{max} of 100 uM Cetiedil <u>versus</u> Lipid Concentration	71
12. Difference Spectral Titration of 400 uM Cetiedil with Human Erythrocyte Membranous Lipids in 5 mM Phosphate Buffer with 150 mM NaCl, pH 7.4 at Room Temperature	74
13. Double Reciprocal Plot of the UV Difference Data, $1/\delta A$ <u>versus</u> $1/[\text{Lipid}]$	76
14. The effects of Cetiedil on the Hyperfine Separation of 5-Doxyl Stearate Labeled Erythrocyte Membrane Samples in 5 mM Phosphate Buffer with 150 mM NaCl at 37 °C	80

15. Change in (W/S) of Mal-6 Labeled Erythrocyte Membranes as a Function of Free Cetiedil Concentration in a Typical Run of Paired Samples of Intact Membrane (o) and Simplified Membrane (+) Interacted with Cetiedil at 20 °C (Top Panel) and 37 °C	83
---	----

I. INTRODUCTION

I.1 Sickle Cell Anemia

Sickle cell anemia is a fatal disease prevalent mainly among the black population in the United States and Africa. It is also found in parts of Latin America, Greece, Italy and India. The sickled erythrocytes are more fragile than normal cells, hemolyze readily and consequently have a shorter life than normal cells (1). The chronic course of the disease is punctuated by crises in which the proportion of the sickled cells in blood capillaries is very high (2). The major manifestations of the sickle cell disease are a chronic hemolytic anemia and vaso-occlusive crises that cause severe pain as well as long term and widespread organ damage (2). Sickle cell patients have been found to have impaired growth and development and are highly susceptible to infections (3).

The disease results from the homozygous expression of a mutant globin gene (2). Individuals who receive the abnormal gene from both parents have sickle cell anemia. Those who receive the abnormal gene from one parent but its normal allele from the other have sickle cell trait. Such heterozygous individuals are usually not symptomatic since only 1 % of the red cells in their venous circulation are sickled (compared to 50 % in the homozygous) (2). As a result of this hemoglobin chain mutation, the solubility of the deoxygenated sickle hemoglobin (HbS) is markedly reduced, but the solubility of the oxygenated sickle hemoglobin is not affected (1). The mutation leads to "sticky" patches in both deoxy and oxy HbS. The sticky patches from two deoxy hemoglobin molecules interact to form long aggregates of deoxy HbS that distort the morphology of the red cells (1).

Abnormalities of membrane transport have also been found in sickle red cells. Deoxygenation of the sickle cells leads to an increase in passive sodium and potassium movements across the sickle cell membranes (4). This has been associated with water loss and cell dehydration. There are some investigations, however, that report no change in cell water content upon deoxygenation of sickle cells (5). Sickle cells have been found to contain high levels of calcium (6). This has been suggested to be responsible for triggering cell dehydration by creating a selective potassium-loss pathway (the Gardos phenomenon) (7). Recently, Berkowitz and Orringer found that during short periods of deoxygenation, sickling caused a balanced sodium gain and potassium loss without a change in cell water content (8). They also found that passive movements of both sodium and potassium in oxygenated sickle cells differed significantly from those in normal cells. They suggest a permanent acquired defect in the sickle cell membrane, and that potassium and water loss may not be direct consequences of deoxygenation. Tosteson and coworkers (9) found that sickle cells exposed to oxygen or carbon monoxide decrease their potassium content through a pathway for potassium transport that is activated by both cell swelling and decrease in internal pH. They also found that the same pathway was responsible for the loss of water in sickle cells and that this pathway was independent of the polymerization of sickle hemoglobin (9). Although the above findings about the mechanism of dehydration of sickle cells differ, they, nevertheless, demonstrate that membrane transport abnormalities exist.

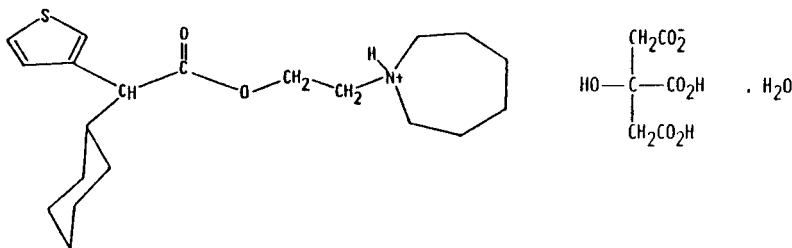
1.2 Antisickling Agents

Although some of the molecular defects of sickle cell anemia are quite

well characterized, there is at present no specific treatment for its cure or prevention. The presence of either normal adult hemoglobin or elevated levels of fetal hemoglobin seems to protect the patients from the manifestations of the disease (2). The protective effect of the fetal hemoglobin however, is variable, and the prognostic value for measuring the levels of fetal hemoglobin is limited (2). Modifying the hemoglobin synthesis by azacytidine has been suggested to be useful (10). Of the numerous antisickling agents that have been proposed for sickle cell anemia, only few have been found to be clinically useful over the years (11). Most of the antisickling agents act by modifying the sickle hemoglobin molecule (HbS) either covalently, like potassium cyanate (12) and carbamyl phosphate (13), or noncovalently, like urea (14) and L-phenylalanine (15), to prevent deoxygenated hemoglobin from forming polymers. Since the concentration of hemoglobin is high inside the red blood cells, rather high concentrations of these agents are required in order for them to be effective. Under such conditions these reagents may be toxic. Therefore, less toxic and more effective drugs, such as the drugs affecting the red blood cell membranes may offer an alternative or supplemental therapeutic approach to the disease. Some of the membrane active drugs, like procaine hydrochloride (17) and zinc (16) inhibit sickling of the sickled erythrocytes by diluting the intracellular hemoglobin concentration through cell volume change.

I.3 Cetiedil

Cetiedil, (α -hexahydro-1H-azepinyl-1-yl) ethyl-2-cyclohexyl -3-thiophenacetate,



2-(HEXAHYDRO-1H-AZEPIN-1-YL)ETHYL α -CYCLOHEXYL-3-THIOPHENACETATE 2-HYDROXY-1,2,3-PROPANETRICARBOXYLATE HYDRATE (1:1:1)

belongs to the class of noncovalent, membrane active drugs. Cetiedil is a multifunctional drug that has been available in Europe since the early 70's for the treatment of ischemic leg pain due to vascular disease (18). Other pharmacological properties of the drug include vascular smooth muscle relaxation (19), inhibition of phosphate diesterase activity (20), blockade of the effects of bradykinin and serotonin (21), analgesia (22), and inhibition of platelet aggregation (23). It has also been used to inhibit the sickling of sickle erythrocytes (24).

I.3.1 Clinical Investigations on the Effects of Cetiedil on Human Erythrocyte

The use of cetiedil as an antisickling agent was first explored by Cabannes (25). He found out that cetiedil could diminish the duration and intensity of painful crises in sickle cell anemia patients. Chromium-51 survival studies of canine erythrocytes treated with 166 μ M cetiedil had a $T_{1/2}$ of 16 days, compared to 18 days for cells incubated in buffer alone. Similar experiments on sickle cells showed that, for control cells, the $T_{1/2}$ was 8.9 days, and that, for the cells treated with 166 M cetiedil, it was 9.4 days (26). This indicates

that cetiedil is not toxic to the sickle erythrocytes. Furthermore, intravenous infusion of cetiedil to male volunteers indicated development of tolerance (27). Thus, cetiedil is considered as a potentially unique antisickling drug by some physicians.

I.3.2 The Effects of Cetiedil on Sickle Cell Morphology

Benjamin and coworkers observed a decrease in the irreversible sickle cells (ISC) count at 100 - 200 μM concentrations of cetiedil, but observed no effect at concentrations less than 50 μM , or greater than 500 μM (26). In another study, 400 μM cetiedil decreased the number of sickle cells under deoxygenated conditions, whereas 10 mM cetiedil decreased ISC counts and the cells became spheroidal, suggesting that ISC's as well as other cells became swollen (24). Marked (80 %) reduction of sickle cells at 100 - 500 μM cetiedil and 3 % oxygen concentration has also been reported (24). However, no significant effect was reported when 500 μM to 1 mM concentration of cetiedil was added to serum at 50 % oxygen saturation (11).

I.3.3 Current Understanding of the Antisickling Mechanism of Cetiedil

The detailed mechanism of cetiedil action on the erythrocyte is not clear. Cetiedil does not appear to affect, or to bind, to HbS. Asakura and coworkers observed a 20 % increase in hematocrit and over 10 % increase in the cell volume after incubating cells with 400 μM cetiedil at 37 °C (24). Schmidt and coworkers observed an increase in the cell sodium and water contents after incubating cells with 100 to 500 μM cetiedil (28, 29). The net sodium gain exceeded the net potassium loss. Furthermore, Berkowitz and Orringer found that cetiedil inhibits a specific increase in the

calcium-dependent potassium permeability across the red cell membrane (30, 31). They also found that cetedil did not prevent calcium accumulation or inhibit the anion movement. It was therefore suggested that cetedil inhibited Gardos phenomenon by preventing the opening of the potassium-specific gate in the erythrocyte membrane. Cetedil has been found to inhibit Ca^{++} -dependent calmodulin interactions with membranes (32) and also calmodulin-stimulated 3', 5'- nucleotide phosphodiesterase and Ca^{++} - ATPase activities (33). Recently, cetedil has been found to affect the trigger mechanism of the plasma membrane to inhibit the activation of NADPH oxidase (34). In brief, cetedil appears to interact with erythrocyte membranes to increase cell volume.

The present study was therefore undertaken in order to better understand the molecular mechanism of cetedil-membrane interaction.

I.4 Some Biophysical Methods Used in the Study of Small Molecule Interaction with Membrane Components

Detailed studies of the interactions of small molecules with membrane components give useful information about the binding sites and the mechanism of interactions. Some common methods that are available to study such interactions include isotopic labeling, equilibrium dialysis, ultraviolet difference spectrometry, fluorescence spectrometry, nuclear magnetic resonance and spin label electron paramagnetic resonance spectroscopy. Each of these methods has its own usefulness and gives specific information about the interaction. Many of these methods may be used concurrently to provide supplementary and complementary information about the system. Some of the major methods that were used in this study to obtain both qualitative and quantitative information about the interaction of cetedil with the human erythrocyte membrane

components are discussed in the following sections.

I.4.1 Spin Label Electron Paramagnetic Resonance (EPR)

The EPR technique is based on the magnetic moment of an unpaired electron. Most biological systems, including erythrocyte membranes, give no obvious intrinsic EPR signal, because they have no easily detectable unpaired electrons. In order to probe the structure of biomembranes and to study their interactions with small molecules, the spin label approach is generally used (35).

Spin labeling generally refers to the introduction of stable nitroxide radicals to biological systems, such as proteins and lipids (36). Different membrane components can be selectively labeled with different nitroxide spin labels. Generally, the protein spin labels are covalently attached to the protein molecules by alkylating, acylating, sulfonylating, or phosphorylating reactions (37). The lipid spin labels intercalate amongst the lipid bilayers (38).

In this study, human erythrocyte membrane proteins were covalently labeled by the commercially available piperidinyl nitroxide derivatives of sulfhydryl reagent, N-(1-oxyl-2,2,6,6-tetramethyl 4-piperidinyl) maleimide (Mal-6). By monitoring the spectral changes of the spin labeled membranes in the presence of the interacting species, information about the binding interaction such as the equilibrium dissociation constant can be obtained (39). Under specific conditions, the labeled proteins exhibit a two-component spectrum consisting a narrow and a broad component (40). The narrow line is from the weakly immobilized (W) component and the broad line is from the strongly immobilized (S) component. The amplitude ratios of these components, (W/S), can be measured easily. The high sensitivity of the W/S ratio (41) has been used to study hemoglobin binding to membrane. This approach was used

in the present study to monitor the interaction of cetiedil with the human erythrocyte membrane proteins.

In order to study the effect of cetiedil on membrane lipids, the fatty acid spin label, (3-carboxypropyl)-4,4-dimethyl-2-tridecyl-3-oxyl (5-doxyl stearate) was used and the change in the hyperfine separation of the extreme peaks (35) was monitored as a function of cetiedil concentration. The measured hyperfine separation values were used to derive information about the effect of cetiedil on the mobility or the environmental polarity of the spin label.

1.4.2 Nuclear Magnetic Resonance Spectroscopy (NMR)

The NMR technique is based on the detections of magnetic moments of nuclei with finite spin I , such as ^{13}C and ^1H . NMR techniques are widely used to provide structural information about molecules in solution. From the chemical shift values, the conformation of a molecule or of a particular moiety in the molecule can be assigned. Accordingly, for the present study, to obtain molecular and structural information about cetiedil in solution, the ^{13}C NMR chemical shifts of the carbon atoms of cetiedil in D_2O , methanol and buffer were measured. The proton chemical shifts of different concentrations of cetiedil in buffer were also measured to obtain additional molecular information about cetiedil.

The observation of binding of a small molecule to membranes by NMR methods depends largely on the existence of a measurable change in at least one NMR parameter of the system resulting from binding. A change in the relaxation times, linewidths, chemical shifts or coupling constants of any observable nucleus may be employed (42). By this technique, it is possible to monitor the spectrum of either the small molecule or the membrane component

and their interactions. Accordingly, to obtain molecular information about the cetiedil-erythrocyte membrane interaction, the change in the chemical shifts and the linewidths of the carbon and proton resonances of cetiedil in buffer, glycerol and membranes were measured in order to monitor the parts of cetiedil molecule that were affected upon interaction with the membranes.

NMR studies may also be used to provide information about the exchange of a molecule between two different environments (43). The proton relaxation time of water has been used to study the exchange of water between the erythrocytes and plasma (44). Water molecules inside red blood cells constantly exchange with water molecules outside (plasma). The exchange time for this process is about 10 msec at 37 °C (44). The NMR relaxation time of the protons of water inside the erythrocytes is longer than that of plasma. When plasma is doped with impermeable paramagnetic ions, such as Mn^{++} , the water protons of plasma relax faster ($\ll 10$ msec) by interacting with the paramagnetic ions. When this plasma water enters the cell, it would have already relaxed and when the excited water molecule inside the cell enters the plasma it would relax faster due to the presence of manganese. This would reduce the population of the excited water molecules inside the cell. By measuring the relaxation time of cell water in the presence and absence of Mn^{++} , and from the population of water outside the cell, the exchange time for water can be calculated (44). Thus, for the present study, to investigate the effect of cetiedil on water transport across the red cell membranes, cell water exchange times were measured in the presence and absence of cetiedil.

I.4.3 Ultraviolet (UV) Difference Spectroscopy

The partitioning of amphiphilic molecules between hydrophobic and

hydrophilic phases is determined by the affinity of the molecule toward a particular environment. Several methods are available to measure the partitioning properties of these amphiphilic molecules. Some of the methods include the separation of the two phases by centrifugation (45), by filtration (46) or by dialysing out the free amphiphiles from the amphiphiles in the hydrophobic phase and determining the concentration of the free amphiphiles in the aqueous phase (47). One should exercise extreme caution in determining the free amphiphile concentration in these methods. For example, if the amphiphile solubilizes the lipid components (as in the case of chlorpromazine and methochlorpromazine (48)), then the lipid bound amphiphiles will also show up as the free amphiphile. This could lead to erroneous results in the estimates of partition coefficients (49).

Recently, a UV difference spectrometric technique was developed to determine the water/lipid partition coefficients of amphiphilic molecules (50). This method takes advantage of a shift in the absorption spectra of the amphiphilic molecule upon going from an aqueous to a hydrophobic environment. It is an equilibrium technique that does not require the separation of the bound and free amphiphile as do the separation methods of determining the membrane-buffer partition coefficients. The UV difference method is useful for any amphiphile that has an appreciable absorbance below its critical micelle concentration and whose absorbance is sensitive to change in the environment. Lower amphiphile concentrations are used in order to avoid the formation of mixed micelles with the membrane lipids (46). Partition coefficients of amphiphilic molecules such as chlorpromazine, methochlorpromazine, cis and trans parinaric acids have been obtained by this method and have been shown to be in good agreement with the values obtained

by other methods (50). Cetiedil has several chromophores that absorb UV light. The UV difference spectrometric method was used to obtain the partition coefficient of cetiedil in membranes.

II. STATEMENT OF THE PROBLEM

II.1 Specific Aims of the Project

The primary goal of this dissertation project was to study cetiedil's molecular structure and properties in solution, and its interactions with the erythrocyte membrane in order to understand its mode(s) of action with erythrocyte membrane components and to evaluate the effectiveness of cetiedil as an antisickling agent. More specifically, experiments were designed to investigate the following four major areas.

II.1.1 The Optical and Structural Properties of Cetiedil in Solution

Does cetiedil contain chromophores so that the optical properties of cetiedil in solution can be characterized by UV spectroscopic technique and used to determine the concentration of cetiedil in solution? Can we determine the structural details of cetiedil in solution and the critical micelle concentration of cetiedil in aqueous solution?

II.1.2 The Partitioning Properties of Cetiedil between the Membranous Lipid and Aqueous Phases

How do cetiedil molecules partition between the lipid and the aqueous phases? Using UV difference spectroscopy the partition coefficient of cetiedil in the lipid bilayer can be obtained.

II.1.3 The Binding Properties of Cetiedil to Membrane Proteins and Lipids

If cetiedil interacts with membrane, what are the binding properties of cetiedil to membrane proteins and lipids? Can we determine the equilibrium

dissociation constant, K_d , for cetiedil-membrane proteins? Does cetiedil affect membrane lipids? Which part(s) of the cetiedil molecule are affected upon binding to the membranes?

II.1.4 The Effect of Cetiedil on Water Transport across Red Cell Membranes

How does cetiedil affect the water transport across the red cell membranes? ^1H NMR relaxation time measurements can be carried out to investigate the problem.

II.2 Significance of the Project

Very little is known about the detailed mechanism of drug action. Clinical investigations on cetiedil have shown an increased amount of cell cations like Na^+ and K^+ . As a result of this, the cell water content increases leading to cell swelling. Since these effects are direct consequences of the alterations in membrane transport properties, it is very important to understand the specific interaction of cetiedil with red cell membranes. Although existing clinical and laboratory investigations have given some phenomenological and biochemical explanation about the drug effects on the whole blood cells, investigations with more sensitive physical methods are necessary to provide molecular understanding of the specific interactions and mode(s) of action of cetiedil in the erythrocytes. With the advent of sensitive and/or sophisticated biophysical techniques, such as spin label EPR and NMR spectroscopy, it is possible to monitor the cellular events at the molecular level. Information on the specific interactions of cetiedil with the membrane components and its effects on water transport across cell membranes may lead to the development of a more effective and more specific drug therapy for sickle cell anemia. This

investigation also serves as a model system for the general study of drug-cell membrane interactions.

42

III. MATERIALS AND METHODS

III.1 Sample Preparation

III.1.1 Buffers

The various buffers used in this study included the commonly used 5 mM sodium phosphate buffer at pH 8.0 (5P8), and 5 mM phosphate buffer with 150 mM NaCl at pH 7.4 (5P7.4/NaCl), or at pH 8.0 (PBS). A pH 4 solution, 5P4/NaCl, was obtained by adding a small amount of HCl to a 5 mM monobasic sodium phosphate solution containing 150 mM NaCl to give a pH value of 4.0. A 0.3 mM phosphate buffer at pH 7.6 (0.3P7.6) was used for spectrin-actin extraction.

III.1.2 Cetiedil Solution

Cetiedil was obtained from McNeil Pharmaceuticals (Spring House, PA) in the form of the citrate salt, and used without further purification.

Cetiedil is only slightly soluble in water, with a solubility of 0.5 g/dL (51). For experiments that required cetiedil concentrations higher than 0.5 g/dL, a 30 mM stock solution was prepared. For volumetric measurements, the Oxford Adjustable Sampler Micropipetting system (Lancer, St.Louis, MO) was used. The accuracy of measurement was within one microliter. 45 mg of cetiedil was added to 1 mL 5P7.4/NaCl buffer, followed by sonication for about 2 min and centrifugation at 1,075 g for 5 min to give a clear supernatant. We found that the concentration of the supernatant was much higher than 0.5 g/dL and was generally about 2.5 - 3.0 g/dL (45 - 54 mM), as determined by UV absorption measurements. Without sonication, the supernatant was cloudy. The final pH of the 30 mM stock solution was 4.0.

For the extinction coefficient determination, a precise amount of cetiedil was weighed to prepare a 150 μ M solution in buffer, which was subsequently diluted with buffer to give cetiedil solutions of various concentrations, ranging from 10 to 150 μ M.

For ^{13}C and ^1H NMR studies, cetiedil was prepared in deuterated 5P7.4/NaCl buffer. High purity D_2O (99.9 % D) (Norell, NJ) was used to prepare the deuterated buffer solutions. For the NMR studies of cetiedil in methanol solvent, cetiedil was dissolved in non-deuterated, reagent grade methanol. The sample of cetiedil in glycerol was prepared by adding glycerol (Baker, N.J.) to a solution of cetiedil in buffer. The viscosity of the solution was checked with a Brookfield Synchro - Lectric viscometer (Model LVT - C/P, Stoughton, MA).

III.1.3 Red Blood Cells Preparation

Homozygous sickle blood cells were obtained from the Outpatient Clinic of the University of Illinois hospital (Chicago, ILL.) and from Dr. M. Westerman of the Mount Sinai Hospital of Chicago. Normal adult human packed red blood cells were obtained from the Chicago chapter of the American Red Cross Society. The red blood cells were washed twice with 40 volumes of PBS at 1,750 g for 6 min at 4 $^{\circ}\text{C}$.

III.1.4 Spin Labeled Membrane Samples

Hemoglobin-free white membrane ghosts in 5P8 were prepared from normal or homozygous sickle cells, according to the methods of Dodge et al (52). Washed red blood cells were lysed and repeatedly washed (4 to 5 times) with 5P8 until white membrane ghosts were obtained. Membrane samples (usually 4

mg/mL in protein concentration) were incubated with the protein spin label N-(1-oxyl-2,2,6,6-tetramethyl 4 piperidiny) maleimide (Mal-6) (from Aldrich, WI) at a concentration of 30-50 g Mal-6 per milligram of protein in the dark at 4 °C for 1 hour (35). Excess spin label was removed by washing with 5P8 buffer until the samples gave constant EPR signals.

Mal-6 spin labeled, spectrin-actin depleted membranes were prepared by incubation of labeled membranes at 37 °C in 0.3P7.6 buffer, to solubilize spectrin-actin, which was then removed by centrifugation (53). Modified Lowry protein assays (54) were used to determine protein concentrations. The assays were done on the intact membrane and the supernatant from centrifugation. Generally, about 30 ± 5 % of the proteins were removed from the membranes to give simplified membranes, which were depleted of the spectrin-actin network. The proteins of this simplified membrane sample were mainly Band 3 protein, as shown by 5 % SDS polyacrylamide gel electrophoresis (Figure 1), using the methods of Fairbanks et al (55).

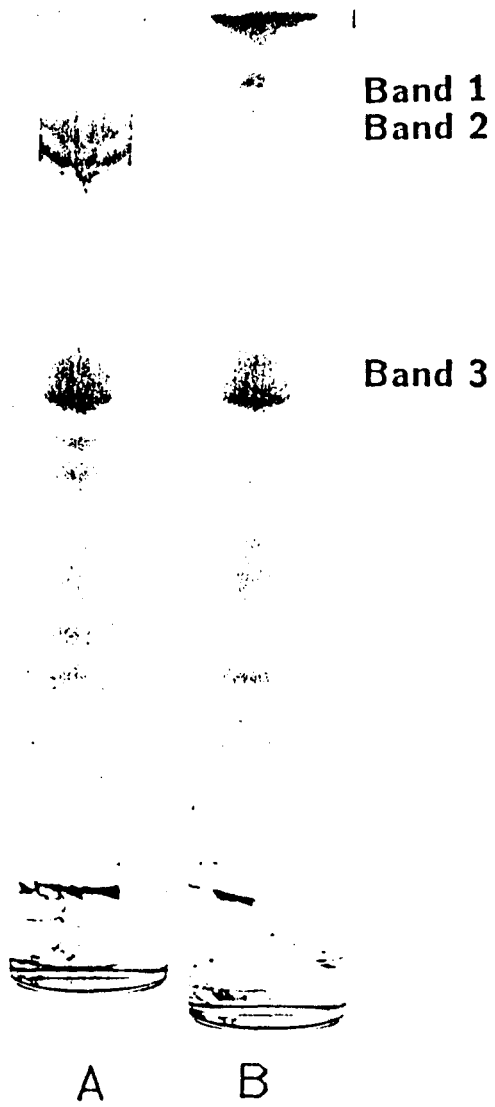
A fatty acid spin probe, (3-carboxypropyl)-4,4-dimethyl-2-tridecyl-3-oxyl (5-doxyl stearate) (from Syva, CA) was also used to probe lipids in membrane ghost samples. Membrane samples in 5P8 buffer were dialyzed in 5P7.4/NaCl buffer before incubation with 5-doxyl stearate at a concentration of 100 g/mg protein for 30 min at room temperature (35). Since the membranes have about equal amounts of proteins and lipids by weight, the spin label to lipid molar ratio was about 1:6.

III.1.5 Preparation of Homogeneous Phospholipid Vesicles

Homogeneous dipalmitoyl phosphatidyl choline (DPPC) vesicles were

Figure 1. SDS gel (5.0 % polyacrylamide) electrophoresis of human erythrocyte membranes (A) and simplified membranes (B).

57



prepared by the method of Barenholz et al. (56). According to this procedure, 20 mg of DPPC was first dissolved in 5 mL of acetone and then dried by rotary evaporation. The sample was then lyophilized to remove all traces of organic solvent. The dry phospholipid was suspended in 5 mL of HEPES buffer (20 mM HEPES, 150 mM NaCl; pH 7.4) and vortexed vigorously for 10 minutes. To make small unilamellar vesicles, the lipid suspension was sonicated with a probe sonicator (Model W-10, Ultrasonics, N.Y.), intermittently (power level 1.5) at 0 °C for 4 minutes, followed by a 2-minute cooling period for a maximum sonication time of 30 minutes. Following sonication, the vesicle dispersion was centrifuged at 101,000 g for 55 minutes to remove large multilamellar liposomes and any probe particles. The clear supernatant, which contained the population of homogeneous minimal size vesicles, was removed. The concentration of the DPPC vesicles was determined by phosphate assay developed by Rouser et al. (57) using ammonium molybdate. Monosodium phosphate in distilled water was used to obtain calibration curve for the assay. The vesicles were stored at 4 °C and used within 3 days of preparation.

III.1.6 Cetedil-Membrane Samples

The Mal-6 spin labeled membrane and the simplified membrane samples were dialyzed in 5P7.4/NaCl overnight. Samples of 5-doxyl stearate spin labeled membrane samples were used directly since they were already in 5P7.4/NaCl. The protein concentrations of these samples were determined, and adjusted to 4 mg/mL for the Mal-6 labeled samples, and 6 mg/mL for the 5-doxyl stearate labeled samples. Various volumes (0 - 200 μ L) of 30 mM cetedil stock solution were added to 100 μ L membrane samples. Appropriate volumes of 5P4/NaCl solution (since the phosphate solution is not a good

buffer at pH 4, we simply used this as a control solution, not buffer for the acidic cetiedil solution) were added to each of the spin labeled membrane and cetiedil mixture to give a constant final volume of 300 μ L. The final pH of all the samples was 6.3. The mixtures of membrane and cetiedil were then centrifuged at 38,750 g for 5 min. The supernatant of each sample was removed, and the free cetiedil concentrations in the supernatants were determined by UV absorption at 233 nm. The pellet membrane samples were used for EPR measurements.

Due to the relatively low sensitivity in the EPR studies, the concentrations of cetiedil (in the millimolar range) and of membrane proteins (in the mg/mL range) needed in this study were higher than those used clinically or in cellular studies, in which μ M concentrations of cetiedil per μ g/mL proteins were used (32, 33). However, the cetiedil-to-protein ratios in both cases are mmoles of cetiedil per gram proteins. In a simple equilibrium process, the interaction depends on the absolute concentrations of cetiedil rather than on the cetiedil-to-protein ratios. This is because the equilibrium will be shifted more toward the cetiedil-membrane association state at higher cetiedil concentration, and toward the dissociation state at lower cetiedil concentration. In the case of limited solubility of cetiedil in the buffer, a precise description of the cetiedil-membrane equilibrium in the buffer requires detailed information on the partitioning of cetiedil between the membrane and buffer phases. For comparison with other studies, simply the "cetiedil added-to-protein" ratio was used as a point of reference for comparison.

III.1.7 Cetiedil-RBC Samples for NMR Studies

To 350 μ L of the washed RBC in PBS (85 % hematocrit), 360 μ L of PBS

and 40 L of cetiedil at 7.26 mM, or 400 L of PBS as controls were added. The samples were incubated at 37 °C for 2 hours and then centrifuged at 1750 g for 6 min. 300 µL of the supernatant was removed from the vials and 20 µL of 20 mM MnCl₂ or PBS was added 1 hour before the NMR measurements. The final concentration of MnCl₂ in the NMR samples was 2 mM, as suggested by Pirkle et al. (58). The samples were allowed to equilibrate for half an hour before NMR measurements to allow interaction of manganese with water molecules outside the cells (59). The hematocrits of the samples at various stages of preparation were measured.

III.2 Experimental Measurements

III.2.1 Cetiedil Extinction Coefficient Measurements

The UV absorption spectra, in the region of 190 to 400 nm, of cetiedil solutions of known concentrations (from 10 to 150 µM of cetiedil in 5P7.4/NaCl buffer) were obtained on a double beam UV-Vis spectrophotometer (Varian DMS 90, CA), and showed a maximum absorption at 233 nm. The absorption values at 233 nm (A_{233}) were measured as a function of cetiedil concentration. A simple linear regression analysis was used to determine the extinction coefficient of cetiedil.

III.2.2 Critical Micelle Concentration Determination

Since cetiedil is an amphiphilic molecule, its solubility in water is limited (51). At high concentration, the molecules appear to form micelles in water, with monomers and micelles in equilibrium. The critical micelle concentration (cmc) of cetiedil was defined and determined according to the method of Phillips (60). A mass-action model of micelle formation was used. At the cmc,

the third derivative of an ideal colligative property of the amphiphile, A_{233} of cetiedil for this work, with respect to concentration ($[C]$) is zero ($d^3A_{233}/d[C]^3 = 0$). The A_{233} of cetiedil solutions in the concentration range of 1 - 15 mM were measured using a narrow path length, 1.0 or 0.2 mm, optical cell. The absorbance values at different concentrations were fitted to polynomial equations of varying order: $A_{233} = a[C] + b[C]^2 + c[C]^3 + \dots + n[C]^m$, where a, b, c, etc., were parameters to be determined from experimental data, and m was the order of the polynomial equation. The third derivatives of these polynomial equations with respect to concentration were set to zero to solve for cmc values.

III.2.3 pH Measurements

For the pH effect studies, various amounts of 30 mM cetiedil stock solution in PBS were added to PBS, or to blood serum, to give a concentration range of cetiedil of 4.3 μ M to 20 mM. The pH was measured at room temperature, in an open system exposed to air by Beckman Digital pH meter (model 3500) with Ingold (Andover, MA) combination pH electrode (model 18513). After adding cetiedil to serum, the contents were constantly stirred. During this time, the dissolved carbon dioxide escaped from the acidified serum. The pH values stabilized usually 5 minutes after the addition of cetiedil.

III.2.4 UV Difference Spectroscopic Measurements

The UV difference spectral measurements were made following the procedure of Welte et al. (50). The Varian DMS 90 spectrophotometer was used for all measurements. Regular absorption spectra were obtained in 1-cm light

path quartz cuvettes with the appropriate reference of either 5P7.4/NaCl buffer or erythrocyte ghost membrane (4 mg/mL) in 5P7.4/NaCl buffer. Difference spectral titrations were done in tandem cuvettes with buffer in a 0.45 - cm compartment and a solution of cetiedil in another equal light path compartment of both the reference and sample cuvettes. With this setup, first a baseline spectrum was recorded and stored. The baseline correction mode was activated to avoid baseline drifts in the subsequent measurements.

A titration was performed by adding various amounts of membrane ghost (4 mg/mL) in 5P7.4/NaCl buffer to the compartment containing cetiedil solution in the sample cuvette and to the compartment containing buffer in the reference cuvette. The solution was mixed by repeated pipetting with a pasteur pipet. Equal volumes of buffer were added to the compartments not containing membranes. The lipid concentration of the membrane ghosts (0.50 μmol of phospholipid per mg of proteins as calculated by Welte et al., (50)) in the sample mixture ranged from 6.7 to 113.2 μM . The concentration of cetiedil in all sample mixtures was 400 μM . After the addition of membrane ghosts, the samples were allowed to equilibrate for 5 min at room temperature before the spectrum was recorded. The difference spectra were recorded between 220 and 290 nm. No settling of the membrane ghosts was detected during the measurements. The positive amplitude of the difference spectra was measured to obtain A values. This was done by measuring from the baseline of the difference spectrum to the maximum of the spectrum (250 nm).

III.2.5 NMR Absorption Spectra Measurement

III.2.5.1 ^{13}C NMR

^{13}C NMR spectra were recorded at 90 MHz and 50 MHz using a Nicolet NIC 360 and Nicolet NIC 200 (Nicolet Magnetics Corporation, WI) spectrometers with 12 mm sample tubes. The "Bilevel" pulse sequence (one-pulse with two-level decoupling) was used to record the spectra (61). The pulse sequence is written as $[D_3, P_2, A, D_2, D_5]$, where D_3 is a delay time that is allowed for relay switching times (usually 1 μsec), P_2 is an excitation pulse, A is the acquisition trigger, D_2 is the acquisition time. A delay time of D_5 was allowed before repeating the pulse sequence.

The "Bilevel" pulse sequence is used typically for heteronuclear broadband decoupling, where high decoupler power is needed during data acquisition, but a lower power level can be used between scans to maintain the nuclear Overhauser enhancement (nOe).

For spectra of cetiedil in different solvents at 26.5 mM, 1000 scans (about 3 hours) were collected. The time averaged free induction decays (FID) were Fourier transformed to give the spectra in the frequency domain.

For the spectrum of cetiedil in methanol, the solvent signal was used as the internal reference to obtain the chemical shifts of cetiedil carbons. As for cetiedil in D_2O and in deuterated buffer solutions, the chemical shifts were obtained by direct comparison to the methanol spectrum. For this, the same offset value of the pulse carrier frequency was used as in the case of the methanol spectrum (62).

For cetiedil in the presence of membranes, more scans were required in order to improve the signal-to-noise. Usually, 20 blocks of 1000 FID/block (about 60 hours) were collected. Typical parameter settings for ^{13}C NMR experiments are given in Table 1.

The linewidths of the carbon resonances were measured by fitting the

data points to a Lorentzian line shape function and reported in units of hertz (Hz). No line broadening factor was used.

III.2.5.2 ^1H NMR

Proton NMR spectra were recorded at 200 MHz using a Nicolet NIC 200 spectrometer with 5 mm sample tubes. The PRESAT (one-pulse with decoupler presaturation) pulse sequence was used to record the spectra (61). According to this pulse sequence, the decoupler is turned on for D_3 seconds before pulsing, so that the solvent peak can be saturated. After a delay of D_4 seconds, the excitation pulse, P_2 is set followed by data acquisition, A and delay for acquisition, D_2 . The pulse sequence is written as, [D_3 , P_2 , A, D_2 , D_5]. Typical parameter settings for the ^1H NMR experiments are given in Table 1.

III.2.6 EPR Experiments

EPR samples were introduced into 50 μL microhematocrit capillary tubes (nonheparinized, Type II glass, American Scientific, ILL.) following the procedures used in this laboratory (35). An EPR spectrometer (Varian model E109) interfaced with a time averager (Nicolet model 535) and a variable temperature set up (Varian), was used to obtain the EPR spectra. The temperature of each EPR measurement was controlled and monitored with copper - constantan thermocouple placed inside the sample tubes to within 0.1 $^\circ\text{C}$. The EPR spectrometer settings used for measuring the spectra are given in Table 2.

Table 1. Spectral Parameters for NMR Experiments

<u>Parameter</u>	<u>¹³C NMR</u>	<u>¹H NMR</u>
Spectrometer Frequency (MHz)	90.80 ^a	
	50.02 ^b	200.07 ^b
Spectral Width (Hz)	20,000	2000
Excitation Pulse, P ₂ (μsec)	13.00	5.50
Memory Size	16 K	8 K
Data Acquisition Time, A (sec)	0.410	2.05
Delay Time, D ₂ /D ₃ (sec)	0.0001	3.00
Pulse Delay D ₆ (sec)	10.00	0.10
Number of Scans	1000 ^c	600 ^d
	20 x 1000 ^e	20 x 600 ^f

^a Nicolet NIC 360 spectrometer.

^b For spectra taken with Nicolet NIC 200 spectrometer.

^c For cetiedil in D₂O, methanol, buffer, and glycerol solvents.

^d For cetiedil in buffer.

^e For cetiedil in membrane.

^f For cetiedil in membrane.

Table 2. Spectral Parameters for EPR Experiments

<u>Parameter</u>	<u>Samples</u>	
	<u>Mal-6 Labeled</u>	<u>5-Doxyl Stearate Labeled</u>
Microwave Power Attenuation (decibals)	16	16
Modulation Frequency (KHz)	100	100
Modulation Amplitude (Gauss)	1	1
Time Constant (sec)	0.128	0.128
Scan Time (min)	2	2
Number of Scans	4	1
Field Set (Gauss)	3181	3205
Microwave Frequency (GHz)	8.65	8.65
Scan Range (Gauss)	25	100

III.2.7 Water Exchange Time Measurements

III.2.7.1 Cell Volume Measurements

III.2.7.1.1 Determination of Hemoglobin Concentration

The procedure devised by Tentori and Salvati (63) was followed for determining the total hemoglobin concentration. According to this procedure, 20 μ L of the blood sample (NMR sample after NMR measurements) was treated with 5 mL of the cyanide reagent which contained 607 μ M potassium ferricyanide ($K_3Fe(CN)_6$), 768 μ M potassium cyanide (KCN), 1 mM potassium dihydrogen phosphate (KH_2PO_4) and a non-ionic detergent (1 mL/L, Triton X-100). Potassium ferricyanide oxidized the hemoglobin to methemoglobin with cyanide as ligand to give $Hb^+ - CN^-$. The detergent enhanced hemolysis and prevented turbidity introduced by the membrane proteins. The absorbance of the resulting solution was read at 540 nm after letting the mixture equilibrate for half an hour. The hemoglobin concentration was calculated from the equation,

$$[Hb] \text{ (g\%)} = \frac{A_{540} \times F \times M}{E_{540} \times L}$$

where, F = dilution factor; M = molecular weight of hemoglobin chain (16 KDa); L = light path in cm; A_{540} = absorbance of $Hb^+ - CN^-$ solution at 540 nm; E_{540} = molar extinction coefficient of the cyanomet hemoglobin at 540 nm ($11,000 \text{ M}^{-1} \text{ cm}^{-1}$).

III.2.7.1.2 Cell Volume

The total number of cells was obtained by dividing hemoglobin

concentration, obtained by the above method, by the mean corpuscular hemoglobin concentration (MCHC, 29 ± 2 pg/cell for normal cells (59), and 32 ± 2 pg/cell for sickle cells (2)). The average cell volume (in mL) was determined by dividing the hematocrit value by the total number of cells. The cell volume measurements were done after each NMR measurement.

III.2.7.2 Spin - Spin Relaxation Time

Water proton spin-spin relaxation times, T_2 , of the blood samples were measured at 37 °C in a Nicolet NIC 200 spectrometer (Nicolet Magnetics Corporation, WI) using the Carr-Purcell-Meiboom-Gill pulse sequence (90-i-180, where i is the delay between the 90 and 180 degree pulses) (64, 65). Sample points were taken on the top of each echo. This was achieved by using a continuously variable delay trigger after the 180 degree pulse of the CPMG sequence. 16 scans were signal averaged for each sample. Independent T_2 measurements were made on packed red blood cells (control) by fitting the relaxation data to a single exponential function which relates the decay of magnetization to T_2 . For Mn - doped samples, the decay of the echo amplitudes was resolvable into two exponential components; a fast component and a slow component. The time constant characteristic of the slower component, which is related to the water diffusion exchange time, T_{ex} , was determined from the decomposition of this decay by a non-linear least squares computer program (section III.3.3). The experimental parameters used for measuring the T_2 values are given in Table 3.

III.2.7.3 Measurement of Change in the Intracellular Water Content

In order to determine the effect of ceticedil on intracellular water

Table 3. Experimental Parameters for ^1H of Water Relaxation Time Measurements

Spectrometer Frequency (MHz)	200.07
Spectral Width (Hz)	1000
Scans	16
90° Pulse (usec)	7.5
180° (µsec)	15.00
Acquisition (msec)	512.00
Recycle Time (msec)	0.100 ^a
	0.200 ^b

^a For cells with Mn^{++} .

^b For cells without Mn^{++} .

content, the changes in the cell water content were measured. This was done by two methods: the NMR method and the hematocrit measurement method.

In the NMR method, as discussed in the previous section, the spin - spin relaxation data of the packed cells were fitted to a single exponential function. The intercept (the echo amplitude) of the CPMG decay curve at $t = 0$, which is directly proportional to the amount of cell water, was measured. From the difference in the echo amplitudes of the samples before and after treatment with cetiedil, the change in the cell water content was determined.

Although the hematocrit measurement is not a direct method of determining cell water content, it could still be used to determine changes in water content. Thus for the present study, the hematocrit values of RBC before and after treatment with cetiedil were measured. From the difference in the hematocrit values of samples before and after treatment with cetiedil, the change in the cell water content was determined.

III.3 Data Analysis

III.3.1 UV Difference Spectral Data Analysis

In order to determine the concentration of cetiedil bound to the membranous lipids accurately, the change in the absorbance of cetiedil in the membranous lipid phase, δA , was measured (50). δA is proportional to the amount of lipid-associated cetiedil. At high membrane lipid concentrations, δA approaches δA_{\max} , the value corresponding to 100 % cetiedil bound. Then $\delta A / \delta A_{\max}$, at a given membrane lipid concentration, is the fraction of total cetiedil associated with membrane lipid. From the knowledge of the fraction of cetiedil in the membrane lipid phase and in the buffer phase, the molar

partition coefficient of cetiedil between buffer (water) and membrane lipid was defined as

$$K_p = \frac{\text{mol of cetiedil in lipid/mol of lipid}}{\text{mol of cetiedil in water/mol of water}} \quad (1)$$

or,

$$K_p = \frac{\text{fraction of cetiedil in lipid}/[\text{lipid}]}{\text{fraction of cetiedil in water}/[\text{water}]} \quad (2)$$

where [lipid] and [water] are expressed as molar concentrations. Since the fraction of cetiedil in lipid and the fraction of cetiedil in water added up to 1,

$$K_p = \frac{(\delta A/\delta A_{\max})/[\text{lipid}]}{(1 - \delta A/\delta A_{\max})/[\text{water}]} \quad (3)$$

The above equation was rearranged to give

$$1/\delta A = \frac{[\text{water}]}{K_p \delta A_{\max}} \cdot \frac{1}{[\text{lipid}]} + \frac{1}{\delta A_{\max}} \quad (4)$$

The above equation was used to obtain δA_{\max} and K_p from the plot of $1/\delta A$ vs $1/[\text{lipid}]$.

III.3.2 EPR Data Analysis

III.3.2.1 5-Doxyl Stearate Labeled Samples

The hyperfine separation (HFS) of the high field and low field EPR signals of labeled membrane samples were measured as a function of cetiedil concentration (35).

III.3.2.2 Mal-6 Labeled Samples

The W/S ratios (39) of membrane samples without cetiedil, $(W/S)_o$, and of membranes with a certain amount of cetiedil present, $(W/S)_{cet}$, were measured. $(W/S)_{cet}$, the difference between $(W/S)_o$ and $(W/S)_{cet}$, was calculated and used to obtain quantitative information on the interaction between cetiedil (C) and membranes (M).

A general cooperative binding model was first assumed for membranes with n binding sites, $M + nC \rightleftharpoons MC_n$. For this model the equilibrium dissociation constant, K_d , was equal to $[C]^n[M]/[MC_n]$, where $[M]$ was the final membrane concentration, $[C]$ was the concentration of free cetiedil, in equilibrium with the bound cetiedil, and $[MC_n]$ was the concentration of the membrane-cetiedil complex. If f_b was the membrane fraction that interacted with cetiedil, then, $f_b = [MC_n]/([MC_n] + [M])$. Combining the K_d and f_b expressions given above, the following expression was obtained:

$$f_b = (1 + K_d/[C]^n)^{-1} \quad (5)$$

Assuming that the changes in the W/S ratio observed upon addition of cetiedil to the membrane were the direct results of cetiedil interacting with the membrane to reduce the spin label mobility, the EPR data could be related to f_b to obtain values for the K_d . Assuming $(W/S)_b$ as the W/S value for

membrane bound with cetiedil, then $(W/S)_{\text{cet}} = f_b(W/S)_b + (1 - f_b)(W/S)_o$, or

$$\Delta(W/S)_{\text{cet}} = f_b \Delta(W/S)_{\infty} \quad (6)$$

where $\Delta(W/S)_{\infty} = (W/S)_o - (W/S)_b$. Substituting equation (5) into equation (6), the following equation was obtained:

$$\Delta(W/S)_{\text{cet}} = \Delta(W/S)_{\infty} (1 + K_d/[C]^n)^{-1} \quad (7)$$

When $n = 1$, this equation became the equation for the two-state binding model for membranes with multiple independent binding sites, $M + C \rightarrow MC$. $\Delta(W/S)_{\text{cet}}$ and $[C]$ values were experimental data. K_d , $\Delta(W/S)_{\infty}$ and n could be obtained from equation (7) using nonlinear regression methods. The n values, which indicate the cooperativity of binding, were also obtained by Hill plots. The half saturation concentration, $C_{1/2}$, was the cetiedil concentration that gave a $\Delta(W/S)_{\text{cet}}$ value that was half of the $\Delta(W/S)_{\infty}$ value, and was obtained from the nonlinear regression analysis.

III.3.3 Water Exchange Time Data Analysis

The measured relaxation time of water protons of RBC results from the water exchange across the cell membranes which is superimposed on the ordinary spin-spin relaxation of water in the cell (66). In order to obtain the exchange time of water across the cell membranes, the relaxation data of the Mn - doped samples were analyzed using the theory of two-site exchange (58). Assuming no significant chemical shift difference between the water molecules inside and outside the cell, Woessner (67) has derived the following normalized

expression for the effect of two-site exchange on the CPMG decay:

$$M(t) = [P_a' \exp (-t/T_{2a}') + P_b' \exp (-t/T_{2b}') + B] \quad (8)$$

where, $M(t)$ represents the magnetization at time t , B is a baseline correction factor, T_{2a}' and T_{2b}' are the apparent relaxation times of water molecules inside and outside the cell, respectively and P_a' and P_b' are the apparent fractions of the echo amplitudes from the intra- and extra- cellular water molecules, respectively.

The relaxation data of Mn-doped sample were first fit by Equation (8) by non-linear least squares method to obtain P_a' , T_{2a}' and T_{2b}' where,

$$1/T_{2a}' = C_1 - C_2 \quad (9)$$

$$1/T_{2b}' = C_1 + C_2 \quad (10)$$

$$P_b' = 1/2 - 1/4[(P_b - P_a)(1/T_{2a} - 1/T_{2b}) + 1/T_{ex} + 1/t_b]/C_2 \quad (11)$$

$$P_a' = 1 - P_b' \quad (12)$$

where,

$$C_1 = 1/2[1/T_2 + 1/T_{2b} + 1/T_{ex} + 1/t_b] \quad (13)$$

$$C_2 = 1/2[(1/T_{2b} - 1/T_2 + 1/t_b - 1/T_{ex})^2 + 4/T_{ex}t_b]^{1/2} \quad (14)$$

$$P_a = 1 - P_b \quad (15)$$

$$P_a/T_{ex} = P_b/t_b \quad (16)$$

In the above equations, T_2 is the spin - spin relaxation time of water inside

the cell (packed cells), T_{2b} is the relaxation time of water outside the cell, t_b is the residence time of water outside the cell, and P_a and P_b are the fractions of the echo amplitudes of water molecules inside and outside the cell respectively. The values of P_a' , T_{2a}' and T_{2b}' were then used in Equations 9-16 and the values of T_{2b} , T_{ex} , t_b , P_a and P_b were calculated. The exchange time is related to the diffusional water permeability constant, P_w , by the equation (44),

$$P_w = (V/A) \cdot 1/T_{ex} \quad (17)$$

where, V is the cell volume and A is the surface area of RBC. For the calculation of the permeability constants, the cell surface area was taken as $140 \times 10^{-8} \text{ cm}^2$ (68). P_w is expressed in cm/sec. Equation 17 was then used to obtain the diffusional permeability constant.

IV. RESULTS AND DISCUSSION

IV.1 Molecular Properties of Cetiedil

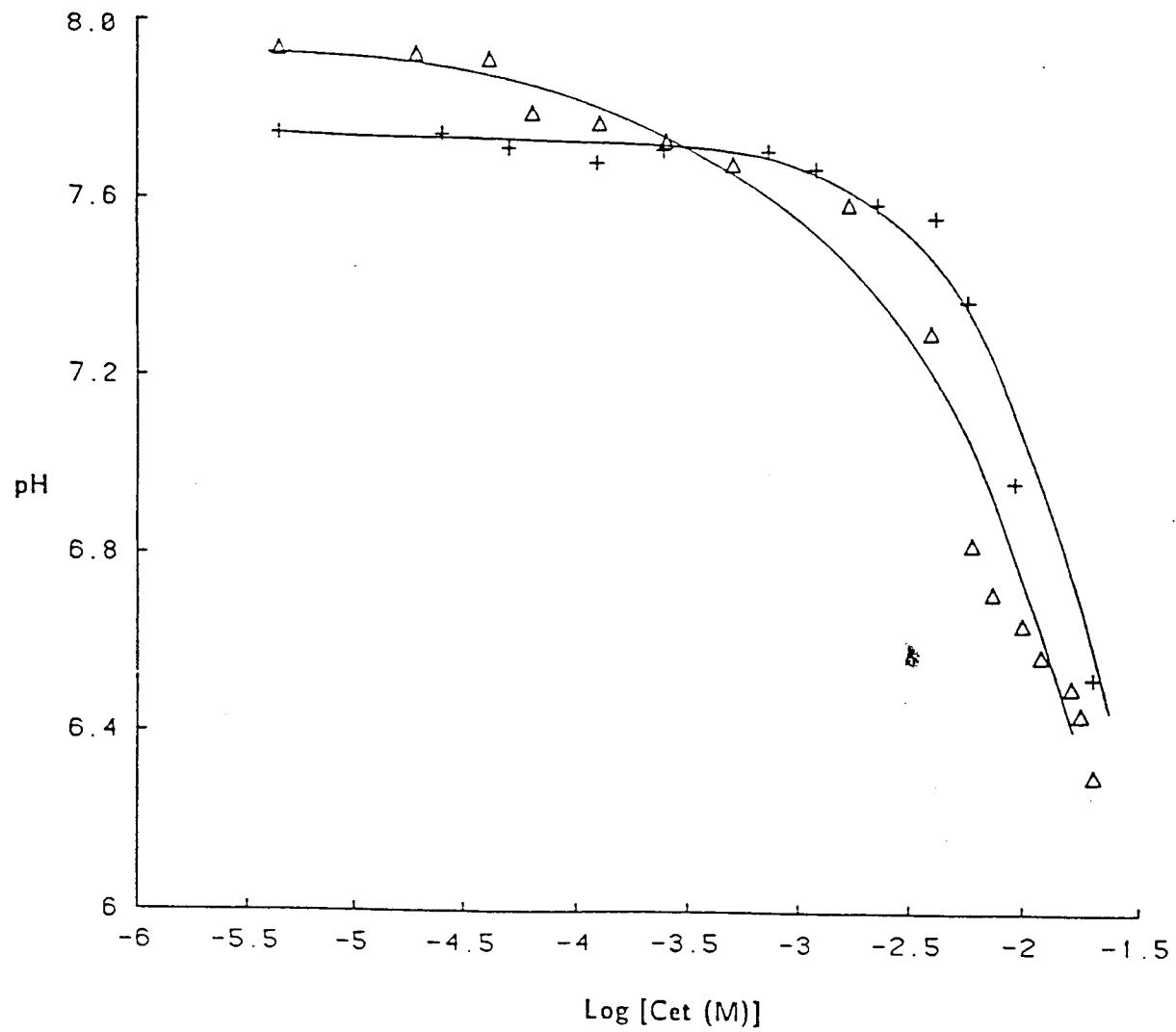
IV.1.1 pH Effects

Figure 2 shows the pH of the drug molecule, cetiedil citrate, in PBS and in blood serum as a function of cetiedil concentration. In PBS, addition of 500 μ M cetiedil causes the pH of the buffer to drop from 8.0 to 7.7. At 20 mM cetiedil, the pH is about 6.3, and at 30 mM, the pH is 4.0.

This sharp change in pH upon addition of cetiedil to buffer was probably due to the citrate moiety that was present with cetiedil as a counterion. The pK_2 of citric acid is 4.76 and pK_3 is 6.4 at 25 °C (69). The first ionizable proton ($pK_1 = 3.1$) of the three carboxylate groups in citrate is neutralized by the positive charge on the tertiary ammonium group of azepine ring, which has a pK_a of about 10. Various concentrations of citric acid solutions in PBS were also prepared and their pH values were compared with those of cetiedil solutions. The pH profiles of cetiedil citrate and citric acid in PBS were similar.

The pH effect of the drug molecule was also tested on blood serum in a similar manner. Although the pH profile of cetiedil in serum in Figure 2 looks similar to that in PBS, the curve is slightly right shifted, indicating that the buffering capacity of blood serum is somewhat better than that of PBS. The pH of the serum remains constant upon addition of cetiedil up to about 0.5 mM, and it drops to about 6.5 at 20 mM cetiedil. Thus the pH titration experiments clearly showed that the drug molecule became acidic at concentrations greater than 500 μ M.

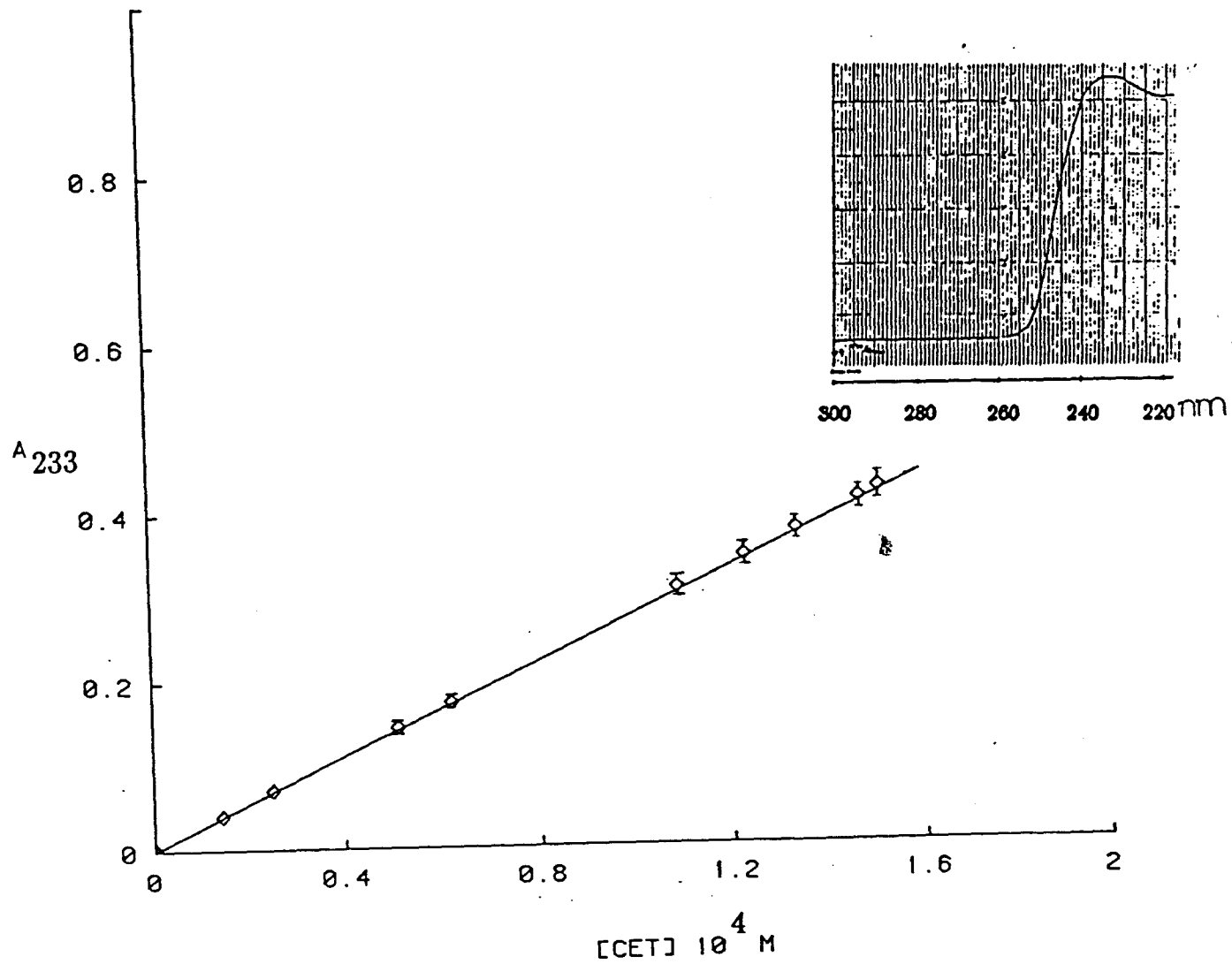
Figure 2. pH profile of cetiedil in blood serum (plus) and in PBS (triangle). pH measurements were made on a Beckman Model 3560 Digital pH meter using an Ingold Micro pH Electrode at room temperature. The pH of the blood serum was 7.78. The lines shown through the data are spline fits and have no theoretical significance.



IV.1.2 Extinction Coefficient of Cetiedil

The maximum UV absorption of cetiedil in 5P7.4/NaCl buffer is at 233 nm (inset of Figure 3). The molar extinction coefficient at 233 nm (E_{233}) determined from the slope of a linear plot of A_{233} versus cetiedil concentration over the range of 10 to 150 M was $2796 \text{ M}^{-1} \text{ cm}^{-1}$ (Figure 3). The chromophores in cetiedil appear to be the thiophene (sulfur-containing 5 membered ring) and the azepine (nitrogen-containing 7 membered ring) groups, both of which absorb in the UV region. For thiophene, the maximum absorption is at 231 nm, and the E_{231} is $7,100 \text{ M}^{-1} \text{ cm}^{-1}$ (70), and for azepine, the maximum absorption is at 226 - 229 nm, and the E_{227} is $13,780 \text{ M}^{-1} \text{ cm}^{-1}$ (71). The low value of the extinction coefficient of cetiedil compared to that of its components suggested that the absorption is less efficient in the case of cetiedil (72). The nitrogen atom of azepine ring in cetiedil is protonated in buffer and so the absorption due to that moiety is affected. Therefore, the spectrum was basically due to the absorption by the substituted thiophene moiety. The observed molar extinction coefficient, $2796 \text{ M}^{-1} \text{ cm}^{-1}$ for cetiedil, however, is much less than 7100. The absorption characteristics of substituted heteroaromatic compounds depend on the substituents present in the ring and also on the solvent (70). The presence of electron withdrawing substituents in thiophene ring such as nitro group ($-\text{NO}_2$) causes a red shift in the absorption maximum to 268 - 272 nm and the extinction coefficient decreases to $6,300 \text{ M}^{-1} \text{ cm}^{-1}$ (70). Thus in cetiedil the decrease in extinction coefficient may be due to the substituent on thiophene ring, the substituted ester group (cyclohexyl and azepinyl).

Figure 3. Plot of A_{233} versus concentration of cetiedil in 5 mM phosphate buffer with 150 mM NaCl. Inset shows the UV spectrum of cetiedil with maximum absorption at 233 nm. The molar extinction coefficient was determined from the slope of the line.



IV.1.3 Cetiedil Micelles

Figure 4 shows that the A_{233} (1 mm light path) values of cetiedil in 5P7.4/NaCl buffer level off at higher cetiedil concentrations, above 8 mM. The instrument performance at high absorbance was checked to ensure linear response. Straight lines were obtained for absorbance versus concentration plots for benzoic acid at 230 nm (Figure 5A), and for hemoglobin solutions at 280 nm (Figure 5B). Light scattering at 233 nm was also checked by monitoring the absorbance of membrane solutions. A linear response was also obtained at high absorbance (2 - 3) (Figure 5C). The levelling off phenomenon in cetiedil solutions at high concentration is then attributed to micelle formation. The relationship between the absorbance and concentration was fit to polynomial equations to determine the critical micelle concentration as discussed in section III.2.2. Polynomial equations with orders equal to 4, 5, 6, 7, and 8 all gave reasonably good fits to the experimental data. The average value of the cmc from these fitted polynomial equations was 8.8 ± 0.3 mM.

IV.1.4 Solvent Effects on the Conformation of Cetiedil Molecules in

Solution

In all the solvent systems studied, the ^{13}C NMR spectra of cetiedil consisted of three distinct regions: the downfield carbonyl region (172 - 180 ppm), the middle region of the aromatic thiophenyl carbons (120 - 139 ppm), and the upfield region of the azepinyl and cyclohexyl carbons and also of the carbons from the rest of the molecule including the citrate moiety (20 - 75 ppm). For cetiedil in D_2O solvent (Figure 6), based on published spectra of the compounds that are close structural analogs

Figure 4. Critical micelle concentration of cetiedil. A_{233} versus cetiedil concentration in 5 mM phosphate buffer with 150 mM NaCl. Optical cells with a 1 mm light path were used to obtain the A_{233} values.

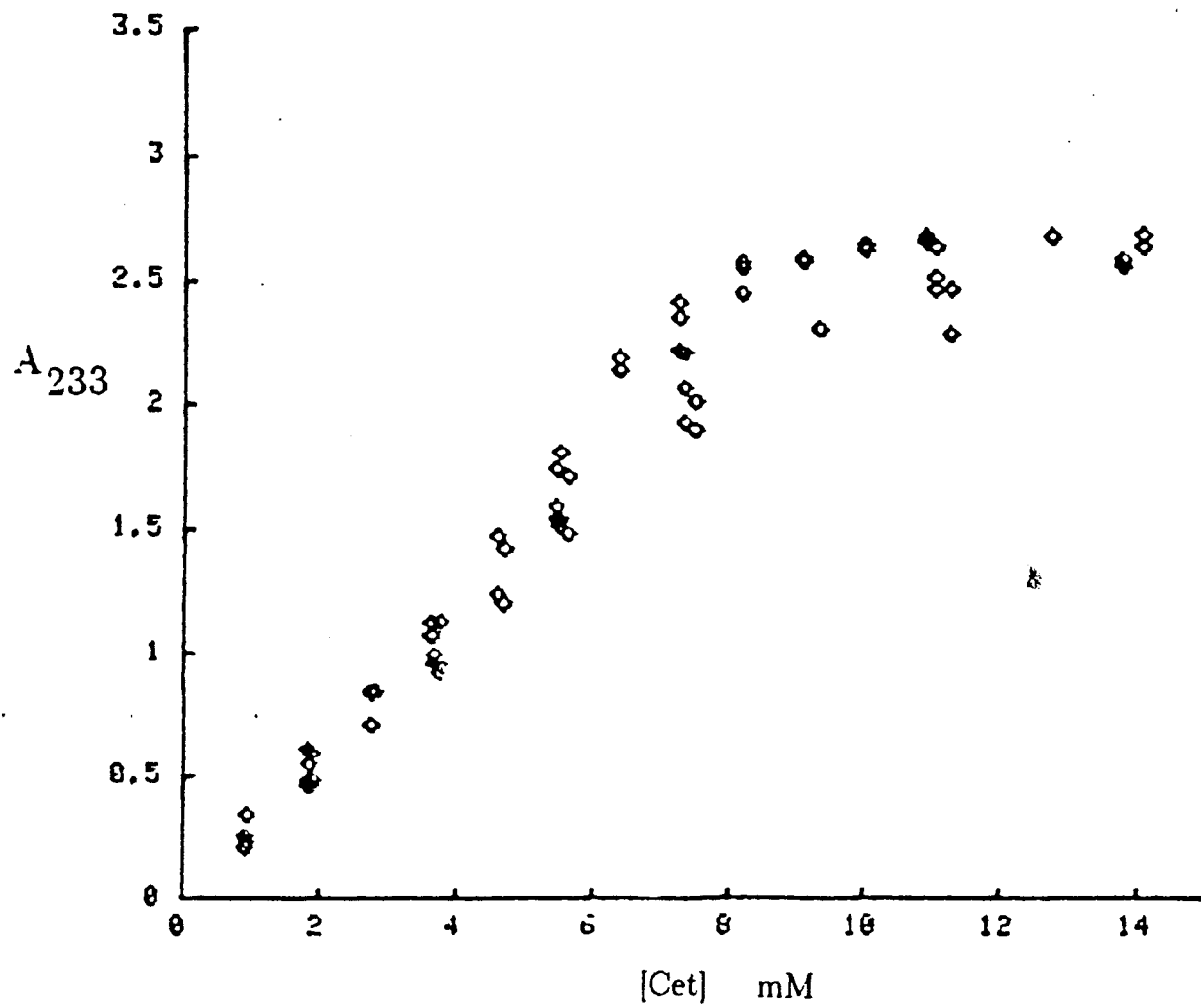


Figure 5. Plot of absorbance versus concentration to check the linearity of the instrument. A: A_{230} versus benzoic acid concentration. B: A_{280} versus hemoglobin concentration. C: A_{233} versus concentration of membrane lipids. The concentration is expressed in terms of phospholipids (4.8×10^8 phospholipids per membrane ghost; $0.5 \mu\text{mol}$ lipid per mg of membrane protein).

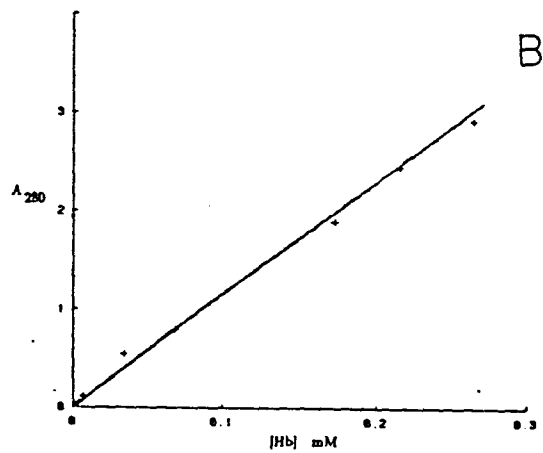
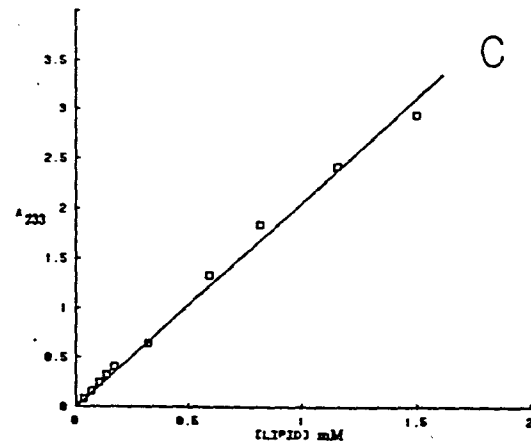
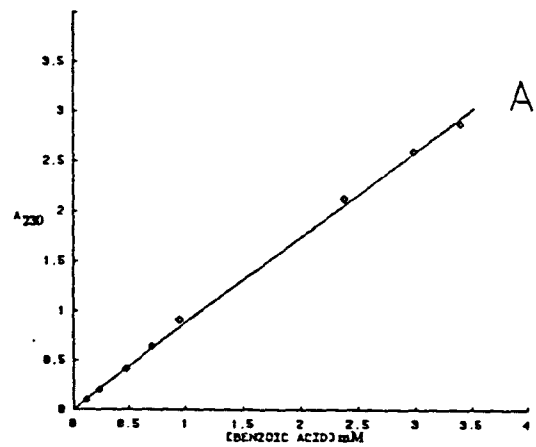
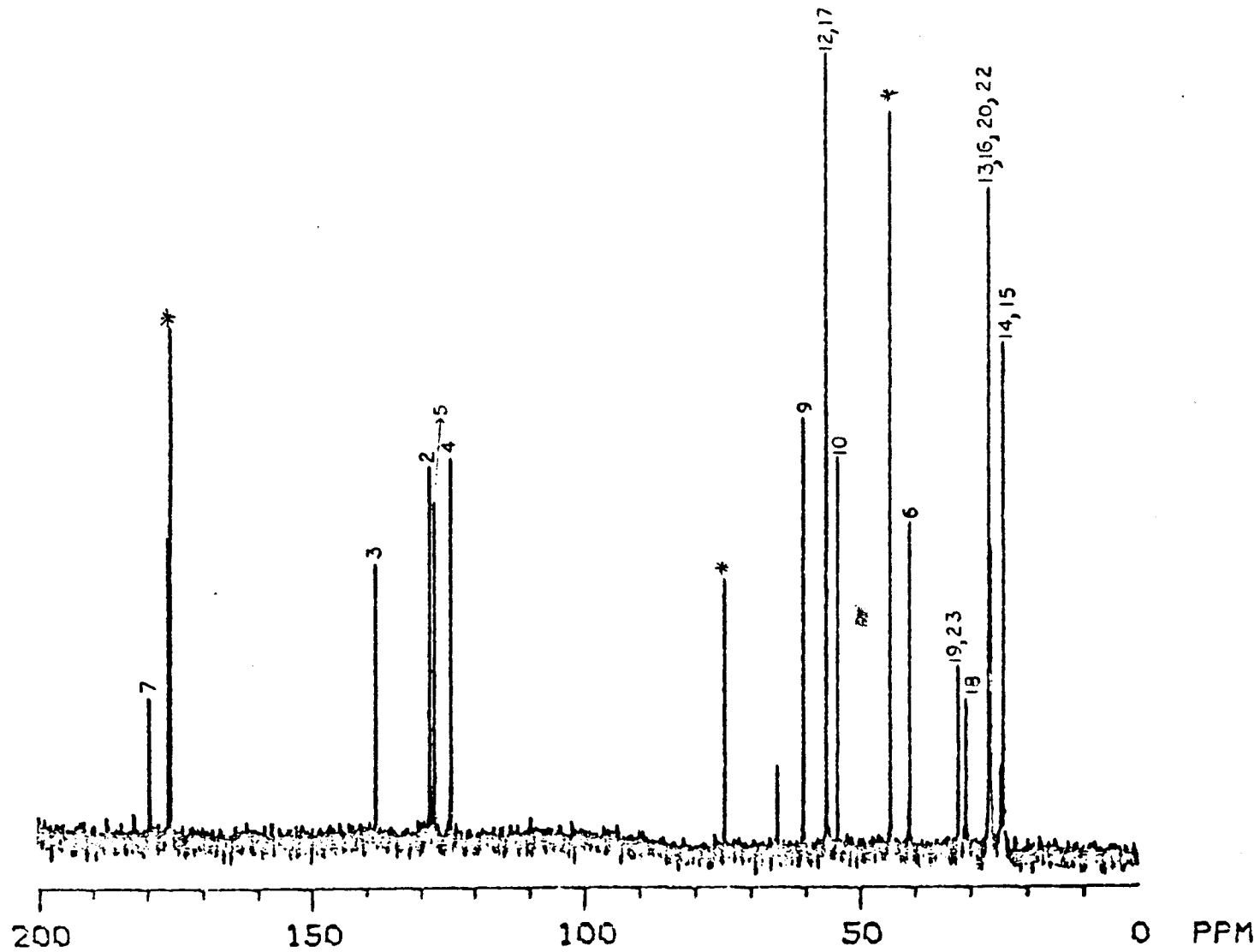


Figure 6. 90 MHz ^{13}C NMR spectrum of cetiedil citrate in D_2O at 23 °C. Concentration 26.5 mM; number of scans 1000 (about 3 hours); spectral width 20,000 Hz. The numbered peaks correspond to the cetiedil carbons (see section I.3) and the peaks with asterisks correspond to the citrate moiety.



of the different groups present in cetiedil, the peak assignments were determined. Accordingly, the carbonyl carbons of the citrate moiety were assigned to the peak at 175.62 ppm using the published spectrum of sodium citrate (73) and the carbonyl carbon of the cetiedil moiety (C-7) was assigned to the peak at 178.52 ppm using the spectrum of ethyl acetate (74). The thiophenyl carbons (C-2 to C-5) were assigned using the published spectrum of 3-substituted thiophene (75). Thus the peaks at 127.57 ppm, 137.12 ppm, 123.33 ppm, and 126.44 ppm were assigned to the thiophenyl carbons, C-2, C-3, C-4, and C-5 respectively. The resonances of cyclohexyl carbons (C-18 to C-23) were assigned using the published spectrum of methyl cyclohexane (76). Thus, C-18 of cetiedil was assigned to the peak at 29.81 ppm; C-19 and C-23 were assigned to the peak at 31.24 ppm and carbons 20 and 22 were assigned to the peak at 25.67 ppm. The chemical shifts of cyclohexyl carbons of cetiedil were very similar to the chemical shifts of the chair form of methyl cyclohexane (77). So, it was concluded that the cyclohexyl group of cetiedil is in the chair conformation. Using N-methyl piperidine as the model compound (78), C-12 and C-17 were assigned to the peak at 55.18 ppm, C-13 and C-16 were assigned to the peak at 25.67 ppm, and C-14 and C-15 were assigned to the peak at 23.10 ppm. The C-6, C-9 and C-10 of cetiedil were assigned to the peaks at 40.15 ppm, 59.43 ppm, and 53.12 ppm respectively, based on the published spectrum of ethyl acetate. The chemical shift assignments of the cetiedil spectra in methanol, buffer and glycerol were made by comparison with the spectrum of cetiedil in D₂O.

The chemical shift assignments of all the cetiedil carbons in methanol, and buffer are also shown in Table 4. The chemical shift values have an estimated precision of ± 0.014 ppm for individual runs. There is a general

Table 4. Carbon Chemical Shifts (δ) of Cetiedil in Different Solvents*

<u>Model</u> <u>Compound</u> <u>Reference</u>	<u>Carbon</u>	<u>δ (ppm)</u>		
		<u>D₂O</u>	<u>Methanol</u>	<u>5P7.4/NaCl</u>
71	2	127.57	127.87	128.22
71	3	137.12	138.29	137.98
71	4	123.33	123.40	124.23
71	5	126.44	126.42	127.25
70	6	40.15	41.56	40.96
70	7	178.52	178.94	179.53
70	9	59.43	59.86	60.28
70	10	53.12	54.18	53.93
74	12,17	55.18	55.69	56.07
72,74	13,16,20,22	25.67	26.91	26.49
74	14,15	23.10	24.03	23.95
73	18	29.81	30.85	30.62
73	19,23	31.24	32.36	32.04

* Cetiedil concentration in all solvents except membrane was 26.5 mM. In the membrane system, the cetiedil concentration was 19.5 mM (in 5P7.4/NaCl with a final pH of 6.3). All spectra were taken at room temperature (23 ± 1 °C).

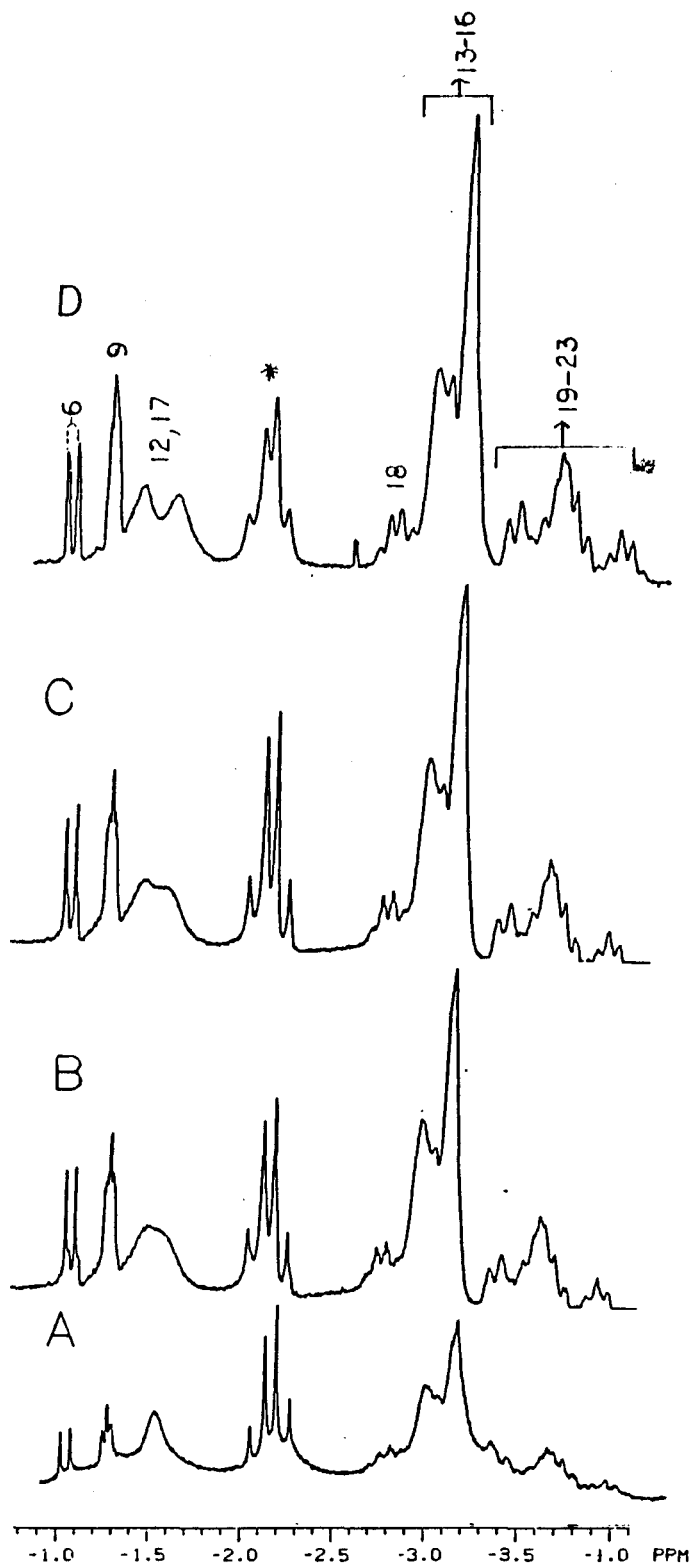
trend in the chemical shifts of cetiedil carbons. The chemical shift of a particular carbon is most upfield in D_2O , and is downfield shifted in methanol solvent, as the polarity of the solvent decreases from that of D_2O .

Comparing the ^{13}C NMR chemical shifts of cetiedil in different solvents showed that cetiedil probably undergoes overall conformational change as the polarity of the solvent changed. For example, the chemical shift of the carbonyl carbon (C-7) of cetiedil is more upfield in D_2O solvent than in the presence of methanol. The hydrogen bonding capability in water is more than that in methanol. For carbonyl carbons, in the absence of other effects, hydrogen bond formation usually leads to downfield shifts (79, 80). In the case of cetiedil however, the hydrogen bond formation seems to lead to upfield shifts. Therefore, there may be other effects such as hydrophobic interactions that mask the effect of hydrogen bonding. Hydrogen bond formation is usually accompanied by a change in the dipole moment of the interacting species. According to the charge-transfer theory, the proton-donor group tends to acquire excess electronic density directly from the basic electron-donor complement (81). In the case of cetiedil, the proton-donor H of water molecule gains electron density from the electron-donor group, carbonyl, of cetiedil. Since cetiedil is an ester, the ester oxygen can also hydrogen bond with water. In the case of amide bonds (peptide linkage), the polarizability of the bond is such that the effects from these two hydrogen bonds (carbonyl oxygen and the amide nitrogen) lead to an upfield shift of the carbonyl carbon (82, 83). A similar effect is thus suggested for the observed upfield shift of carbonyl carbon resonance. At the concentrations of cetiedil used in the present ^{13}C NMR studies (26.5 mM), cetiedil would exist as micelles in D_2O solvent (Section IV.1.3). Since methanol is a less polar solvent than D_2O , the

molecular properties of cetiedil may be different which may be responsible for the observed changes in the ^{13}C NMR chemical shifts.

The ^1H NMR spectra of cetiedil at different concentrations are shown in Figure 7. Two distinct regions could be observed in all the cetiedil spectra; the aromatic region that consists of the thiophenyl protons is about 2.5 ppm downfield from the solvent (HOD) peak and the aliphatic region is upfield from the solvent peak. Proton chemical shifts were referenced with respect to the water signal, which was 4.75 ppm downfield from the proton resonance of tetramethyl silane (TMS) at the ambient temperature of the probe. Chemical shifts downfield from water were assigned positive values and the chemical shifts upfield from water were assigned negative values. As in the case of the carbon spectra, the chemical shifts were assigned by using the published spectra of the analogous compounds. The spectrum of 3-methylthiophene was used to assign the peaks from the thiophenyl protons in the aromatic region (84). Thus, the peaks in the region 2.38 - 2.70 ppm were assigned to the thiophenyl protons of cetiedil, H-2, H-4, and H-5. For assigning the azepinyl protons, the spectrum of chloroethyl derivative of azepine hydrochloride was used (84). Methylcyclohexane spectrum (84) was used to assign the chemical shifts of the cyclohexyl protons (H-13 to H-16) of cetiedil to the peak at -3.10 ppm. By comparing the spectrum of sodium citrate, the methylene protons of the citrate moiety were assigned. The broad envelope around -1.5 ppm was assigned to the azepinyl protons H-12 (2 protons) and H-17 (2 protons). H-10 (2 protons) were assigned to the peak at -0.35 ppm.

Figure 7. 200 MHz ^1H NMR spectra of the aliphatic region of cetiedil citrate at different concentrations: A) 5 mM, B) 6 mM, C) 6.5 mM, D) 7 mM. For each spectrum, 600 FID's were collected and then Fourier transformed.



By spectral integration of the aliphatic region, 28 of the 33 aliphatic protons were accounted for (Table 5). The proton attached to nitrogen was probably broadened due to the quadrupolar coupling by nitrogen (85). The integration of the peaks close to the water signal was difficult because of the relatively large intensity of the water signal. The chemical shifts of the protons and their assignments are shown in Table 5.

Comparison of the proton NMR spectra of cetiedil at different concentrations showed that as the concentration was increased to about 6.5 mM, a new peak was observed at -1.60 ppm. Spectral integration of the 5 mM cetiedil spectrum showed 4 protons (H-12 and H-17) under the -1.5 ppm peak. For the 6.5 mM or higher concentration samples, spectral integration showed 2 protons each under the peaks at -1.5 ppm (H-12 or H-17) and -1.6 ppm (H-17 or H-12). Thus, at higher concentrations of the drug, the molecule seems to be in equilibrium with two forms. These two forms may be the cetiedil aggregates and the monomers. The UV data however, showed that cetiedil formed micelles only above 8 mM. Thus the peak at -1.6 ppm may be suggesting the involvement of the protons H-12 and/or H-17 in the formation of cetiedil aggregates. Further investigation of this property of cetiedil molecules might give more useful information.

IV.2 Binding Properties of Cetiedil to Membrane

IV.2.1 Membrane Effects on Cetiedil Conformation

The ^{13}C NMR spectra of membrane, cetiedil in membrane and that of the difference spectrum after subtracting the contribution from the membranes are shown in Figure 8. The difference in chemical shifts of cetiedil in buffer and in the presence of membranes are shown in Table 6. In general, the

Figure 8. 50 MHz spectra of cetiedil citrate in the presence of membranes at 23 °C. A: difference spectrum of cetiedil after subtracting from spectrum B (membrane + cetiedil), spectrum C, the contribution due to the membrane components.

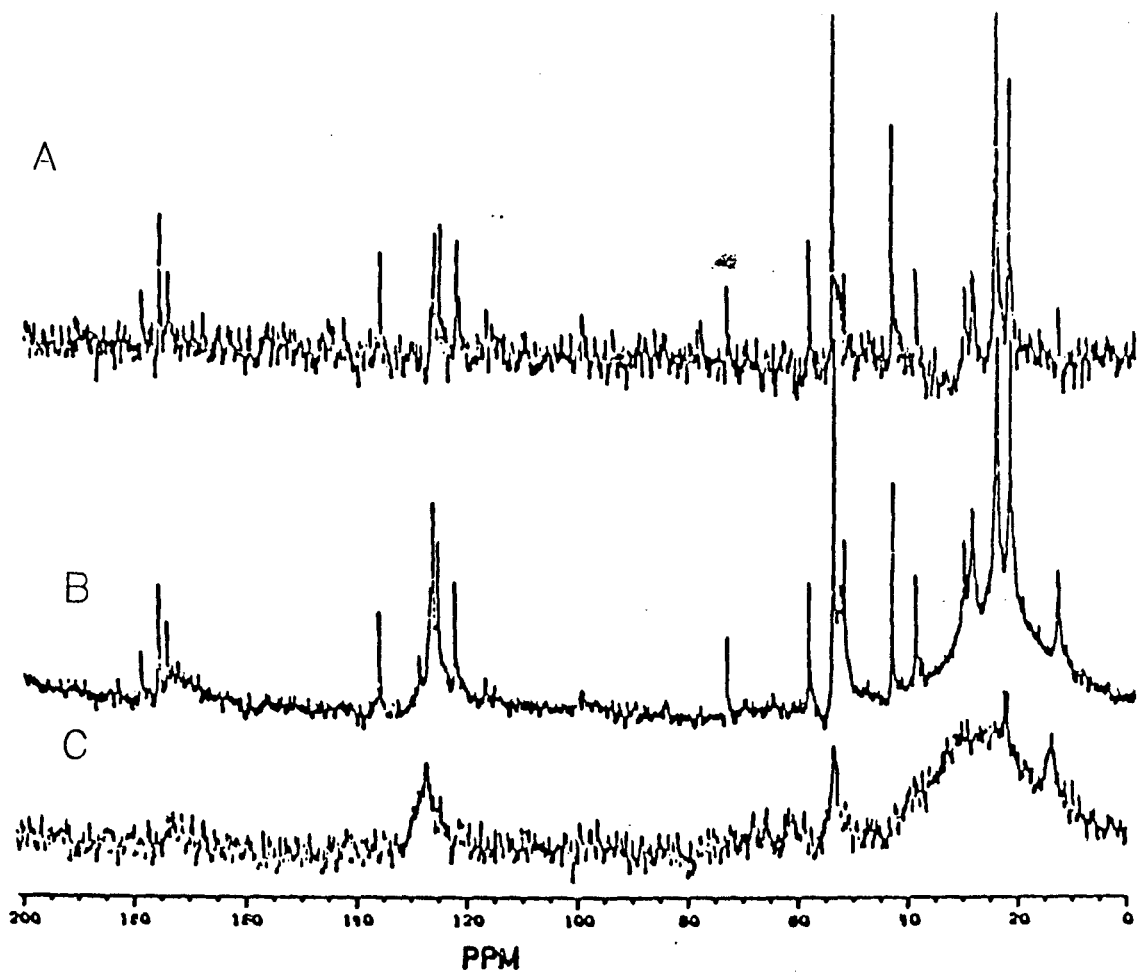


Table 5. Proton Chemical Shifts (δ ppm) of Cetiedil

<u>Proton</u>	<u>δ(ppm)</u>	<u>Number of Protons</u>	
		<u>Expected</u>	<u>Observed[*]</u>
2,4,5	2.38 - 2.70	3	(3)
6	-1.00	1	1.0 ^a 1.0 ^b
9	-1.30	2	2.0 ^a 2.0 ^b
10	-0.35	2	(2)
11	-----	1	(1) ^c
12,17	-1.50	4	4.0 ^a 2.0 ^b
12,17	-1.60	(2)	0.0 ^a 2.3 ^b
13-16 & (19-23)	-3.10	11	10.0 ^a 11.3 ^b
18	-2.80	1	--- ^a 0.8 ^b
(19-23)	-3.4 to -4.2	7	5.5 ^a 5.0 ^b
Citrate	-2.10	4	4.5 ^a 4.3 ^b

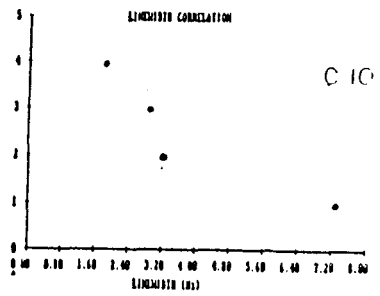
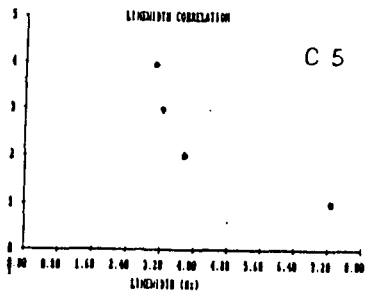
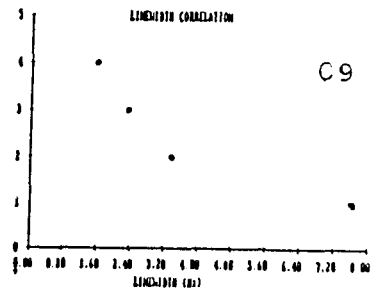
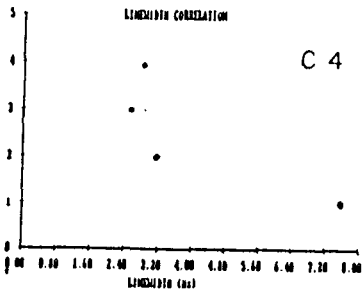
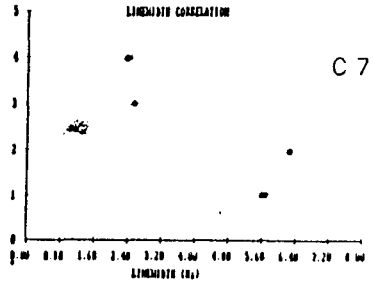
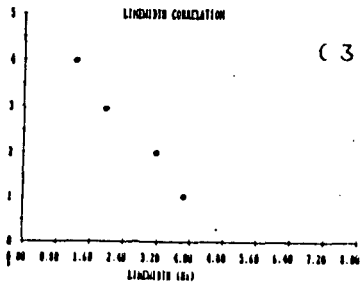
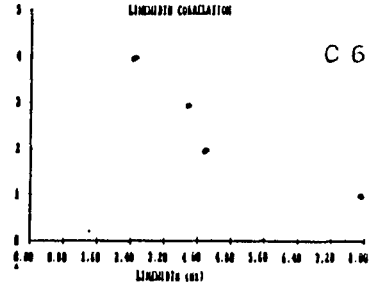
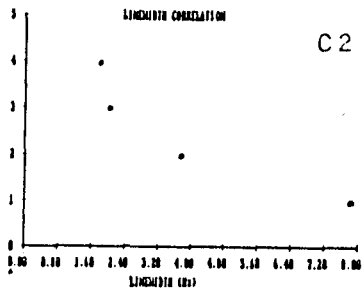
- * From the spectral integration of the aliphatic region
- ^a For 5.0 mM cetiedil solution in 5 mM phosphate buffer with 150 mM NaCl with a final pH of 6.3.
- ^b For 7.0 mM cetiedil solution in 5 mM phosphate buffer with 150 mM NaCl with a final pH of 6.3.
- ^c The number in parenthesis means that the peak was either not integrable or not integrated. All spectra were taken at room temperature (22 ± 1 °C).

resonances of cetiedil in buffer and in membranes are shifted downfield compared to methanol and D₂O solvents. For the samples of cetiedil in buffer and in membranes, the ionic strength of the medium is much higher than that of water. Under high ionic strength conditions, the carbonyl carbon chemical shifts of esters have been shown to be shifted by up to ± 2.0 ppm (83). Compared to cetiedil in water (D₂O), the chemical shift of the carbonyl carbon (C-7) of cetiedil in buffer is shifted downfield by about 1.0 ppm (Table 4) and the chemical shift of cetiedil in membranes is shifted downfield by about 2.2 ppm (Table 6). Thus, the chemical shift changes of carbonyl carbon of cetiedil in buffer and in membranes are attributed to ionic strength effects. Overall, the conformation of the cetiedil molecules in the presence of membranes seems to be affected.

Figure 9 shows the linewidth correlation diagram of cetiedil carbons in solvents of different polarities and in membranes. For a particular carbon of cetiedil, the linewidth is broader in the presence of membrane compared to the other systems. The linewidths in general increase in the order: methanol < D₂O < buffer < membrane. For the thiophenyl carbons 2 and 4, the linewidths increase from about 2 - 3 Hz in methanol to about 7.5 Hz in membrane. For C-5 the increase is about 4 Hz, in going from methanol to membrane. For the cyclohexyl carbons (C-18 to C-23), the linewidth is in the range 14 - 18 Hz in membrane, compared to about 2 Hz in methanol. Similarly, for the azepinyl carbons, the linewidths are broader in membranes compared to methanol. In general, the linewidths of cetiedil carbons are broadened in the presence of membranes. In order to test whether the line broadening in the presence of membranes is due to viscosity effects, a sample of cetiedil in buffer with glycerol was prepared, with viscosity slightly

Figure 9. Linewidth correlation diagram of cetiedil carbons. Linewidths (Hz) of cetiedil carbons are plotted versus different solvent systems and membranes. Y-axis: 1 refers to membrane, 2 refers to glycerol, 3 refers to D₂O and 4 refers to methanol. Each plot corresponds to the assigned peaks in Table 5.

57



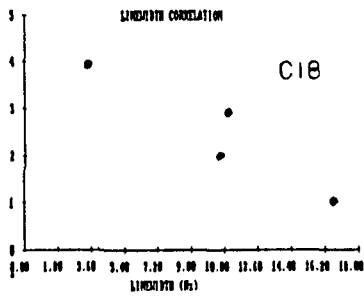
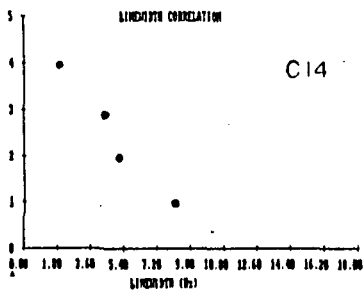
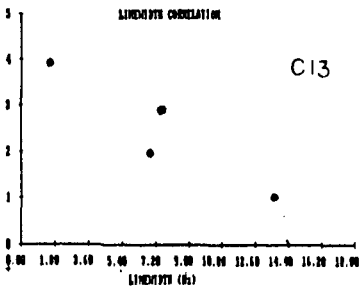
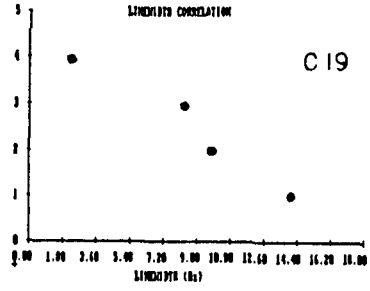
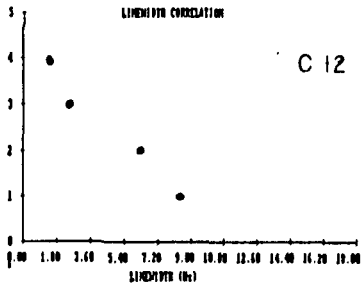


Table 6. Chemical Shift Differences of Cetiedil in Buffer and Membrane Compared to D₂O

<u>Carbon</u>	<u>Difference ($\delta - \delta_{D_2O}$) ppm</u>	
	<u>Buffer</u>	<u>Membrane</u>
2	0.65	0.59
3	0.86	0.73
4	0.90	0.75
5	0.81	0.72
6	0.81	0.69
7	1.01	2.21
9	0.85	0.73
10	0.81	0.77
12,17	0.89	0.74
13,16,20,22	0.82	0.68
14,15	0.85	0.74
18	0.81	0.72
19,23	0.80	0.71

greater than that of the membrane-cetiedil sample. If the line broadening observed in the case of membrane is simply due to viscosity effects, then the linewidths in the glycerol sample should be similar or larger than those in membrane. Since the linewidths in the glycerol sample is narrower than in the membrane samples, the linebroadening is probably due to the interaction of cetiedil with the membrane components and not because of the viscosity effects.

Analysing the linewidths of cetiedil carbons in the presence of membrane shows that the carbonyl carbon of the molecule is relatively less affected than the rest of the molecule (3.2 Hz increase), and the cyclohexyl and the thiophenyl carbons are affected more (5.5 - 13.5 Hz increase). This may be indicative of the involvement of the nonpolar regions of the molecule in the interaction with the membrane components. In the proton spectra, the effects were even more drastic. At very low membrane concentrations (cet/membrane molar ratio 5/1), the line broadening in the cetiedil proton resonances was very significant.

The presence of a single broad resonance for the peak means that the bound and the free molecules are probably in a fast exchange process (exchange rate greater than 10^5 to 10^{12} sec⁻¹) (43). A similar effect was also observed when the proton NMR spectra of cetiedil in buffer and cetiedil in the presence of membranes were compared. Thus, both carbon and proton spectra of cetiedil provided information about the parts of cetiedil molecule that were affected upon interaction with membranes.

IV.2.2 Cetiedil - Membrane Interaction

The free cetiedil concentration in the presence of membrane ghosts was determined with UV absorbance method on supernatant after centrifugation, as

discussed in section III.1.5. Figure 10 shows the concentration relationship between free cetiedil and total cetiedil added in the presence of 1.33 mg/mL membranes. The slope of the fitted line is 0.88. About 88 % of cetiedil remains in solution as free cetiedil. For example, at 5 mM cetiedil concentration, about 0.6 micromoles of cetiedil associate with 1.33 mg membranes or 1.6×10^8 cetiedil molecules per ghost (assuming 5.7×10^{-10} mg protein per ghost (68)), which is an enormous amount of cetiedil associated with membranes.

IV.2.3 Cetiedil Partitioning between the Membranous Lipid and Buffer Phases

IV.2.3.1 Absorption Spectral Changes Induced by Membrane Lipids

When DPPC vesicles were added to a solution of cetiedil (100 μ M) in buffer, some of the cetiedil molecules partitioned into the lipid phase. This produced a spectrum that included both the absorbance of cetiedil in buffer (with a maximum at 233 nm) and the absorbance of cetiedil in the lipid phase (with a maximum at a higher wavelength). The difference in the wavelength maxima for the two systems was too small for the two peaks to be resolved. Instead, the two peaks appeared as one with an increasing wavelength maximum on lipid addition. A plot of lipid concentration versus wavelength maximum (nm) is shown in Figure 11. After adding 90 μ M DPPC, the wavelength maximum shifted to 237 nm. In this range of lipid concentration, the extinction coefficient of cetiedil remained constant.

Next, the shift in wavelength maximum of cetiedil was followed after adding erythrocyte membrane. A similar shift in the wavelength maximum of

Figure 10. The relationship between the total and the free cetiedil concentrations in a membrane sample (1.33 mg/mL) in 5 mM phosphate buffer with 150 mM NaCl.

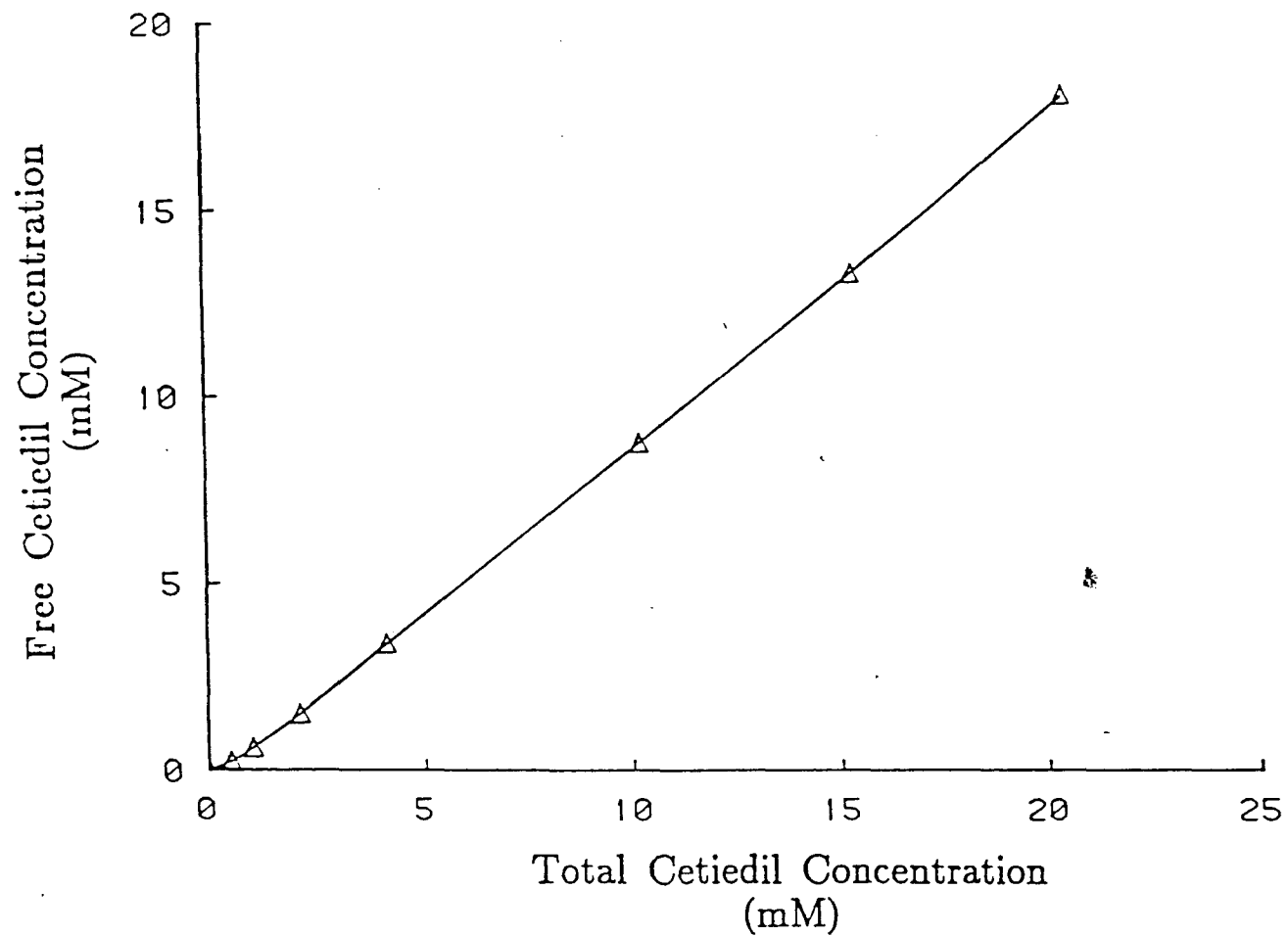
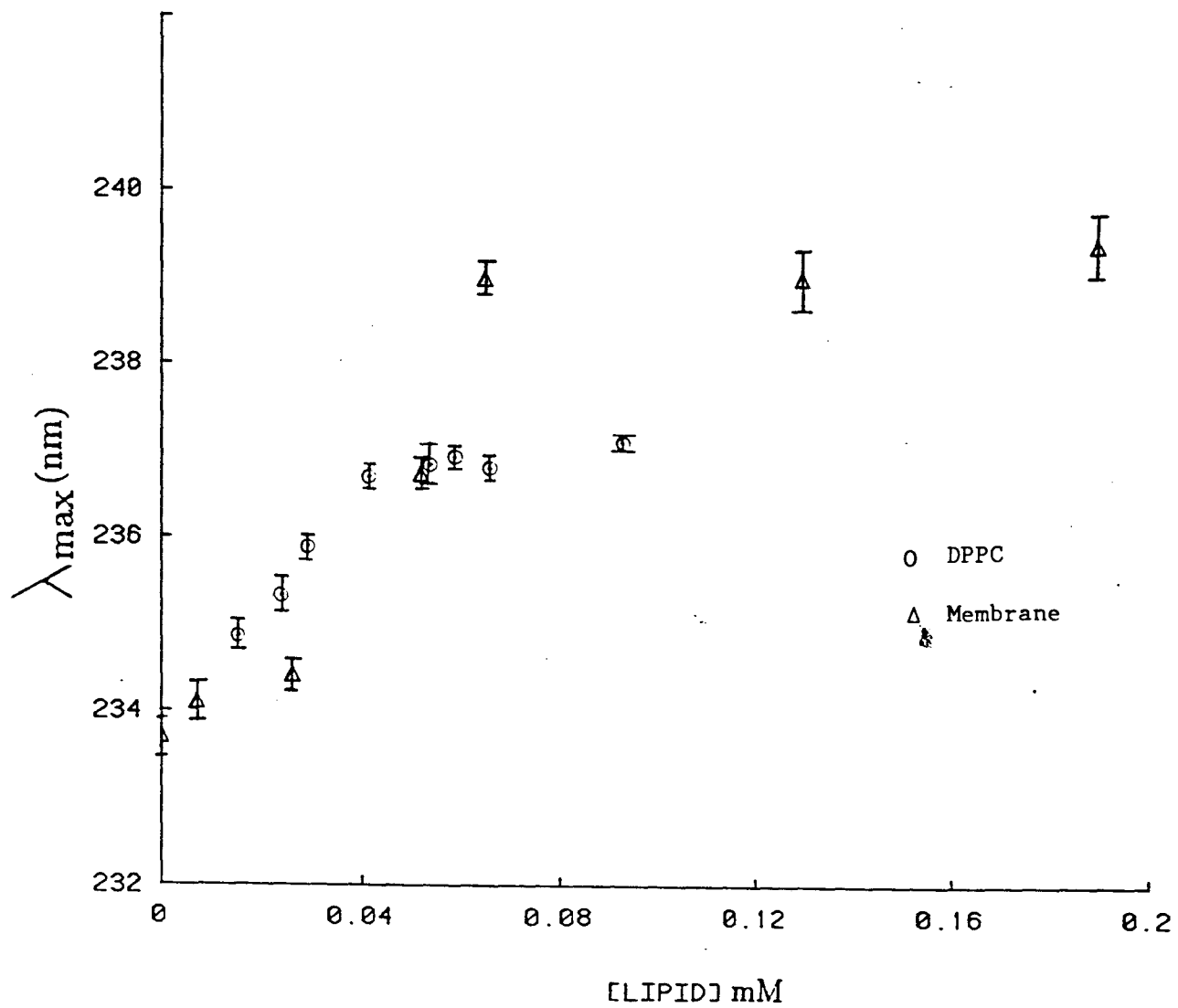


Figure 11. Plot of λ_{max} of 100 μM cetiedil versus lipid concentration. The spectra were scanned in the region 290 - 220 nm to determine the absorption maxima.



cetiedil was observed as in the case of DPPC vesicles. This suggested that the shift in the wavelength maximum of cetiedil in the presence of erythrocyte membranes was due to the partitioning of cetiedil in the lipid phase in membrane. An isosbestic point was observed at about 235 nm, which indicated that there were only two spectrally distinct forms of cetiedil. These forms were assumed to be the free form and the lipid associated form of cetiedil.

IV.2.3.2 Partition Coefficient of Cetiedil in Membrane Lipid

Figure 12 shows a typical difference spectral titration of 400 μM cetiedil with erythrocyte membrane lipids in 5P7.4/NaCl buffer at room temperature. As the lipid concentration increased, the spectral amplitude also increased, indicating increased partitioning of cetiedil into the membranous lipid phase (51). From the double reciprocal plot of $1/[\text{Lipid}]$ vs $1/A$ (Figure 13), K_p , the partition coefficient of 400 M cetiedil was determined as $3.51 \pm 0.85 \times 10^5$ ($n=5$ runs and 53 data points).

Using the K_p value of cetiedil, the number of molecules of cetiedil associated with the lipids can be calculated. Accordingly, the number of cetiedil molecules associated with 665 μM lipids (equivalent to 1.33 mg/ml protein concentration used to calculate bound cetiedil in section IV.2.2) was calculated as 3.8×10^8 . From the centrifugation method, under similar conditions, the number of cetiedil molecules bound to the membrane (both proteins and lipids) was calculated as 1.28×10^7 (Section IV.2.2).

The calculated number of cetiedil molecules associated with the lipid phase does not agree with the total number of cetiedil molecules associated with the membrane. Although the double reciprocal plot gave a good fit,

Figure 12. Difference spectral titration of 400 μ M cetiedil with human erythrocyte membranous lipids in 5 mM phosphate buffer with 150 mM NaCl, pH 7.4 at room temperature. Increasing size curves correspond to increasing lipid concentrations.

50

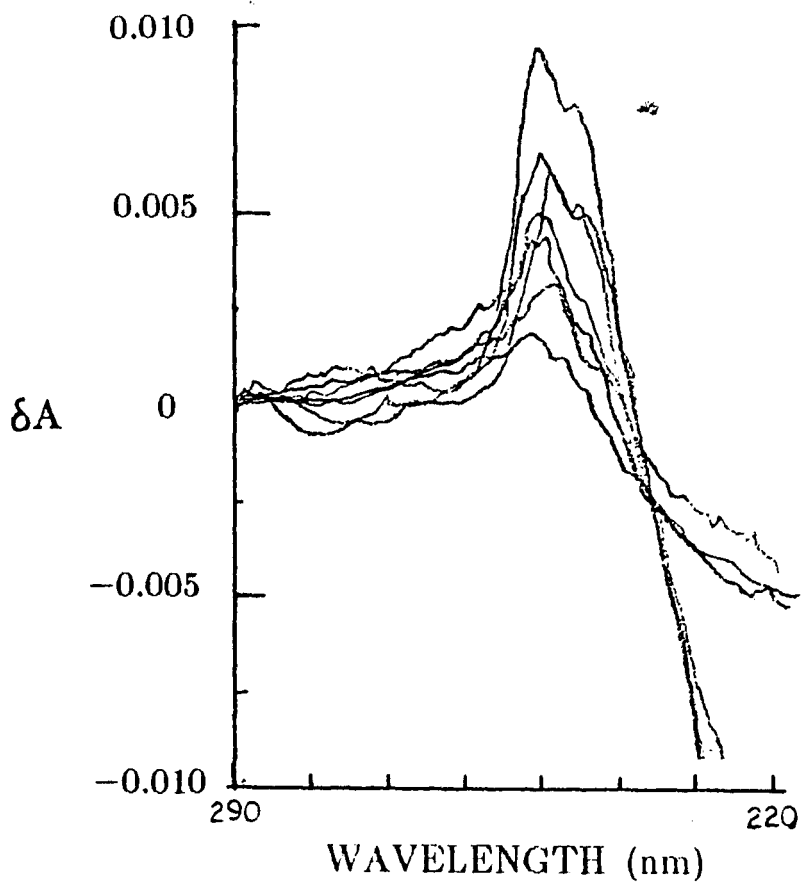
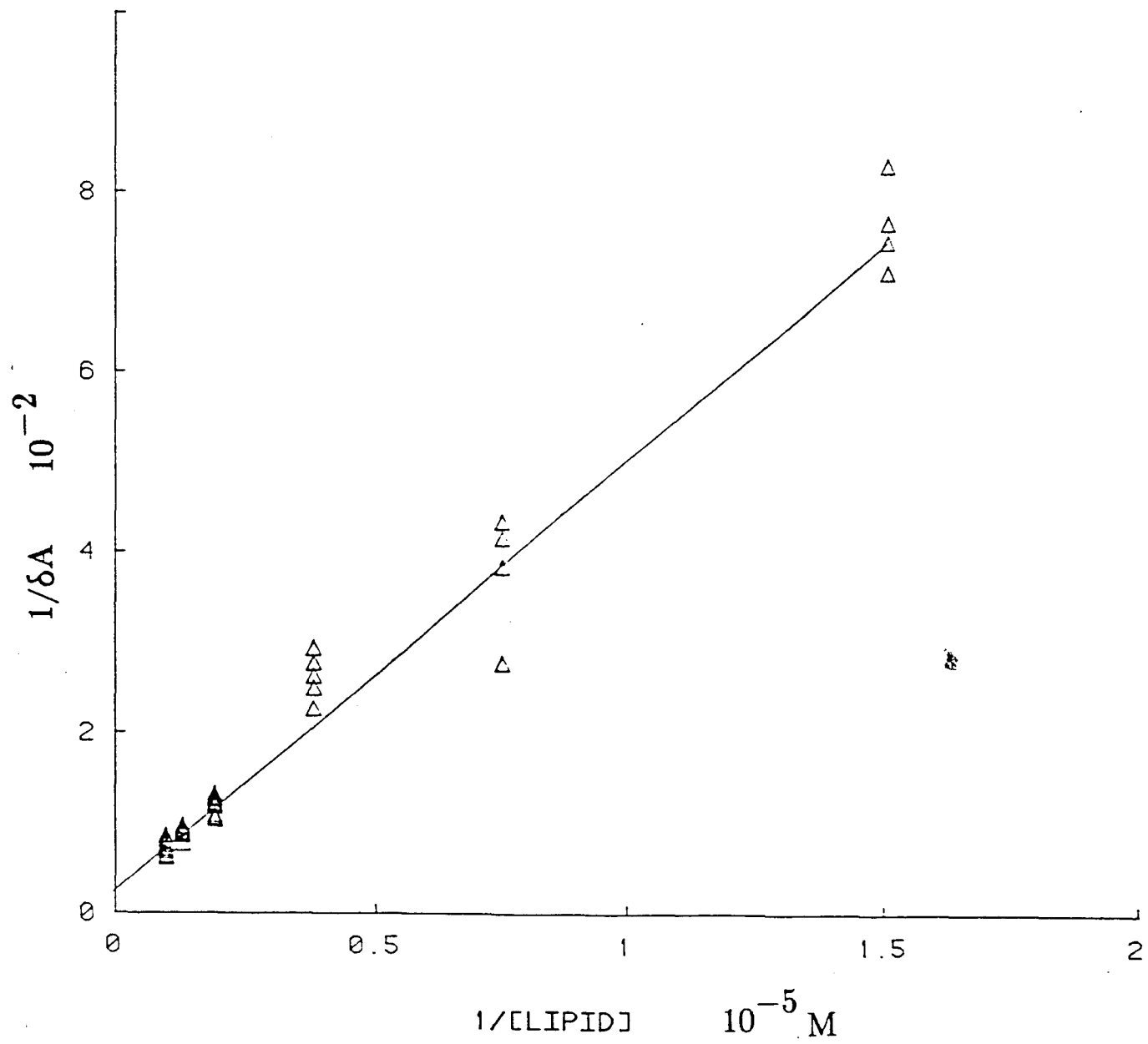


Figure 13. Double reciprocal plot of the UV difference data, $1/\delta A$ vs $1/[\text{Lipid}]$.



there is 24% error associated with the estimated K_p value. One of the possible sources of error in the K_p estimate is in the accuracy of the lipid concentration used in the spectral titrations. A 10% error in the lipid concentration significantly changes the slope and intercept of the double reciprocal plot, which in turn affects the K_p . With this variation in the lipid concentration, the K_p value is in the range 10^4 to 10^5 . If K_p is 10^4 rather than 3.5×10^5 , the calculated bound cetiedil would be 1.09×10^7 . Another source of error could be from the centrifugation method. Amphiphilic molecules such as chlorpromazine are known to solubilize membrane lipids (50). Since the centrifugation method is a separation technique, it is possible that some of the lipid - associated cetiedil may be in the supernatant. This would reflect as somewhat higher free cetiedil concentration in the aqueous phase. Thus, the value for the number of cetiedil molecules associated with the membrane lipids calculated from the partitioning experiments (10^7 to 10^8) is a maximum estimate. The number of cetiedil associated with ghosts is about 1×10^7 (probably an underestimate) and the number of cetiedil associated with Band 3 is about 2×10^6 . Thus most of the cetiedil that are associated with the ghosts are distributed among the lipid phase in the membrane.

IV.2.4 Effect of Cetiedil on Lipid Spin Label Mobility

The fatty acid spin probe, 5-doxyl stearate, intercalates amongst the lipid molecules in the membrane, with the nitroxide moiety of the 5-doxyl stearate located near the carbonyl group of phospholipid molecules, and has been used to monitor the behavior of the lipid molecules near the polar head groups (86). Although these spin probes are easy to use, there has been some criticism of their uses in membrane studies since the spectral data are often over

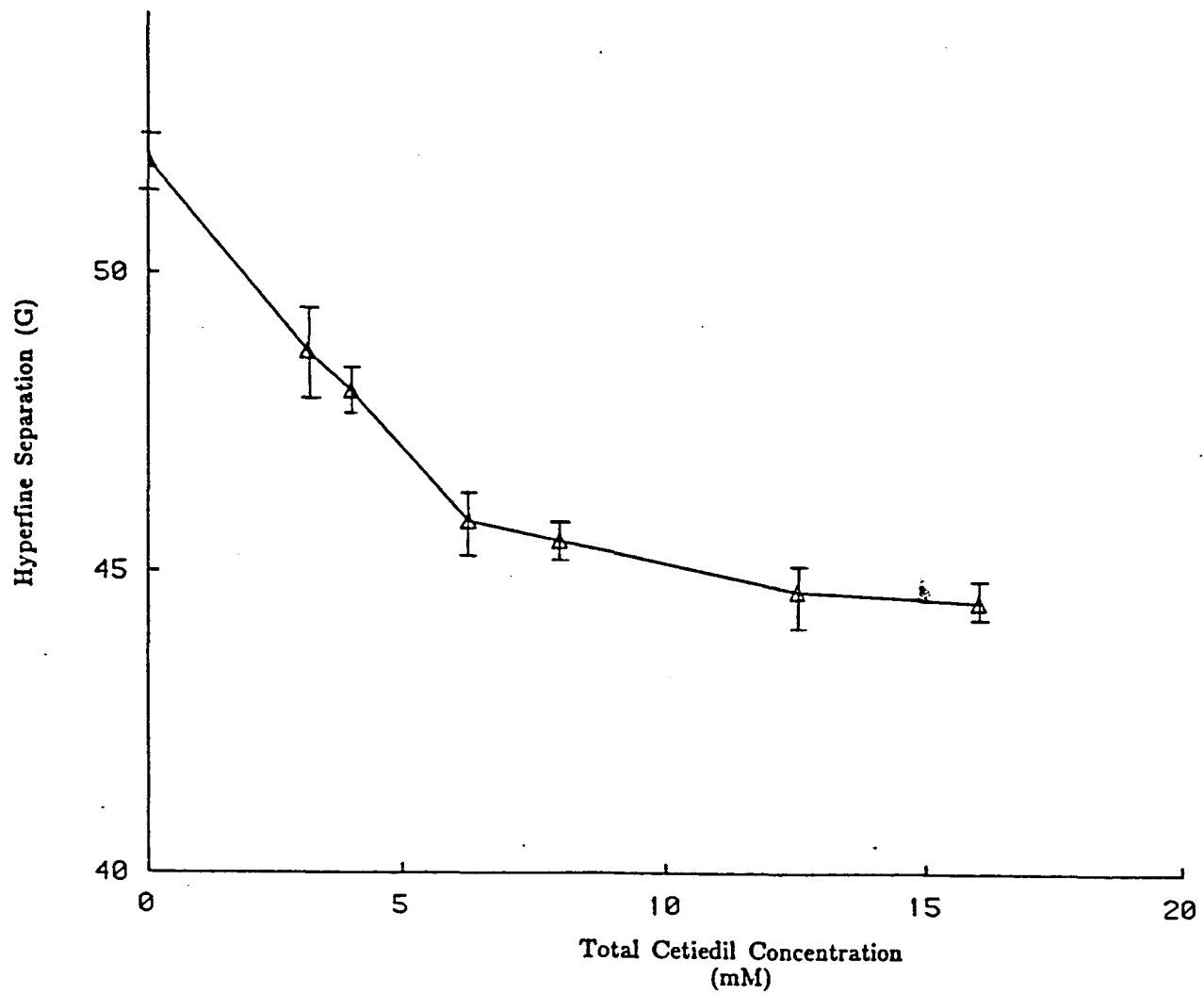
interpreted (87). In this study, the label was simply used to find out whether cetiedil affected the lipid component in membrane, and no attempt was made to obtain quantitative information on the dynamics of the lipid molecules. Figure 14 shows a plot of the hyperfine separation as a function of total cetiedil concentration in the membrane sample. As the concentration of cetiedil increased, the HFS values decreased indicating a change in the mobility or environmental polarity of the spin probe upon addition of cetiedil to the membrane. This change may be due to the effect of cetiedil on the organization of the lipid molecules. At a pH of about 6.3 (in 5P7.4/NaCl buffer) and 37 °C, the HFS values decrease from about 52 G to about 45 G when 10 to 15 mM cetiedil was present in the membrane sample that had a protein concentration of 2 mg/mL. The effect appears to level off at about 6 mM cetiedil. This suggests that the interaction of cetieil with the membrane lipids is a saturable process under the conditions of the present study.

IV.2.5 Effect of Cetiedil on Membrane Proteins

Mal-6 spin label was used to monitor the effect of cetiedil on membrane proteins of both normal and sickle cells. The Mal-6 spin labels alkylate primarily the sulfhydryl (SH) groups of the protein molecules (40). Our earlier finding shows that about 20 % of the erythrocyte membrane protein SH groups are alkylated by Mal-6, and about 80 % of the spin label intensity arises from label sites at the cytoplasmic membrane surface, with most of the spin labels attached to the peripheral proteins, the spectrin-actin complex (88), and one spin label to the Band 3 molecule. The amplitude ratio, W/S, of the EPR spectrum of Mal-6 labeled membranes is very sensitive to such experimental conditions as temperature, ionic strength and pH as well as to molecules

Figure 14. The effects of ceteil on the hyperfine separation of 5-doxyl stearate labeled erythrocyte membrane samples in 5 mM phosphate buffer with 150 mM NaCl at 37 °C.

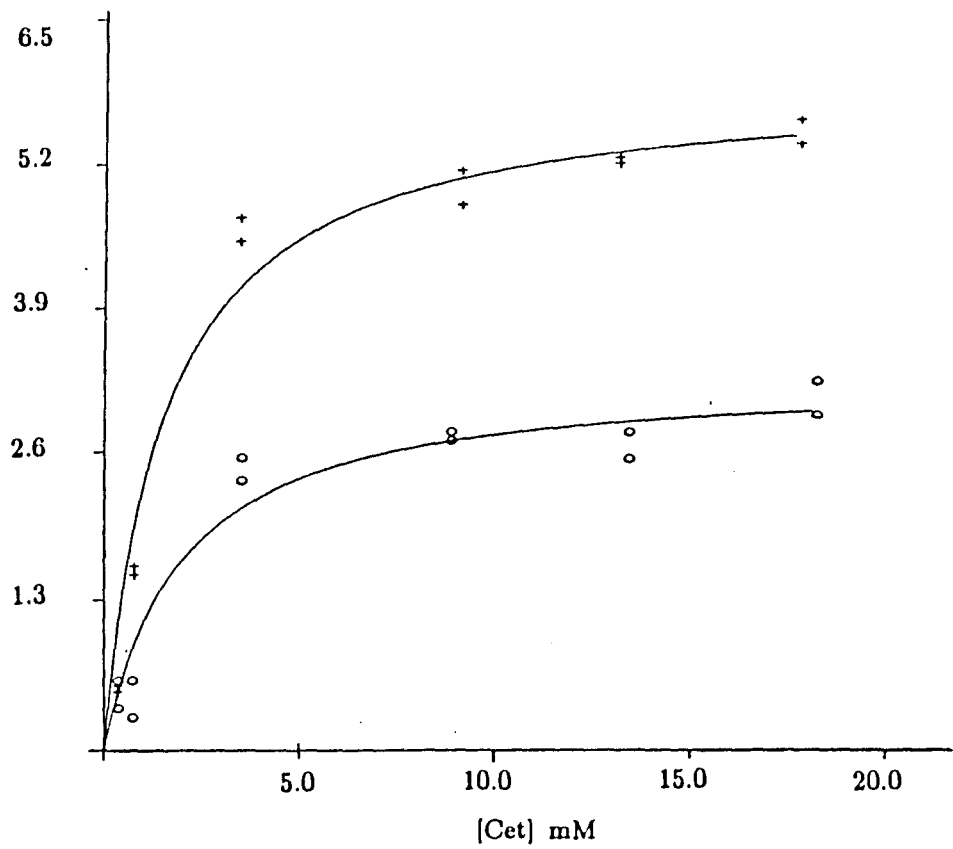
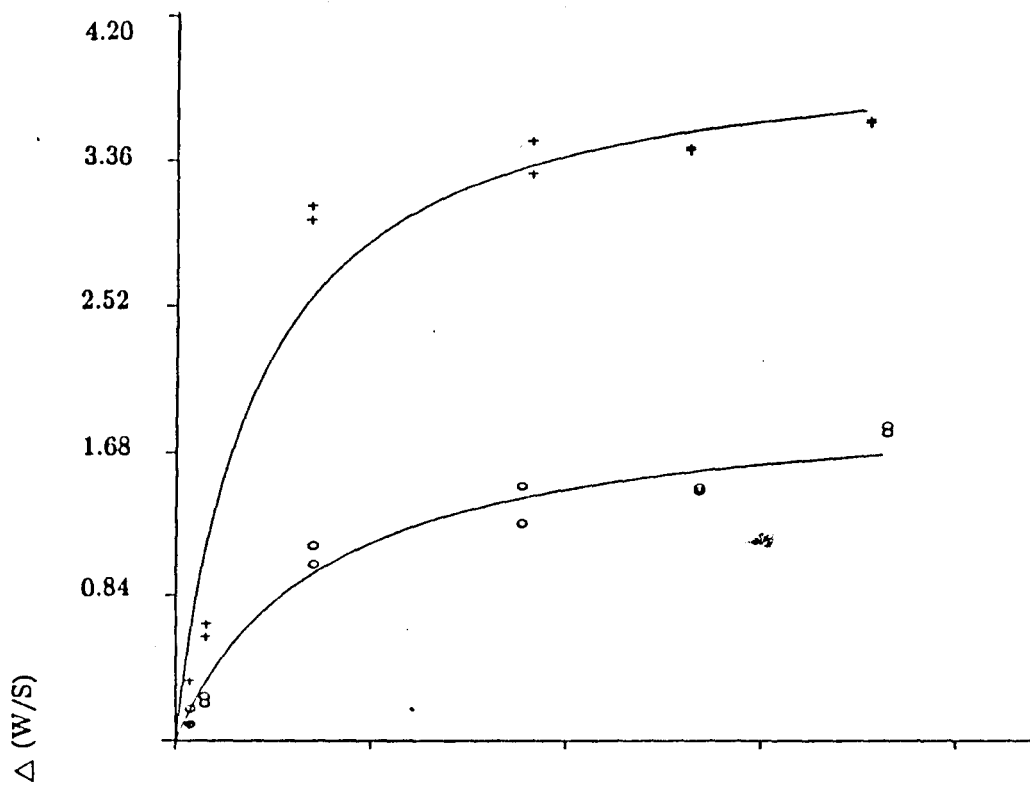
300



binding to the cytoplasmic surface of the membranes (40, 41). The W/S values of Mal-6 labeled membranes were measured, in the presence of various amounts of cetiedil in 5 mM phosphate buffer with 150 mM NaCl at 20 ° and 37 °C. As shown in Figure 15, the initial addition of cetiedil to both membrane and simplified membrane samples of normal cells gave a gradual increase in (W/S) at both 20 °C and 37 °C. The four curves shown in Figure 15 were qualitatively similar to each other. They demonstrated that the binding of cetiedil molecules to membranes caused immobilization of some of the spin labels on these membrane samples. In our previous studies, we have shown that changes in the W/S ratios can be directly related to the membrane binding process. The addition of bovine serum albumin, for example, causes no change in the W/S ratios, whereas the addition of hemoglobin causes the W/S values of membrane to decrease (40). The $\Delta(W/S)_{cet}$ values approached constant values at high concentrations of cetiedil, suggesting that the interaction of cetiedil with membrane proteins was a saturable process under the conditions we studied. Similar data were obtained on membranes from sickle cells at 37 °C.

We also interacted cetiedil with the spectrin-actin sample in 5P7.4/NaCl buffer, and monitored the W/S ratios of the spectrin-actin samples as a function of cetiedil added. Although we observed decreases in the W/S ratios, we also found protein aggregation upon addition of cetiedil, probably due to the acidity of cetiedil causing spectrin-actin precipitation. The pI of spectrin-actin is about 4.5. Thus little quantitative information was obtained by directly interacting spectrin-actin with cetiedil. We have found that the association of cetiedil with the erythrocyte membrane was reversible. The EPR signals of the membrane samples with and without cetiedil were first

Figure 15. Change in (W/S) of Mal-6 labeled erythrocyte membranes as a function of free cetiedil concentration in a typical run of paired samples of intact membrane (o) and simplified membrane (+) interacted with cetiedil at 20 °C (top panel) and 37 °C. The smooth curves are obtained by a nonlinear regression method using the equation discussed in the text.



measured. These samples were then dialyzed overnight in buffer solutions with buffer to sample ratio volume ratios of at least 1,000. The EPR signals of the dialyzed samples were measured again after dialysis. Both samples gave W/S ratios similar to that of the membrane sample without cetiedil before dialysis, indicating that the cetiedil - membrane interaction was non-covalent in nature, and did not cause irreversible changes in the erythrocyte membrane. This is in good agreement with the previous finding that the effect of cetiedil on the erythrocyte is reversible (29).

To obtain quantitative information on cetiedil and membrane binding, such as the apparent K_d values, from the W/S data, the free cetiedil concentration, $[C]$, in cetiedil - membrane mixtures, as shown in Figure 9 was used. After substituting $[C]$ and $(W/S)_{cet}$ into Equation 5, K_d , n and $\Delta(W/S)_{\infty}$ could be obtained. The n values obtained from these data, both by non-linear regression methods and by the Hill plot were all about 1, indicating that a simple two-state model with multiple independent binding sites that we have previously used was adequate to describe the binding of cetiedil to membrane proteins.

Table 7 shows the values of apparent K_d , $\Delta(W/S)_{\infty}$ and $C_{1/2}$ for cetiedil - membrane, cetiedil - simplified membrane systems at 20 °C and 37 °C. All the K_d values are about 2 mM. The half saturation concentration ranges from 1 to 3 mmoles cetiedil per gram membrane proteins.

By using the protein spin label, Mal-6, cetiedil was shown to bind to membranes as well as to simplified membranes (Figure 15). Direct comparison

Table 7. Equilibrium Binding Parameters in 5 mM Phosphate Buffer with 150 mM NaCl at pH 6.3

<u>Sample</u>	$\Delta(W/S)_{\infty}$	$K_d+S.D.(mM)$	$C (\mu M/ g)$	<u>N</u>	<u>t</u>	p^*
<u>20° C</u>						
Membrane	1.92±0.15	2.95±0.64	2.5	7	3.186	<0.02
Simplified Membrane	3.34±0.57	1.89±0.27	1.1	7		
<u>37° C</u>						
Membrane	3.06±0.43	2.34±0.74	1.4	7	2.682	<0.05
Simplified Membrane	5.30±0.85	1.57±0.56	0.9	7		

* The p values were obtained from paired sample student t-test by null-hypothesis.

of the averaged K_d values of the membrane and the simplified membrane samples in Table 7 indicated a slightly lower K_d values for the simplified membrane samples than those for intact membrane samples. However, a paired sample Student's t-test of the K_d values indicated that the differences in the K_d values between membrane and simplified membrane samples were not statistically significant either at 20 °C ($p < 0.02$) or at 37 °C ($p < 0.05$), as shown in Table 7. Removal of the spectrin-actin network from the membrane thus did not significantly affect the binding of cetedil to erythrocyte membrane. The spectrin-actin network is the major component in maintaining the shape of the erythrocyte. The lack of interaction between cetedil and the spectrin-actin network, as observed by EPR data, suggested that the action of cetedil in returning sickle to normal shapes was not accomplished by modifying the spectrin-actin network in sickle cells. Other studies indicate that cetedil inhibits calmodulin-stimulated calcium ATPase activity (34). Calmodulin is present in the erythrocyte, but does not appear to bind to spectrin molecules (89, 90). These findings are consistent with our EPR data.

The simplified membrane sample consists of lipid bilayer and Band 3 protein and other proteins, including ATPases (91). However, the major protein component is the Band 3 molecule. Most of the protein spin labels, if not all, in the simplified membranes are on the Band 3 molecules. Therefore our data suggested interaction of cetedil with the Band 3 proteins in membranes, with an apparent K_d of about 2 mM at 37 °C. However, these results did not exclude the interaction of cetedil with other minor proteins in the simplified membranes. The spin label EPR approach will not be sensitive enough to detect such interactions. Additional information on the partitioning of cetedil in membranes will provide quantitative information on the concentrations of

cetiedil interacting with individual membrane components.

Band 3 is an anion transport protein (92), and may have a role in the membrane to regulate water movement in erythrocyte (93-96). More detailed studies of interactions between cetiedil and Band 3 molecules and interactions between cetiedil and ATPases, for example, may provide insight toward understanding its various drug actions in affecting erythrocyte water contents and Na^+ and K^+ movements across cell membranes.

Since Band 3 seems to be the major protein that interacts with cetiedil, the K_d value of cetiedil-simplified membrane interaction (Table 7) can be used to calculate the number of cetiedil (C) molecules bound to the membrane proteins (P) under the equilibrium conditions, $\text{P} + \text{C} \rightleftharpoons \text{PC}$. From this equation and using the value of K_d , PC, the equilibrium concentration of bound cetiedil was evaluated. Accordingly, at equilibrium, at 400 M cetiedil concentration, the number of cetiedil molecules associated with the membrane proteins was calculated to be 2.06×10^5 ($\text{PC} = (1/K_d)/\{([P] - [\text{PC}]) - ([C] - [\text{PC}])\}$, where P and C are the initial concentrations of protein and cetiedil, respectively). Comparing this value with the number of cetiedil molecules associated with the membrane lipids showed that cetiedil preferentially associated with the membrane lipids than with the proteins.

IV.2.6 Effect of cetiedil on Water Transport across Red Cell Membranes

Treatment of normal RBC with 390 μM cetiedil increases the hematocrit value of the RBC samples from 60.3 to 67.7 % (Table 8). This indicates that there is an increase in hematocrit value of the samples by 12.3 %. The cell volume of normal control samples was $(9.6 \pm 0.2) \times 10^{-11}$ mL and that of the samples treated with cetiedil was $(10.6 \pm 0.2) \times 10^{-11}$ mL. For sickle cells, the cell volume of the control samples was $(11.4 \pm 0.8) \times 10^{-11}$ mL and that of

Table 8. Effect of Cetiedil on the Hematocrit Values of RBC

<u>Sample</u> ¹	<u>RBC</u>	<u>RBC + Cetiedil</u>	<u>SRBC</u>	<u>SRBC + Cetiedil</u>
<u>Hematocrit</u>				
Before Incubation	36.7±0.5	36.7±0.5	--	--
After Incubation at 37 °C for 2 hours.	36.7±0.5	41.7±0.5	--	--
NMR Sample	60.3±1.0	67.7±1.0	55.0±1.0	63.5±0.5
Cell Volume (10 ⁻¹¹ mL)	9.6±0.2	10.6±0.2	11.4±0.8	12.7±0.9

¹ See section III.1.6

cells treated with cetiedil was $(12.7 \pm 0.9) \times 10^{-11}$ mL (Table 8). Thus cetiedil increased cell volume by 10.4 % for normal cells and 11.4 % for sickle cells, in good agreement with published values of 10 % (24).

Table 9A gives the results of the NMR relaxation measurements of both normal and sickle cells. All the relaxation measurements were performed, as mentioned in the Methods section, on the 200 MHz spectrometer. Measurements of normal cells were made on different batches of samples, whereas for sickle cells, the sample was from a single patient. Hence, the statistics for the comparison of normal and sickle cells would only be qualitative at best.

The relaxation time of water protons decreased for both normal and sickle cells, after treatment with 390 μ M cetiedil. The T_2 of normal cells is 0.168 ± 0.0165 sec and that for the sickle cells is 0.056 ± 0.003 sec. The T_{ex} value of normal control cells is 0.0247 ± 0.0028 sec whereas for sickle cells is 0.0529 ± 0.0036 sec. The paired sample Student's t-test of the relaxation times of normal and sickle cells showed that the difference in the relaxation times is significant ($p < 0.0001$) (Table 9B). After incubating the samples with cetiedil, the T_2 of normal cells decreased to 0.152 ± 0.0093 sec and that for the sickle cells decreased to 0.0442 ± 0.0022 sec. The difference between the decreased T_2 values for both normal and sickle cells was also found to be statistically significant. Similarly comparing the T_{ex} values of both normal and sickle cell samples before and after treatment with cetiedil showed a significant decrease in the exchange times after addition of cetiedil (Table 9A and 9B). A decrease in the exchange time of water would mean an increase in the water permeability (Equation 17). Water permeability of sickle cells was significantly less than that of normal cells, as shown by Student's t-test ($p < 0.001$). The

Table 9A. Effect of Cetiedil on the Water Exchange Time across RBC

Sample	T₂(s)	T_{ex}(s)	P_w(cm/s)	N
RBC	0.1680 ±0.0165	0.0247 ±0.0028	0.00281 ±0.0003	8
RBC w/Cet	0.1520 ±0.0093	0.0152 ±0.0018	0.0050 ±0.0006	8
Sickle	0.0560 ±0.0028	0.0529 ±0.0036	0.00155 ±0.0001	4
Sickle w/Cet	0.0442 ±0.0022	0.0393 ±0.0023	0.00232 ±0.0001	4

→

Table 9B. t and p Values of Student's t- test of paired samples on Data Given in Table 9A

		RBC & RBC+Cet	SRBC¹ & SRBC+Cet	RBC & SRBC	RBC+Cet & SRBC+Cet
T₂	t	5.25	26.36	5.51	5.88
	p	0.0006	0.0001	0.0004	0.0002
T_{ex}	t	5.53	17.10	4.71	6.17
	p	0.0004	0.0001	0.0011	0.0002

¹ SRBC refers to sickle RBC.

p values were obtained from paired sample Student's t-test by null- hypothesis.

diffusional water permeability of normal control cells was 0.00281 ± 0.00029 cm/sec and that for sickle cells was 0.00155 ± 0.00011 cm/sec, at 37 °C. Treatment of sickle cells with cetiedil however, seemed to enhance the permeability. The permeability of cetiedil-treated sickle cells was comparable to that of normal control cells. The diffusional permeability of normal cells after incubating with cetiedil was 0.00504 ± 0.00059 cm/sec and for the sickle cells was 0.00232 ± 0.00014 cm/sec. Comparison of the permeability values showed that addition of cetiedil to RBC significantly enhances the water permeability of membranes ($p < 0.001$).

As indicated by previous studies (24), an increase in the cell volume of RBC was observed after treatment with 390 μ M cetiedil (10.4 % for normal cells and 11.4 % for sickle cells). This increase in cell volume was attributed to the increase in cell sodium and cell water contents (29).

The observed decrease in the relaxation time of water in RBC treated with 390 μ M cetiedil indicates a change in the water environments upon addition of cetiedil. A similar examination of the water exchange times also indicated that water exchange was faster in the presence of cetiedil in both normal and sickle cells. Therefore, cetiedil seems to facilitate the water movements across red blood cell membranes in both cases.

The NMR data showed that the exchange time for sickle cells is greater than that of normal cells. This means that the exchange rate of water in sickle cells is slower compared to normal cells. Previous studies, using a three-state model for cell water, comparing the correlation times of water in the sickle and normal cells indicated that there were more bound water molecules in sickle cells than in normal cells with the correlation time of water molecules of sickle cells greater (10^{-6} sec) than that of normal cells

(10^{-9} sec) (97,98). Osmotic permeability studies on sickle and normal cells showed reduced water permeability in sickle cells (99). Decreased osmotic or diffusional water permeability of sickle cells is being speculated as being due to increased amounts of sickle hemoglobin bound to the cell membrane which affect the aqueous channels that transport water across the membranes (100, 101). Fung and coworkers have shown that sickle hemoglobin has a higher affinity toward membrane surface than does normal hemoglobin (102). The altered ion and water transport in sickle cells are also attributed to permanent changes in the sickle cell membrane such as irreversibly modified membrane proteins (9), and increased amounts of bound intracellular calcium (7), compared to the normal membranes. Thus, the decreased diffusional water permeability of sickle cell membranes observed in the present study may be due to the bound water molecules inside the sickle cells in addition to the above-mentioned membrane abnormalities.

There seems to be some correlation between the cell volume increase and the corresponding permeability increase, upon addition of cetiedil. Cetiedil has been shown to increase cell sodium and cell water contents. At $300 \mu\text{M}$ cetiedil concentration Schmidt and coworkers observed a 11 % increase in the cell water (28). From the hematocrit measurements of the normal RBC samples, comparison of the volume of water inside the cells indicated a 12.3 % increase after incubating the cells with $395 \mu\text{M}$ cetiedil, at 37°C for 2 hours. The hematocrit value increased from 60.3 before incubation to 67.7 after incubation. Similarly, for sickle cells, the increase in water content inside the cells after incubating with cetiedil was 15.5 % (Table 10).

In order to correlate the increase in water content inside the cells with the changes in the relaxation behavior of water, the echo amplitude of the

water before and after incubating the cells with cetiedil was measured. The packed cells were used for this purpose, since the echo amplitude represented mainly the contribution from intracellular water. For normal cells, there was a 12.3 % increase in the echo amplitude after incubating the cells with cetiedil, which is the same as the increase measured from the hematocrit values. For sickle cells, the increase in the echo amplitude was 28.7 %, compared to 15.5 % increase from the hematocrit values (Table 10). The source of the discrepancy between these two values is not known. These increases in amplitudes for both normal and sickle cells suggested that the water content of the cells increased after incubating with cetiedil.

Water transport across the red cell membranes is usually explained in terms of "channels" or "pores" (94 - 96). Although the mechanism of water transport is far from clearly understood, the presence of aqueous channels at the interface between the Band 3 subunits has been suggested (95). Water transport by "leak" pathway (diffusion through lipids) also has been suggested and observed (66). For the present study, the "composite" diffusional permeability (both channel as well as leak) was measured. The increase in the diffusional permeability of the membranes to water after incubating with cetiedil suggests that these pathways are affected.

Table 10. Effect of cetiedil on the cellular water content

<u>Sample</u>	<u>W_i^1</u> (mL)	<u>% increase²</u>	<u>A³</u>	<u>% Increase⁴</u>
RBC	0.603 ±0.010		485.74 ±54.33	
		12.3		12.3
RBC w/Cet	0.677 ±0.010		545.46 ±14.45	
Sickle cells	0.550 ±0.010		206.59 ±4.47	
		15.5		28.7
Sickle Cells w/Cet	0.635 ±0.005		265.88 ±5.32	

¹ W_i is water inside the cell (mL)
See section III.1.6 for sample volume measurements.

² % increase = $[W_i (\text{Cell} + \text{Cet}) - W_i (\text{Cell})] / W_i (\text{Cell})$

³ Echo amplitude measured in arbitrary units.

⁴ % Increase = $[A (\text{Cell} + \text{Cet}) - A (\text{Cell})] / A (\text{Cell})$

V. CONCLUSIONS

Optical data of cetiedil show that it has a maximum absorption at 233 nm with an E_{233} of $2796 \text{ M}^{-1} \text{ cm}^{-1}$. Cetiedil citrate molecule at high concentration is quite acidic, and forms micelles. The critical micelle concentration of cetiedil in phosphate buffer with 150 mM NaCl is about 8.8 mM.

Conformational studies of cetiedil in D_2O using ^{13}C NMR spectroscopy, show that the cyclohexyl moiety of cetiedil is in the chair conformation. The study also indicates that the molecule seems to undergo an overall conformational change as the polarity and the ionic strength of the solvent change. ^1H NMR studies of cetiedil show that at concentrations above 7 mM, cetiedil exists as an equilibrium mixture of, possibly, monomers and aggregates.

^{13}C and ^1H NMR data of cetiedil in the presence of membranes show that the molecule may have a preferred orientation in the membranes. Cetiedil resonances in general are broader in the presence of membranes. The carbonyl carbon of cetiedil is relatively less affected than the rest of the molecule. The linewidth of the carbonyl carbon increases by 3.2 Hz in the presence of membranes compared to 5.5 - 13.5 Hz increase for the remaining carbon atoms in the molecule. This may suggest that the nonpolar regions of the molecule are more involved with the membrane components than the polar regions.

This study shows that a large amount of cetiedil may associate with membranes. The partition coefficient of 400 μM cetiedil in the membrane lipids at 23 °C and pH 7.4 is about $10^4 - 10^5$ and the free energy of transfer from the aqueous phase to the membranous lipid phase is about -7.5 kcal/mol at 23 °C.

Cetiedil seems to associate preferentially with the membrane lipids rather

than with the membrane proteins. From the partition coefficient of cetiedil into the membrane lipids, $10^7 - 10^8$ cetiedil molecules are found to be associated with the lipids. The partitioning properties of cetiedil are comparable to those of the amphiphilic amines such as chlorpromazine and methochlorpromazine. Their pharmacological properties (tranquilizing) have been correlated with their membrane solubility, but the mechanism of drug action is not clearly understood. The amphipathic agents are likely to act in four general ways (103); (1) physical expansion of a lipid bilayer leaflet with the displacement or disruption of existing structural lipids and lipid domains (104,105); (2) capture or replacement of essential or regulatory lipids needed for protein function or cell regulation such as polyphosphoinositides (106); (3) disruption of the membrane permeability barrier, such as facilitated ion diffusion or channel formation (107); and (4) inhibition of the membrane protein function by direct modification or damage (108).

The EPR data show that the drug interacts with the membrane proteins, and the binding is saturable and reversible. The half saturation concentration for binding is in the range of 1 - 3 mmoles cetiedil per gram membrane proteins at physiological temperature. The equilibrium dissociation constant for membranes is about 2 mM at pH 6.3 and 37 °C. Removal of spectrin-actin from the membrane does not appear to affect the binding properties of cetiedil significantly, indicating that the spectrin-actin network is not involved in the mechanism of drug action. The results suggest the existence of an interaction between cetiedil and Band 3 molecules, with an equilibrium dissociation constant of about 2 mM. From the equilibrium dissociation constant of cetiedil obtained from the EPR measurements, about 2×10^5 cetiedil molecules are found to be associated with the membrane proteins. Thus the interaction of cetiedil with

membrane proteins is relatively weak compared to its interaction with the lipids. Our results suggest that at 400 μM concentration, cetiedil molecules distribute in the membrane lipids and proteins and would exist as monomers. At this level, cetiedil does not alter the blood pH, which is in very good agreement with the published studies on the metabolic action of cetiedil (23).

The EPR data also show that cetiedil affects the mobility of the spin labels that intercalate amongst the head groups of the lipid molecules in the membrane. The hyperfine separation (HFS) of the spin label decreases as the concentration of cetiedil increases, and tends to level off about 6 mM cetiedil concentration. The HFS data suggest that cetiedil affects the organization of the membrane lipids.

Cetiedil also has been found to affect the calcium-dependent calmodulin interactions with the membranes (33). The protein spin label EPR data from the present study show that cetiedil interacts with the membrane proteins and lipids. NMR studies, under the same conditions of cetiedil/membrane concentration ratio, temperature and pH, show that cetiedil may have a preferred orientation upon interacting with the membrane components.

In summary, cetiedil seems to exert its action by partitioning preferentially into the membranous lipid phase as well as interacting with the membrane protein Band 3.

Further studies of the interaction of cetiedil with the isolated membrane components such as Band 3 molecules and ATPases, may provide insight toward understanding its various drug actions in affecting the sodium and potassium movements across the cell membranes.

Incubation of normal as well as sickle cells with 390 μM cetiedil at 37 $^{\circ}\text{C}$ for 2 hours increases the hematocrit of the samples. The cell volume of the

normal cells increased by 10.4 % and that of sickle cells increased by 11.4 %. Due to the presence of more bound water molecules inside the sickle cells compared to normal cells, our NMR relaxation data of water protons of both normal and sickle red cells which show that the water molecules in sickle cells exchange slower with the water molecules outside than the normal cells are in good agreement with previous studies (99). The diffusional water permeability of sickle cells is significantly less than that of normal cells. Treatment of both normal and sickle cells with 390 μM cetiedil significantly decreases their exchange times to increase their diffusional permeability to water. At 37 °C, the permeability of normal cells is 0.0028 cm/sec, and in the presence of cetiedil, this permeability increases to 0.0051 cm/sec. For sickle cells, the permeability is 0.0016 cm/sec, a value much less than that of the normal cells. In the presence of cetiedil, the permeability is increased to 0.0023 cm/sec, a value more similar to that of normal cells. The increase in the diffusional water permeability in the presence of cetiedil is suggested to be due to the effect of cetiedil on the membrane proteins and lipids. The NMR method, however, does not distinguish between the protein and the lipid pathways of water transport. Water transport by leak pathway has been studied in the vesicles formed from the extracted membrane lipids (109). A similar study in the presence and absence of cetiedil might prove useful to determine the effect of cetiedil on the diffusion of water through the lipid bilayers.

BIBLIOGRAPHY

1. F.I.D. Konotey-Ahulu, (1974). The Sickle Cell Diseases: Clinical Manifestations including the "Sickle Crisis", Arch. Intern. Med., 133, 611-619.
2. J. Dean and A.N. Schechter (1978). Sickle-Cell Anemia: Molecular and Cellular Bases of Therapeutic Approaches, New Eng. J. Med., 299, 752-763.
3. G.R. Serjeant, (1974). The Clinical Features of the Sickle Cell Disease. Elsevier.
4. D.C.E. Tosteson, E. Carlson, and E.T. Dunham (1952). The Effect of Sickling on Ion Transport, J. Clin. Invest., 31, 406-411.
5. B.E. Glader, and D.G. Nathan, (1978). Cation Permeability Alterations during Sickling: Relationship to Cation Composition and Cellular Hydration of Reversibly Sickled Cells, Blood, 51, 983-989.
6. J.W. Eaton, T.D. Skelton, H.S. Swofford, C.E. Kolpin, and H.S. Jacob, (1973). Elevated Erythrocyte Calcium in Sickle Cell Disease, Nature (London), 246, 105-106.
7. L.R. Berkowitz, and E.P. Orringer, (1981). The Effect of Cetiedil, an In Vitro Antisickling Agent, on Erythrocyte Membrane Cation Permeability, J. Clin. Invest., 68, 1215-1220.
8. L.R. Berkowitz, and E.P. Orringer, (1985). Passive Sodium and Potassium Movements in Sickle Erythrocytes, Am. J. Physiol., 249, C208-C214.
9. C. Brugnara, H.F. Bunn, and D.C. Tosteson, (1986). Regulation of Erythrocyte Cation and Water Content in Sickle Cell Anemia, Science, 232, 388-390.
10. J. DeSimone, P. Heller, L. Hall and D. Zwiers, (1982). 5-Azacytidine

- Stimulates fetal Hemoglobin Synthesis in Anemic Baboons. Proc. Natl. Acad. Sci., 79, 4428-4431.
11. H. Chang, S. M. Ewert, R.M. Bookchin and R.L. Nagel, (1983). Comparative Evaluation of Fifteen Antisickling Agents, Blood, 61, 693-704.
 12. A. Cerami, J.M. Manning (1971), Potassium Cyanate as an Inhibitor of the Sickling of Erythrocyte in vitro, Proc. Natl. Acad. Sci. USA, 68, 1180-1183.
 13. E. Elbaum, E.F. Roth, G. Neuman, E.R. Jaffe, R.L. Nagel (1976), Molecular and Cellular Effects of Antisickling Concentrations of Alkylureas, Blood, 48, 273-287.
 14. R.M. Nalbandian, G. Schultz, and J.M. Lusher, (1971). Sick Cell crisis Terminated by Intravenous Urea in Sugar Solutions- A Preliminary Report, Am. J. Med. Sci., 261, 309-324.
 15. C.T. Naguchi and A.N. Seechter: Inhibition of Sick Hemoglobin Gelation by Amino Acids and Related Compounds (1978), Biochemistry, 17, 5445-5459.
 16. G.J. Brewer, L.F. Brewer and A.S. Prasad (1977), Suppression of Irreversibly Sickled Erythrocytes by Zinc Therapy in Sick cell Anemia, J. Lab. Clin. Med., 90, 549-554.
 17. R. Backer, D. Powers, L.J. Haywood (1974), Restoration of the Deformability of Irreversibly Sickled Cells by Procaine Hydrochloride, Biochem. Biophys. Res. Commun., 59, 548-556.
 18. M. Linquette, P. Fossati, and G. Luez, (1973). Interet Therapeutique d'une Nouvelle Medication Antiischemique et Vaso-regulatrice: Le Cetiedil, Lille Med. Acutal., 18, 1303-1312.
 19. J.A. Simaan and D.M. Aviado, (1976). A Comparative Study between the

- Cardiovascular Effects of Cetiedil, a New Vasodilator, and Papaverine and Aminophylline, *J. Pharmacol. Exp. Ther.*, 198, 176-186.
20. W.R. Kukovetz and G. Poch, (1970). Inhibition of Cyclic 3', 5'-Nucleotide-Phosphodiesterase as a Possible Mode of Action of Papaverine and Similarly Acting Drugs, *Naunyn-Schmiedebergs Arch. Pharmacol.*, 267, 189-194.
 21. D.M. Aviado, (1975). Peripheral Vasodilators, *Drug Inform. J.*, 36-40.
 22. J.R. Bossier, M. Arousseau, J.-F. Giudicelli, and D. Duval, (1978). Pharmacological Findings on Cetiedil, *Arzneim.-Forsch./Drug Res.*, 28 (II), 2222-2228.
 23. A. Yamaguchi, T. Asakura, K. Tanoue and H. Yamazaki, (1985). Effect of Cetiedil on Platelet Aggregation and Thromboxane Synthesis, *Thromb. Res.*, 37, 391-400.
 24. T. Asakura, S.T. Ohnishi, K. Adachi, M. Ozguc, K. Hashimoto, M. Singer, M.O. Russell and E. Schwartz (1980), Effect of Cetiedil on Erythrocyte Sickling: New Type of Antisickling Agent that may Affect Erythrocyte Membranes. *Pro. Natl. Acad. Sci. USA.*, 77, 2955-2959.
 25. R. Cabannes (1977), Preliminary Study on the Effects of Cetiedil in Acute Episodes of Sickle Cell Anemia, Presented at Sickle Cell Conference, Washington D.C.
 26. L.J. Benjamin, G. Kokkini and C.M. Peterson (1980), Cetiedil: Its Potential Usefulness in Sickle Cell Disease. *Blood*, 55, 265-270.
 27. G.P. Lewes and Y.W. Cho (1982), Tolerance of Healthy Adult Males in Intravenous Infusion of Cetiedil, a Vasoerythroactive Drug. *J. Clin. Pharmacol. (USA)*, 22, 243-249.
 28. W.F. Schmidt, T. Asakura and E. Schwartz (1982), The Effect of

- Cetiedil on Red Cell Membrane Permeability. *Blood Cells*, 8, 289-298.
29. W.F. Schmidt, T. Asakura and E. Schwartz (1982), Effect of Cetiedil on Cation and Water Movements in Erythrocytes. *J. Clin. Invest.*, 69, 589-594.
 30. L.R. Berkowitz and E.P. Orringer (1982), Effects of Cetiedil on Monovalent Cation Permeability in the Erythrocyte; An Explanation of the Efficacy of Cetiedil in the Treatment of Sickle Cell Anemia. *Blood Cells*, 8, 283-288.
 31. L.R. Berkowitz and E.P. Orringer, (1984). An Analysis of the Mechanism by which Cetiedil Inhibits the Gardos Phenomenon, *Am. J. Hematol.*, 17, 217-223.
 32. P. Agre, D. Virshup, and V. Bennett, (1984). Bepridil and Cetiedil. Vasodilators which Inhibit Calcium-dependent Calmodulin Interactions with Erythrocyte Membranes, *J. Clin. Invest.*, 74, 812-820.
 33. S.N. Levine, L.R. Berkowitz and E.P. Orringer, (1984). Cetiedil Inhibition of Calmodulin-stimulated Enzyme Activity, *Biochem. Pharmacol.*, 33, 581-584.
 34. H. Kohzaki, K. Kakinuma, T. Asakura, and T. Yamakawa, (1985). Effects of Cetiedil on the Oxidative Metabolism of Activated Polymorphonuclear Leucocytes, *Br. J. Haematol.*, 60, 531-539.
 35. L.W. Fung (1981), Spin Label Studies of the Lipid and Protein Components of Erythrocyte Membranes, *Biophys. J.*, 33, 253-262.
 36. L.J. Berliner, (1976). In, "Spin Labeling. Theory and Applications", (L.J. Berliner Ed). pp 1-4.
 37. J.D. Morrisett, (1976). The Use of Spin Labels for Studying the Structure

- and Function of Enzymes. In, "Spin Labeling. Theory and Applications" (L.J. Berliner, ed) pp 273-338.
38. B.J. Gaffney, (1976). Practical considerations for the Calculation of Order Parameters for Fatty Acid or Phospholipid Spin Labels in Membranes. In, "Spin Labeling. Theory and Applications" (L.J. Berliner, ed) pp 567-571.
 39. L.W. Fung (1981), Spin-Label Detection of Hemoglobin-Membrane Interaction at Physiological pH. *Biochemistry*, 20, 7162-7166.
 40. D. Chapman, M.D. Barratt, V.B. Kamat, (1969). A Spin-Label Study of Erythrocyte Membranes. *Biochim. Biophys. Acta.*, 173, 154-157.
 41. L.W. Fung and M. Ostrowski (1982), Spin Label EPR Studies of Huntington Disease Erythrocyte Membranes. *Am. J. Hum. Genet.*, 34, 469-480.
 42. O. Jardetzky and G.C.K. Roberts (1981). *NMR in Molecular Biology*, Academic Press, pp 328-378.
 43. L.M. Jackman and F.A. Cotton, eds (1975). *Dynamic Nuclear Magnetic Resonance Spectroscopy*. Academic Press.
 44. T. Conlon and R. Outhred, (1972). Water Diffusion Permeability of Erythrocytes Using an NMR Technique, *Biochim. Biophys. Acta*, 288, 354-361.
 45. S. Roth and P. Seeman (1972). The Membrane Concentrations of Neutral and Positive Anaesthetics (Alcohols, Chlorpromazine, Morphine) Fit the Meyer-Overton Rule of Anesthesia; Negative Narcotics Do Not. *Biochim. Biophys. Acta* 255, 207-219.
 46. M.J. Conrad and S.J. Singer, (1981). The Solubility of Amphiphilic Molecules in Biological Membranes and Lipid Bilayers and its Implications for Membrane Structure, *Biochemistry*, 20, 808-818.

47. K.E. Van Holde (1985). *Physical Biochemistry*, Prentice-Hall. pp 41-42.
48. P. Maher and S.J. Singer (1984). Structural Changes in Membranes Produced by the Binding of Small Amphipathic Molecules, *Biochemistry*, 23, 232-240.
49. L.A. Sklar, B.S. Hudson and R.D. Simoni, (1977). Conjugated Polyene Fatty Acids as Fluorescent Probes: Synthetic Phospholipid Membrane Studies, *Biochemistry*, 16, 819-828.
50. R. Welti, L.J. Mullikin, T. Yoshimura, and G.M. Helmkamp, Jr., (1984). Partition of Amphiphilic Molecules into Phospholipid Vesicles and Human Erythrocyte Ghosts: Measurements by Ultraviolet Difference Spectroscopy, *Biochemistry*, 23, 6086-6091.
51. McNeil Pharmaceuticals, Physical Data Sheet (McN-R-2009-49-98).
52. J.T. Dodge, C. Mitchell and D.J. Hanahan (1963), The Preparation and Chemical Characteristics of Hemoglobin-free Ghosts of Human Erythrocytes. *Arch. Biochem. Biophys.*, 100, 119-130.
53. V. Bennett and D. Branton (1977), Selective Association of Spectrin with the Cytoplasmic Surface of Human Erythrocyte Plasma Membranes. Quantitative Determination with Purified P-32 Spectrin. *J. Biol.Chem.*, 252, 2753-2763.
54. G.L. Peterson, (1979). Review of the Folin Phenol Protein Quantitation Method of Lowry, Rosebrough, Farr and Randall, *Anal. Biochem.*, 100, 201-220.
55. G. Fairbanks, T.L. Steck and D.F.H. Wallach (1971). Electrophoretic Mobility of the Major Polypeptides of the Human Erythrocyte Membrane. *Biochemistry*, 10, 2606-2617.
56. Y. Barenholz, D. Gibbs, B.J. Litman, J. Goll, T.E. Thompson, and F.D.

- Carlson, (1977). A Simple Method for the Preparation of Homogeneous Phospholipid Vesicles. *Biochemistry*, 16, 2806-2810.
57. G. Rouser, S. Fleischer and A. Yamamoto, (1970). Two Dimensional Thin Layer Chromatographic Separation of Polar Lipids and Determination of Phospholipids by Phosphorus Analysis of Spots. *Lipids*, 5, 494-496.
58. J.L. Pirkle, D.L. Ashley, and J.H. Goldstein, (1979). Pulse Nuclear Magnetic Resonance Measurements of Water Exchange across the Erythrocyte Membrane Employing a Low Mn Concentration, *Biophys. J.*, 25, 389-406.
59. M.E. Fabry, and M. Eisenstadt, (1978). Water Exchange across Red Cell Membranes: II. Measurement by Nuclear Magnetic Resonance T_1 , T_2 , and T_{12} Hybrid Relaxation. The Effects of Osmolarity, Cell Volume and Medium, *J. Memb. Biol.*, 42, 375-398.
60. J.N. Phillips (1955), Energetics of Micelle Formation. *Trans. Faraday Soc.*, 51, 561-569.
61. NMC-1280 Manual (1982), Nicolet Magnetics Corporation. pp 18-19.
62. M.L. Martin, J.-J. Delpeuch and G.J. Martin, (1980). Practical NMR Spectroscopy. Heyden. pp 177-179.
63. L. Tentori, and A.M. Salvati, (1981). Hemoglobinometry in Human Blood, *Methods in Enzymology*, 76, 707-715.
64. H.Y. Carr and E.M. Purcell, (1954). Effects of Diffusion on Free Precession in Nuclear Magnetic Resonance Experiments, *Phys. Rev.*, 94, 360-365.
65. S. Meiboom and D. Gill, (1958). Proton Relaxation in Water, *Rev. Sci. Instrum.* 29, 688-694.
66. T.F. Moura, R.I. Macey, D.Y. Chien, D. Karan, and H. Santos, (1984).

Thermodynamics of All-or-None Water Channel Closure in Red Cells,
J. Mem. Biol., 81, 105-111.

67. C.F. Hazelwood, D.C. Chang, B.L. Nichols, and D.E. Woessner, (1974). Nuclear Magnetic Resonance Transverse Relaxation Times of Water Protons in Skeletal Muscle. *Biophys. J.*, 14, 583-606.
68. R. S. Weinstein (1974). The Morphology of Adult Red Cells in "The Red Blood Cells". (D.M. Surgenor, ed), Academic Press. p. 232.
69. D.A. Skoog and D.M. West (1982). *Fundamentals of Analytical Chemistry (Fourth Edition)*. Saunders College Publishing, p 833.
70. R.M. Silverstein, C.G. Bassler and T.C. Morrill (1981). *Spectroscopic Identification of Organic Compounds (Fourth Edition)*. John Wiley. p 327.
71. M. Anderson and A.W. Johnson, (1965). Preparation and Reactions of Some Derivatives of Azepine, *J. Chem. Soc.*, 2411-2422.
72. C.R. Cantor and P.R. Schimmel (1980). *Biophysical Chemistry, Volume II*, W.H. Freeman. pp 364-367.
73. V. Formacek, L. Desnoyer, H.P. Kellerhals, T. Keller, and J.T. Clerc, (1976). ¹³C Data Bank Vol. 1, Bruker.
74. R.J. Abraham and P. Loftus, (1980). Proton and Carbon-13 NMR Spectroscopy. Heyden. pp 98, 120.
75. J.B. Stothers, (1972). Carbon-13 NMR Spectroscopy. Academic Press. pp 64, 426.
76. J.B. Stothers, (1972). Carbon-13 NMR Spectroscopy. Academic Press. p 256.
77. R.J. Abraham and P. Loftus, (1980). Proton and Carbon-13 NMR Spectroscopy. Heyden. p 30.
78. R.J. Abraham and P. Loftus, (1980). Proton and Carbon-13 NMR

Spectroscopy. Heyden. p 32.

79. A. Bundi, C. Grathwohl, J. Hochmann, R.M. Keller, G. Wagner and K. Wuthrich, (1975). Proton NMR of the Protected Tetrapeptides TFA-Gly-Gly-L-X-L-Ala-OCH₃, where X Stands for one of the 20 Common Amino Acids. *J. Mag. Resonance*, 18, 191.
80. D.W. Urry and L. Mitchell, (1976). Carbon-13 Magnetic Resonance Spectra of Aortic -Elastin in Solution, Coacervate and Fibrous states, *Biochem. Biophys. Res. Commun.*, 68, 1153.
81. M. Llinas and M.P. Klein, (1975). Charge Relay at the Peptide Bond. A Proton Magnetic Resonance Study of Solvation Effects on the Amide Electron Density Distribution, *J. Am. Chem. Soc.*, 97, 4731-4737.
82. M. Llinas, W.J. Horsley, and M.P. Klein, (1976). Nitrogen-15 Nuclear Magnetic Resonance Spectrum of Alumichrome. Detection by Double Resonance Fourier Transform Technique, *J. Am. Chem. Soc.*, 98, 7554-7560.
83. O.W. Howarth and D.M.J. Lilley, (1978). Carbon-13-NMR of Peptides and Proteins, *Prog. NMR Spectroscopy*, 1-40.
84. C.J. Pouchert, (1983). *Aldrich Library of NMR Spectra*, Volumes 1 and 2, Aldrich Chemical Company.
85. E. Fukushima and S.B.W. Roeder, (1981). *Experimental Pulse NMR. A Nuts and Bolts Approach*. Addison-Wesley. pp 157-161.
86. W.L. Hubbel and H.M. McConnell (1979), Orientation and Motion of Amphiphilic Spin Labels in Membrane. *Proc. Natl. Acad. Sci., USA*, 64, 20-27.
87. L.W. Fung and M.E. Johnson (1984), Recent Developments in Spin Label EPR Methodology for Biomembrane Studies. *Current Topics in Bioenergetics*, C.P. Lee (Ed.), Acad. Press, 13, 107-157.

88. L.W. Fung and M.J. Simpson (1979), Topology of a Protein Spin Label in Erythrocyte Membranes, FEBS Lett., 108, 269-273.
89. P. Boivin and C. Galand, (1984). Is Spectrin a Calmodulin-Binding Protein ?, Biochem. Intl., 8, 231-236.
90. A. Berglund, L. Backman and V.P. Shanbag, (1984). Calmodulin Binding to Human Spectrin, FEBS Letters, 172, 109-113.
91. V. Niggli, E.S. Adunyah, J.T. Penniston, and E. Carafoli, (1981). Purified (Ca²⁺ - Mg²⁺) - ATPase of the Erythrocyte Membrane. Reconstitution and Effect of Calmodulin and Phospholipids, J. Biol. Chem., 256, 395-401.
92. M.L. Jennings, (1984). Oligomeric Structure and the Anion Transport Function of Human Erythrocyte Band 3 Protein, J. Mem. Biol., 80, 105-117.
93. F.L. Vieira, R.L. Sha'afi and A.K. Solomon, (1970). The State of Water in Human and Dog Red Cell Membranes, J. Gen. Physiol., 55, 451-466.
94. R.I. Macey, D.M. Karan, and R.E.L. Farmer, (1972). Properties of Water Channels in Human Red Cells, Biomembranes, 3, 331-340.
95. A.K. Solomon, B. Chasan, J.A. Dix, M. Lukacovic, M.R. Toon and A.S. Verkman, (1983). The Aqueous Pore in the Red Cell Membrane: Band 3 as a Channel for Anions, Cations, Non-electrolytes, and Water, Ann. N.Y. Acad. Sci., 97-124.
96. C.V. Pagnelli, and A.K. Solomon, (1957). The Rate of Exchange of Tritiated Water across the Human Red Cell Membrane, J. Gen. Physiol., 41, 259-277.
97. B.C. Thompson, M.R. Waterman, and G.L. Cottam, (1975). Evaluation of Water Environments in Deoxygenated Sickle Cells by Longitudinal and Transverse Water Proton Relaxation Rates, Arch. Biochem. Biophys., 166, 193-200.

98. A. Zipp, T.L. James, I.D. Kuntz and S.B. Shoet, (1976). Water Proton Magnetic Resonance Studies of Normal and Sickle Erythrocytes, *Biochim. Biophys. Acta*, 428, 291-303.
99. C.T. Craescu, R. Cassoly, F. Galacteros and C. Prehu, (1985). Kinetics of Water Transport in Sickle Cells, *Biochim. Biophys. Acta*, 812, 811-815.
100. R. Cassoly, and J. Salhany, (1983). Spectral and Oxygen-Release Kinetic Properties of Human Hemoglobin Bound to the Cytoplasmic Fragment of Band 3 Protein in Solution, *Biochim. Biophys. Acta*, 745, 134-139.
101. R. Cassoly, (1983). Quantitative Analysis of the Association of Human Hemoglobin with the Cytoplasmic Fragment of Band 3 Protein, *J. Biol. Chem.*, 258, 3859-3864.
102. L.W.-M. Fung, S.D. Litvin, and T.M. Reid, (1983). Spin-Label Detection of Hemoglobin-Membrane Interaction at Physiological pH. *Biochemistry*, 22, 864-869.
103. J.S. Marrow and R.A. Anderson, (1986). Shaping the Too Fluid Bilayer, *Lab. Invest.*, 54, 237-240.
104. N.P. Franks, and W.R. Lieb, (1981). Is Membrane Expansion Relevant to Anaesthesia ?, *Nature (London)*, 292, 248-255.
105. L.A. Sklar, G.P. Miljanich, and E.A. Dratz, (1979). Phospholipid Lateral Phase Separation and the Partition of cis-Parinaric Acid and trans-Parinaric Acid among Aqueous, Solid Lipid, and Fluid Lipid Phases, *Biochemistry*, 18, 1707-1716.
106. J.E. Farrell and W.H. Huestis, (1984). Phosphoinositide Metabolism and the morphology of Human Erythrocytes, *J. Cell Biol.*, 98, 1992-1999.
107. M.J. Selwyn, A.P. Dawson, M. Stockdale and N. Gains, (1970). Chloride Hydroxide Exchange across Mitochondrial, Erythrocyte and Artificial Lipid

Membranes Mediated by Trialkyl- and Triphenyltin Compounds,
Eur. J. Biochem., 14, 120-130.

108. G.L. Nicolson, (1976). Cell Shape Changes and Transmembrane Receptor Uncoupling Induced by Tertiary Amine Local Anaesthetics, J. Supramol. Struct., 5, 65-72.
109. J.A. Dix and A.K. Solomon, (1984). Role of Membrane Proteins and Lipids in Water Diffusion across Red Cell Membranes, Biocim. Biophys. Acta, 773, 219-230.

APPENDIX I

Molecular Properties of Cetiedil and its Interactions with Erythrocyte Membranes

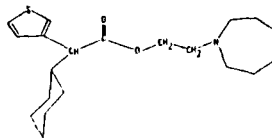
C. NARASIMHAN AND L. W.-M. FUNG*

Received December 2, 1985, from the Department of Chemistry, Loyola University of Chicago, Chicago, IL 60626. Accepted for publication April 14, 1986.

Abstract—Cetiedil, an antisickling agent and a vascular smooth muscle relaxant, is an amphiphilic molecule. The critical micelle concentration in 5 mM phosphate buffer with 150 mM NaCl is \approx 8.8 mM. The molecule, as the citrate salt, is highly acidic at millimolar concentrations. The UV absorption extinction coefficient at 233 nm, E_{233} , is 2796 M⁻¹ cm⁻¹. The studies of free cetiedil concentrations in the presence of membrane ghosts show that large amounts of cetiedil associate with membrane samples. Spin label electron paramagnetic resonance experiments showed that the lipids and the proteins of erythrocyte membrane samples were both affected by the addition of cetiedil. However, the cetiedil effects on membrane components are reversible. The protein spin label results demonstrate the binding of cetiedil to the membrane with an apparent equilibrium dissociation constant of \approx 2 mM. The binding is saturable. The apparent half-saturation concentrations for the binding at physiological ionic strength and temperature are in the range of 1–3 mmoles of cetiedil per gram of membrane proteins. Our studies also indicate that binding is not affected by the removal of the spectrin and actin network from the membranes. Interaction of cetiedil with Band 3 molecules in the erythrocyte membrane is suggested. The regions near the lipid head groups in the membrane samples are also affected by cetiedil.

branes.^{9,10,14} When 400 μ M cetiedil is added, a 20% increase in hematocrit, and an increase $>10\%$ in cell volume are reported.⁹ Recently, cetiedil has been found to inhibit Ca²⁺-dependent calmodulin interactions with membranes.^{15,16} In brief, cetiedil appears to interact with erythrocyte membranes to prevent sickling under some conditions^{7,8,10} but not others.¹ Evaluating the effectiveness of cetiedil as an antisickling drug requires a detailed knowledge of its molecular properties in solution, and an understanding of its mode of action with erythrocyte membrane components.

We have studied the optical and pH properties of cetiedil in solution, and have determined its critical micelle concentration. We have also used spin label electron paramagnetic resonance (EPR) techniques to study the effects of cetiedil on membrane proteins and lipids.



Cetiedil

Experimental Section

Cetiedil Solution—Cetiedil was obtained from McNeil Pharmaceuticals (Spring House, PA) in the form of the citrate salt, and was used without further purification.

Cetiedil is only slightly soluble in water, with a solubility of 0.5 g/dL.¹⁷ For experiments that required concentrations >0.5 g/dL, a stock solution was prepared by adding 45 mg of cetiedil to 1 mL of 5 mM phosphate buffer with 150 mM NaCl at pH 7.4 (5P7.4/NaCl) buffer, followed by sonication for \approx 2 min and centrifugation at 1075 \times g for 5 min to give a clear supernatant, which was then diluted to 30 mM with buffer. The concentration of the supernatant was generally about 2.5–3 g/dL (45–54 mM), as determined by UV absorption measurements. Without sonication, the supernatant was cloudy. The final pH of the 30 mM cetiedil stock solution in 5P7.4/NaCl buffer was 4.0.

For the pH effect studies, various amounts of 30 mM cetiedil stock solution in 5 mM phosphate with 150 mM NaCl at pH 8 (phosphate buffered samples, PBS) were added to PBS, or to blood serum, to give a concentration range of cetiedil of 4.3 μ M–20 mM. The pH was measured in an open system exposed to air, after the pH values had reached constant values.

For the extinction coefficient determination, a precise amount of cetiedil was weighed to prepare a 150 μ M solution, which was subsequently diluted with buffer to give cetiedil solutions of various concentrations.

Cetiedil Extinction Coefficient Measurements—The UV absorption spectra, between 190 and 400 nm, of cetiedil solutions of known concentrations (10–150 μ M cetiedil in 5P7.4/NaCl buffer) were obtained and showed a maximum absorption at 233 nm, as shown in the inset of Fig. 2. A simple linear regression of the absorbance values at 233 nm (A_{233}) versus cetiedil concentration provided a slope that gave the extinction coefficient of cetiedil.

Although many of the molecular defects of sickle cell disease are quite well characterized, there is at present no specific treatment for its cure or prevention. Few antisickling agents have been found to be clinically useful.^{1,3} Most antisickling agents act by modifying the sickle hemoglobin (HbS) molecule either covalently,² or noncovalently.⁴ Modifying hemoglobin synthesis has also been suggested to be useful.⁵ However, cetiedil belongs to another class of antisickling agents which interacts with the erythrocyte membrane.^{6,10} Cetiedil has also been used in Europe as a vasodilator for chronic cardiovascular disease.^{11,12}

The use of cetiedil, (2-hexahydro-1H-azepin-1-yl)ethyl α -cyclohexyl-3-thiopheneacetate, as an antisickling agent was first explored by Cabannes.⁶ Chromium-51 survival studies of cetiedil-treated sickle cells indicated that cetiedil is not toxic to the red cell.⁷ Furthermore, intravenous infusion of cetiedil to male volunteers indicated the development of tolerance.¹³ Cetiedil is thus considered as a unique, non-toxic antisickling drug by some physicians. Benjamin et al.⁷ observed a decrease in the irreversible sickle cell (ISC) count at 100–200 μ M concentrations of cetiedil, but observed no effect at concentrations <50 μ M or >500 μ M. In another study, 400 μ M cetiedil decreased the number of sickle cells under deoxygenated conditions, whereas 10 mM cetiedil decreased ISC counts.⁸ Marked (80%) reduction of sickle cells at 100–500 μ M cetiedil and 3% oxygen concentrations has also been reported.¹¹ However, no significant effect was reported when 500 μ M to 1 mM concentrations of cetiedil were added to serum at 50% oxygen saturation.¹ The detailed mechanism of the drug action on the erythrocyte is not clear. Cetiedil does not appear to affect or to bind to HbS.^{1,7,8} Cetiedil increases passive Na⁺ movement, and inhibits Ca²⁺-dependent K⁺ movement (the Gardos pathway) across cell mem-

Critical Micelle Concentration Determination—Since cetidil is an amphiphilic molecule, its solubility in water is limited.¹⁴ At high concentration, the molecules appear to form micelles in water, with monomers and micelles in equilibrium. The critical micelle concentration (CMC) of cetidil was defined and determined according to the method of Phillips.¹⁵ A mass-action model of micelle formation was used. At the CMC, the third derivative of an ideal colligative property of the amphiphile, A_{233} , of cetidil for this work, with respect to concentration, C , is zero ($d^3A_{233}/dC^3 = 0$). The A_{233} of cetidil solutions in the concentration range of 1–15 mM were measured using a narrow path length, 1.0 or 0.2 mm, optical cell. The absorbance values at different concentrations were fitted to polynomial equations of varying order: $A_{233} = aC + bC^2 + cC^3 + \dots + nC^n$, where a, b, c, \dots were parameters to be determined from experimental data, and n was the order of the polynomial equation. The third derivatives of these equations with respect to concentration were set at zero to solve for the CMC values.

Spin Labeled Membrane Samples—Hemoglobin-free white membrane ghosts in 5 mM phosphate buffer at pH 8 (5P8) were prepared from adult human erythrocytes of normal donors and homozygous sickle cell anemia patients.^{19,20} Membrane samples (usually 4 mg/ml, in protein concentration) were incubated with the protein spin label 4-maleimido-2,2,6,6-tetramethyl-1-piperidinyloxy (Aldrich Chemical Co., Milwaukee, WI) at a concentration of 30–50 μ g/mg of protein in the dark at 4°C for 1 h.²¹ Excess spin label was removed by washing with 5P8 buffer until the samples gave constant EPR signals.

The maleimide spin labeled, spectrin-actin depleted membranes were prepared by incubation of labeled membranes at 37°C in 0.3 mM phosphate buffer at pH 7.6 (0.3P7.6) buffer, to solubilize spectrin-actin, which was then removed by centrifugation.²² Lowry protein assays were carried out on the intact membrane and the supernatant resulting from centrifugation. Generally, $\pm 30 \pm 5\%$ of the proteins were removed from the membranes to give simplified membranes, depleted of the spectrin-actin network. The proteins of this simplified membrane sample were mainly Band 3 protein, as shown by 5% SDS polyacrylamide gel electrophoresis, using the methods of Fairbanks et al.²³

A fatty acid spin probe, (3-carboxypropyl)-4,4-dimethyl-2-(tridecyl-3-oxyl-15-doxyl stearate) (Syva, Palo Alto, CA) was also used to label membrane ghost samples. Membrane samples in 5P8 buffer were dialyzed in 5P7.4 NaCl buffer before incubation with 5-doxyl stearate at a concentration of 100 μ g/mg protein for 30 min, at room temperature. Since the membranes have about equal amounts of proteins and lipids by weight, the spin label to lipid molar ratio was 1:6.

Cetidil-Membrane Samples—The maleimide spin labeled membrane and simplified membrane samples were dialyzed in 5P7.4 NaCl overnight. Samples of the 5-doxyl stearate spin labeled membranes in 5P7.4 NaCl were used directly. The protein concentrations of these samples were determined by the modified Lowry assay, and adjusted to 4 mg/ml, for the maleimide spin labeled samples, and to 6 mg/ml, for the 5-doxyl stearate labeled samples. Various volumes (0–200 μ L) of cetidil stock solution were added to 100 μ L membrane samples. A solution of 150 mM NaCl and 5 mM NaH_2PO_4 with HCl added to give a pH of 4.0 was used as control solution (5P4 NaCl), since the cetidil stock solution in 5P7.4 NaCl has a final pH value of 4. A volume of this solution was added to each spin-labeled membrane and cetidil mixture to give a final volume of 300 μ L. The final pH of all samples was 6.3. The mixtures of membrane and cetidil were then centrifuged at $38750 \times g$ for 5 min. The supernatant of each sample was removed, and the free cetidil concentrations in the supernatants were determined by UV absorption at 233 nm. The pellet membrane samples were used for EPR measurements.

Due to the relatively low sensitivity in the EPR studies, the concentrations of cetidil (in the millimolar range) and of membrane proteins (in the mg/mL range) needed in this study were higher than those used clinically or in cellular studies, in which μ M concentration cetidil per μ g/mL proteins were used.^{7,10} However, the cetidil-to-protein ratios in both cases are millimoles of cetidil per gram of protein. In a simple equilibrium process, the interaction depends on the absolute concentrations of cetidil rather than on the cetidil-to-protein ratios since the equilibrium will be shifted more toward the cetidil-membrane association state at higher cetidil concentration, and toward the dissociation state at lower cetidil concentration. In the case of limited solubility of cetidil in buffer as well as preferential partitioning of cetidil in the lipid phase, a precise description of

the cetidil-membrane equilibrium in the buffer requires detailed information on the partitioning of cetidil between the various membrane components and buffer. For comparison with other studies, we have simply used the ratio of "cetidil added-to-protein present" as a point of reference.

Electron Paramagnetic Resonance Experiments—EPR samples were introduced into 50 μ L capillary tubes, following the procedures used in this laboratory.²⁴ An EPR spectrometer (Varian model E109) interfaced with a time averager (Nicolet model 535), was used to obtain the EPR spectra. The temperature of the EPR measurement was controlled and monitored to ± 0.1 °C. Standard EPR spectrometer settings were used.²⁵

Electron Paramagnetic Resonance Data Analysis of 5-Doxyl Stearate Labeled Samples—The hyperfine separation (HFS) of the high field and low field EPR signals²⁶ of labeled membrane samples were measured as a function of cetidil concentration.

Electron Paramagnetic Resonance Data Analysis of the Maleimide Labeled Samples—The W/S ratios²⁴ of membrane samples without cetidil, $(W/S)_0$, and of membranes with a specific amount of cetidil present, $(W/S)_{\text{cet}}$, were measured. The difference between $(W/S)_0$ and $(W/S)_{\text{cet}}$, $\Delta(W/S)_{\text{cet}}$, was calculated and used to obtain quantitative information on the interaction between cetidil (C) and membranes (M).

A general cooperative binding model is first assumed for membranes with n binding sites, $M + nC \rightarrow MC_n$. The equilibrium dissociation constant, K_d , is equal to $C^n/M/C_n$, where M is the final membrane concentration, C is the concentration of free cetidil, in equilibrium with the bound cetidil, and MC_n is the concentration of the membrane-cetidil complex. If f_b is the fraction of membrane interacting with cetidil, then $f_b = MC_n/(MC_n + M)$. Combining the aforementioned K_d and f_b expressions, we obtain:

$$f_b = (1 + K_d/C^n)^{-1} \quad (1)$$

Assuming that the changes in the W/S ratio observed on addition of cetidil to the membrane are the direct results of cetidil interacting with the membrane to reduce the spin label mobility, the EPR data could be related to f_b to obtain values for the K_d . Assuming $(W/S)_0$ as the W/S value for membrane bound with cetidil, then $(W/S)_{\text{cet}} = f_b(W/S)_0 + (1 - f_b)(W/S)_0$, or:

$$\Delta(W/S)_{\text{cet}} = f_b \Delta(W/S)_0 \quad (2)$$

where $\Delta(W/S)_0 = (W/S)_0 - (W/S)_f$. Substituting eq. 1 into eq. 2 gives:

$$\Delta(W/S)_{\text{cet}} = \Delta(W/S)_0 (1 + K_d/C^n)^{-1} \quad (3)$$

When $n = 1$, eq. 3 became the equation for the two-state binding model for membranes with multiple independent binding sites, $M + C \rightarrow MC$.²⁴ Values of $\Delta(W/S)_{\text{cet}}$ and C are experimentally determined and K_d , $\Delta(W/S)_0$, and n are obtained from eq. 3 using nonlinear regression methods. The n values, which indicate the cooperativity of binding, are also obtained by Hill plots. The half saturation concentration, $C_{1/2}$, is the cetidil concentration that gives a $\Delta(W/S)_{\text{cet}}$ value that was one-half of the $\Delta(W/S)_0$ value, and is obtained from the nonlinear regression fitted curves.

Results and Discussion

The pH Effect of Cetidil—Figure 1 shows the pH of the drug molecule, cetidil citrate, in phosphate buffered saline (PBS) and in blood serum as a function of concentration. In PBS, addition of 500 μ M cetidil citrate causes the pH of the buffer to drop from 8.0 to 7.7. At 20 mM cetidil citrate, the pH is ~ 6.3 , and at 30 mM, the pH is 4.0.

This sharp change in pH on addition of cetidil citrate to buffer is probably due to the citrate moiety present with cetidil as a counterion. The pK_2 of citrate acid is 4.76 and the pK_3 is 6.4 at 25°C. The first ionizable proton ($pK_1 = 3.1$) of the three carboxylate groups in citrate is neutralized by the positive charge on the tertiary ammonium ion of the azepine ring, which has a pK_a of ~ 10 . We also prepared various concentrations of citric acid solutions in PBS and measured their pH values. The pH profiles of cetidil citrate and citric acid in PBS were similar.

The pH effect of the drug molecule was also tested on blood serum in a similar manner. Although the pH profile of

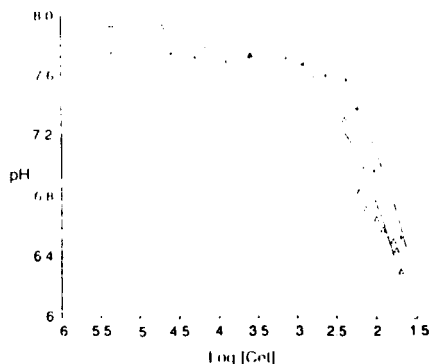


Figure 1—The pH profile of cetiedil in blood serum (+) and in PBS (Δ). The pH measurements were made on a Beckman Model 3560 Digital pH meter, using an Ingold Micro pH Electrode at room temperature. The pH of the blood serum was 7.78. The lines shown through the data are spline fits and have no theoretical significance.

cetiedil citrate in serum in Fig. 1 looks similar to that in PBS, the curve is shifted slightly to the right indicating that the buffering capacity of blood serum is somewhat better than that of PBS. The pH of the serum remains constant on addition of cetiedil citrate up to about 0.5 mM, and it drops to about 6.5 at 20 mM cetiedil citrate.

The concentration of cetiedil citrate used in clinical and cellular studies is usually in the range 100–500 μM . If this amount of cetiedil citrate is evenly distributed, then the change in pH due to cetiedil will be minimal. However, if cetiedil is more soluble in one part of the membrane than another (for example, more soluble in hydrophobic or hydrophilic environments), then accumulation of the drug in the membrane may lead to local concentrations higher than 100–500 μM , which may change the local pH in the membrane. The acidic citrate ions are more soluble in aqueous solution or serum, and less soluble in membrane bilayers. The basic cetiedil moiety is more soluble in the membrane bilayers than in an aqueous solution. Since patients treated with cetiedil citrate received 25–50 mg cetiedil per treatment,^{6,10} it is important to ensure that the concentration of cetiedil or the solution administered to patients is not great enough to cause a sudden pH drop in serum. It also appears that a different counterion which has a more neutral pK may be more desirable.

Extinction Coefficient of Cetiedil—The molar extinction coefficient at 233 nm (E_{233}) was determined to be $2796 \text{ M}^{-1} \text{ cm}^{-1}$ from a linear plot of A_{233} versus cetiedil concentration over the range of 10–150 μM . The chromophores in cetiedil appear to be the thiophene (sulfur-containing five-membered ring) and the azepine (nitrogen-containing seven-membered ring) groups, both of which absorb in the UV region. For thiophene, the maximum absorption is at 231 nm, and the E_{231} is $7100 \text{ M}^{-1} \text{ cm}^{-1}$, and for azepine, the maximum absorption is at 226–229 nm, and the E_{227} is $13,780 \text{ M}^{-1} \text{ cm}^{-1}$.²⁶

Critical Micelle Concentration of Cetiedil—Figure 2 shows that the A_{233} values of cetiedil in 5P7.4/NaCl buffer level off at higher cetiedil concentrations. The instrument performance at high absorbance was checked to ensure linear response. Straight lines were obtained for absorbance versus concentration plots for benzoic acid at 230 nm, and for hemoglobin solutions at 280 nm. Light scattering at 233 nm was also checked by monitoring the absorbance of membrane

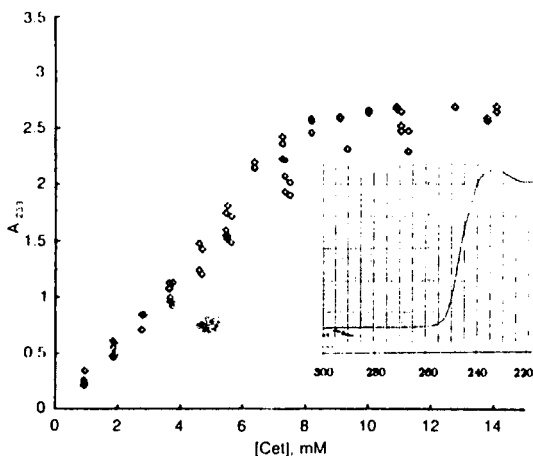


Figure 2— A_{233} versus cetiedil concentration plot in 5 mM phosphate buffer with 150 mM NaCl. Inset shows the UV spectrum of cetiedil at pH 6.3 with maximum absorption at 233 nm. Optical cells with a 1-mm light path were used to obtain the A_{233} . The performance of the instrument was checked for linearity (see text).

solutions. A linear response was also obtained at high absorbance (2–3). The leveling-off phenomenon in cetiedil solutions at high concentration must thus be due to micelle formation. The relationship between the absorbance and concentration was fit to polynomial equations to determine the critical micelle concentration. Polynomial equations with orders of 4, 5, 6, 7, and 8 all gave reasonably good fits to the experimental data. The average value of the CMC obtained from these fitted polynomial equations was $8.8 \pm 0.3 \text{ mM}$.

Since the CMC was well above the 500 μM concentration range used in clinical and cellular studies,^{6,10} cetiedil would exist as monomers in these studies, if it were evenly distributed. In the case where a local accumulation of cetiedil to a concentration above 8.8 mM could occur, then cetiedil would exist as both monomers and micelles.

Cetiedil-Membrane Interaction—We determined the free cetiedil concentration in the presence of membrane ghosts, by measuring the UV absorbance of the supernatant resulting from centrifugation, as discussed above. Figure 3 shows the concentration relationship between free cetiedil and total cetiedil citrate added in the presence of 1.33 mg/ml membranes. The slope of the fitted line is 0.88. About 85% of

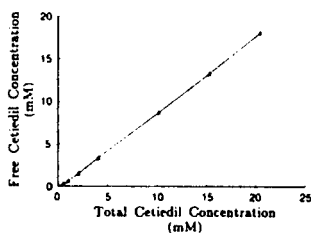


Figure 3—The relationship between total and free cetiedil concentrations in a membrane sample (1.33 mg/mL) in 5 mM phosphate buffer with 150 mM NaCl. At 5 mM concentration, about 1.6×10^8 cetiedil molecules associate with each ghost.

ctetiedil remains in solution as free cetiedil. For example, at a 5 mM cetiedil citrate concentration, 0.5 μ mol of cetiedil associates with 1.33 mg membranes, or 1.6×10^8 cetiedil molecules per ghost (assuming 5.7×10^{10} mg protein per ghost), which is an enormous amount of cetiedil associated with membranes.

Effect of Cetiedil on Membrane Lipids—The fatty acid spin probe, 5-doxyl stearate, intercalates among the lipid molecules in the membrane, with the nitroxide moiety of the 5-doxyl stearate located near the carbonyl group of phospholipid molecules, and has been used to monitor the behavior of the lipid molecules in the region near the polar head groups.²⁶ Although these spin probes are easy to use, there has been some criticism of their uses in membrane studies since the spectral data are often over interpreted.²⁷ In this study, we simply use the label to find out whether cetiedil affected the lipid component in membrane, and no attempt was made to obtain quantitative information on the dynamics of the lipid molecules. Figure 4 shows a plot of the hyperfine separation (HFS) as a function of total cetiedil concentration in the membrane sample. As the concentration of cetiedil increased, the HFS values decreased indicating a change in the mobility or environmental polarity of the spin probe upon addition of cetiedil to the membrane. At a pH of ~ 6.3 (in 5P7.4 NaCl buffer) and 37 °C, the HFS values decrease from ~ 52 G to ~ 45 G when 10–15 mM cetiedil was present in the membrane sample that had a protein concentration of 2 mg/mL.

Effect of Cetiedil on Membrane Proteins—We used the maleimide spin label to monitor the effect of cetiedil on membrane proteins of both normal and sickle cells. The maleimide spin labels alkylate primarily the sulfhydryl (SH) groups of the protein molecules. Our earlier finding shows that $\sim 20\%$ of the erythrocyte membrane protein SH groups are alkylated by the maleimide spin label, and $\sim 80\%$ of the spin label intensity arises from label sites at the cytoplasmic membrane surface, with most of the spin labels attached to the peripheral proteins, the spectrin-actin complex,²¹ and one spin label to the Band 3 molecule. The amplitude ratio, W/S, of the EPR spectrum of the maleimide labeled membranes is very sensitive to such experimental conditions as temperature, ionic strength and pH as well as to molecules binding to the cytoplasmic surface of the membranes.^{24,28} We measured the W/S values of the maleimide labeled membranes in the presence of various amounts of cetiedil in 5 mM phosphate buffer with NaCl at 20 and 37 °C. As shown in Fig. 5, the initial addition of cetiedil to both membrane and simplified membrane samples of normal cells gave a gradual increase in $\Delta(W/S)$ at both 20 and 37 °C. The four curves shown in Fig. 5 were qualitatively similar to each other.

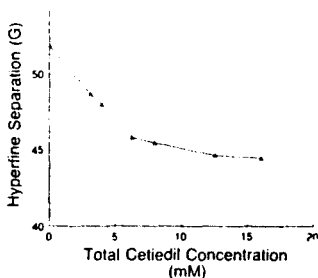


Figure 4—The effects of cetiedil on the hyperfine separation of 5-doxyl stearate labeled erythrocyte membrane samples in 5 mM phosphate buffer with 150 mM NaCl at 37 °C.

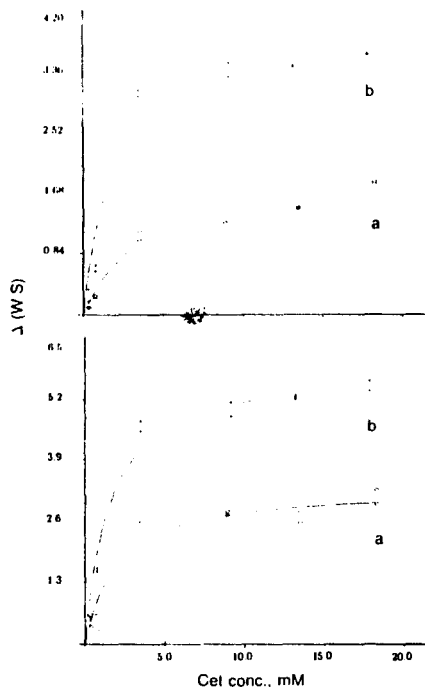


Figure 5—Change in (W/S) of the maleimide labeled erythrocyte membranes as a function of free cetiedil concentration in a typical run of paired samples of intact membrane (a) and simplified membrane (b) that were allowed to interact with cetiedil at 20 °C (top panel) and 37 °C (bottom panel). The smooth curves are obtained by a nonlinear regression method using the equation discussed in the text.

They demonstrated that the binding of cetiedil molecules to membranes caused immobilization of some of the spin labels on these membrane samples. In our previous studies, we have shown that changes in the W/S ratios can be directly related to the membrane binding process. The addition of bovine serum albumin, for example, causes no change in the W/S ratios, whereas the addition of hemoglobin causes the W/S values of membrane to decrease.²⁴ The $\Delta(W/S)_{\text{net}}$ values approached constant values at high concentrations of cetiedil, suggesting that the interaction of cetiedil with membrane proteins was a saturable process under the conditions we studied. Similar data were obtained on membranes from sickle cells at 37 °C.

We also studied the interaction of cetiedil with the spectrin-actin sample in 5P7.4/NaCl buffer, and monitored the W/S ratios of the spectrin-actin samples as a function of the cetiedil added. Although we observed decreases in the W/S ratios, we also found protein aggregation upon addition of cetiedil, probably due to the acidity of cetiedil causing spectrin-actin precipitation. The isoelectric point, pI, of spectrin-actin is ~ 4.5 . Thus little quantitative information was obtained.

We have found that the association of cetiedil with the erythrocyte membrane was reversible. The EPR signals of the membrane samples with and without cetiedil were first measured. These samples were then dialyzed overnight in buffer solutions with buffer to sample volume ratios of at

least 1000. The EPR signals of the dialyzed samples were measured again after dialysis. Both samples gave W/S ratios similar to that of the membrane sample without cetiedil before dialysis, indicating that the cetiedil-membrane interaction was noncovalent in nature, and did not cause irreversible changes in the erythrocyte membrane. This is in good agreement with the previous finding that the effect of cetiedil on the erythrocyte is reversible.⁹

In order to obtain quantitative information on cetiedil and membrane binding, such as the apparent K_d values, from the W/S data, we determined the free cetiedil concentration, C_f , in cetiedil-membrane mixtures, as shown in Fig. 3. After substituting C_f and $\Delta(W/S)_{1-4}$ into eq. 3, K_d , n and $\Delta(W/S)$, could be obtained. The n values obtained from these data, both by non-linear regression methods and by the Hill plot, were all ~ 1 , indicating that a simple two-state model with multiple independent binding sites that we have previously used²⁴ was adequate to describe the binding of cetiedil to membrane proteins.

Table I shows the values of apparent K_d , $\Delta(W/S)$, and $C_{1/2}$ for cetiedil-membrane, cetiedil-simplified membrane systems at 20 and 37 °C. All the K_d values are ~ 2 mM. The half saturation concentration ranges from 1–3 mmol of cetiedil per gram of membrane proteins.

Direct comparison of the averaged K_d values of the membrane and simplified membrane samples in Table I indicated a slightly lower K_d values for the simplified membrane samples than those for intact membrane samples. However, a paired sample t test of the K_d values indicated that the differences in K_d values between membrane and simplified membrane samples were not statistically significant either at 20 °C ($p < 0.02$) or at 37 °C ($p < 0.05$), as shown in Table I. Removal of the spectrin-actin network from the membrane thus did not significantly affect the binding of cetiedil to erythrocyte membrane. The spectrin-actin network is the major component in maintaining the shape of erythrocyte. The lack of interaction between cetiedil and the spectrin-actin network, as observed by EPR data, suggested that the action of cetiedil in returning sickle cell to normal shapes was not accomplished by modifying the spectrin-actin network in sickle cells. Other studies indicate that cetiedil inhibits calmodulin-stimulated calcium-ATPase activity. Calmodulin is present in the erythrocyte, but does not appear to bind to spectrin molecules.^{29,30} These findings are consistent with our EPR data.

The simplified membrane sample consists of lipid bilayer and Band 3 protein and other proteins, including ATPases.³¹ However the major protein component is the Band 3 molecule. Most of the protein spin labels, if not all, in the simplified membranes are on the Band 3 molecules. Therefore our data suggested interaction of cetiedil with the Band 3 proteins in membranes, with an apparent K_d of ~ 2 mM at 37 °C. However, these results did not exclude the interactions

of cetiedil with other minor proteins in the simplified membranes. The spin label EPR approach will not be sensitive enough to detect such interactions. Additional information on the partitioning of cetiedil in membranes will provide us with quantitative information on the concentrations of cetiedil interacting with individual membrane components.

Band 3 is an anion transport protein,³⁴ and may have a role in the membrane to regulate water movement in erythrocytes.^{32,33} More detailed studies of interactions between cetiedil and Band 3 molecules and interactions between cetiedil and ATPases, for example, may provide insight toward understanding its various drug actions in affecting erythrocyte water contents and Na^+ and K^+ movements across cell membranes.^{9,10,14}

Conclusions

Our optical data show that cetiedil has a maximum absorption at 233 nm with a E_{233} of $2796 \text{ M}^{-1} \text{ cm}^{-1}$. The cetiedil citrate molecule at high concentration is quite acidic, and may form micelles. The critical micelle concentration of cetiedil in phosphate buffer with 150 mM NaCl is ~ 8.8 mM.

This study shows that a large amount of cetiedil may associate with membranes. The study further demonstrates that cetiedil interacts with both the lipid component and the protein component in the membranes.

The EPR data show that the drug interacts with the membrane proteins, and that the binding is saturable and reversible. The half saturation concentration for binding is in the range of 1–3 mmol cetiedil per gram membrane proteins at physiological temperature. The equilibrium dissociation constant for membranes is ~ 2 mM at pH 6.3 and 37 °C. Removal of spectrin-actin from the membrane does not affect the binding properties of cetiedil, indicating that the spectrin-actin network is not involved in the mechanism of drug action. Our results suggest the existence of an interaction between cetiedil and Band 3 molecules, with an equilibrium dissociation constant of ~ 2 mM.

The EPR data also show that cetiedil affects the mobility of the spin labels that intercalate amongst the head groups of the lipid molecules in the membrane. The detailed effects of cetiedil on lipid molecules are not clear at this point.

References and Notes

- Chang, H.; Ewert, S. M.; Bookchin, R. M.; Nagel, R. L. *Blood* 1983, 61, 693–704.
- Cyrami, A.; Manning, J. M. *Proc. Natl. Acad. Sci. U.S.A.* 1971, 68, 1180–1183.
- Elbaum, E.; Roth, E. F.; Neuman, G.; Jaffe, E. R.; Nagel, R. L. *Blood* 1976, 48, 273–287.
- Naguchi, C. T.; Schechter, A. N. *Biochemistry* 1978, 17, 5445–5459.
- DeSimone, J.; Heller, P.; Hall, L.; Zwiars, D. *Proc. Natl. Acad. Sci. U.S.A.* 1982, 79, 4428–4431.
- Cabannes, R. *Clin. Trials J.* 1981, 18, 114–127.
- Benjamin, L. J.; Kokkini, G.; Peterson, C. M. *Blood* 1980, 55, 265–270.
- Asakura, T.; Ohnishi, S. T.; Adachi, K.; Ozguc, M.; Hasimoto, K.; et al. *Proc. Natl. Acad. Sci. U.S.A.* 1980, 77, 2955–2959.
- Schmidt, W. F.; Asakura, A.; Schwartz, E. *Blood Cells* 1982, 8, 289–298.
- Berkowitz, L. R.; Orringer, E. P. *Blood Cells* 1982, 8, 283–288.
- Simaan, J. A.; Aviado, D. M. *J. Pharm. Exp. Ther.* 1976, 198, 176–186.
- Boissier, J.-R.; Arousseau, M.; Giudicelli, J.-F.; Duval, D. *Arzneim.-Forsch./Drug Res.* 1978, 28(11), 2222–2228.
- Lewes, G. P.; Cho, Y. W. *J. Clin. Pharmacol.* 1982, 22, 243–249.
- Schmidt, W. F.; Asakura, T.; Schwartz, E. *J. Clin. Invest.* 1982, 69, 589–594.
- Agre, P.; Virshup, D.; Bennet, V. J. *Clin. Invest.* 1984, 74, 812–820.
- Levine, S. N.; Berkowitz, L. R.; Orringer, E. P. *Biochem. Pharmacol.* 1984, 33, 581–584.

Table I—Equilibrium Binding Parameters of Cetiedil in Membrane Systems and Statistical Analysis Results of K_d Values^a

Sample	$\Delta(W/S)$	$K_d \pm \text{SD}$, mM	$C_{1/2}$ mmol/g	t^b	p^b
Membrane ^c	1.92 ± 0.15	2.95 ± 0.64	2.5	3.186	<0.02
Simplified Membrane ^c	3.34 ± 0.57	1.89 ± 0.27	1.1		
Membrane ^d	3.06 ± 0.43	2.34 ± 0.74	1.4	2.682	<0.05
Simplified Membrane ^d	5.30 ± 0.85	1.57 ± 0.56	0.9		

^a Membrane systems were in 5 mM phosphate buffer with 150 mM NaCl. Seven determinations at each temperature for each membrane preparation were made. ^b The t and p values were obtained from a paired sample t test by null-hypothesis. ^c Run at 20 °C. ^d Run at 37 °C.

17. Physical Data Sheet (McN-R-2009-49-98), McNeil Pharmaceuticals: Spring House, PA.
18. Phillips, J. N. *Trans. Faraday Soc.* 1955, *51*, 561-569.
19. Dodge, J. T.; Mitchell, C.; Hanahan, D. J. *Arch. Biochem. Biophys.* 1963, *100*, 119-130.
20. Fung, I. W. M. *Biophys. J.* 1981, *33*, 253-262.
21. Fung, I. W. M.; Simpson, M. J. *FEBS Lett.* 1979, *108*, 269-273.
22. Bennett, V.; Branton, D. *J. Biol. Chem.* 1977, *252*, 2753-2763.
23. Fairbanks, G.; Steck, T. L.; Wallach, D. F. H. *FEBS Lett.* 1971, *108*, 269-273.
24. Fung, I. W. M. *Biochemistry* 1981, *20*, 7162-7166.
25. Anderson, M.; Johnson, A. W. *J. Chem. Soc.* 1965, 2411-2422.
26. Hubbel, W. L.; McConnell, H. M. *Proc. Natl. Acad. Sci. U.S.A.* 1969, *64*, 20-27.
27. Fung, I. W. M.; Johnson, M. E. "Current Topics in Bioenergetics", vol. 13, Lee, C. P., Ed.; Acad. Press: New York, 1984; pp 107-157.
28. Fung, I. W. M.; Ostrowski, M. S. *Am. J. Hum. Genet.* 1982, *34*, 469-480.
29. Biovin, P.; Galand, C. *Biochem. Int.* 1984, *8*, 231-236.
30. Berglund, A.; Backman, L.; Shambhag, V. P. *FEBS Lett.* 1981, *172*, 109-113.
31. Niggli, V.; Adunyah, E. S.; Penniston, J. T.; Carafoli, E. *J. Biol. Chem.* 1981, *256*, 395-401.
32. Vieira, F. L.; Shu'ali, R. L.; Solomon, A. K. *J. Gen. Physiol.* 1970, *55*, 451-466.
33. Macey, R. I.; Karan, D. M.; Farmer, R. E. L. *Biomembranes* 1972, *3*, 331-340.
34. Jennings, M. L. *J. Membrane Biol.* 1981, *80*, 105-117.

Acknowledgments

We thank Dr. M. Westerman and his staff of Mount Sinai Hospital of Chicago for providing us with sickle cells, and thank the staff of American Red Cross Blood Services, Chicago, for normal blood. We would also like to thank McNeil Pharmaceuticals, PA, for their generous supply of ceticidil citrate throughout this project. This research was supported in parts by the National Institutes of Health (HL-31145 and HL-16008, Wayne State University Comprehensive Sickle Cell Center Grant). I.W.-M.F. is a National Institutes of Health Research Career Development Awardee (K04 HL-01190).

APPROVAL SHEET

The dissertation Submitted by Chakravarthy Narasimhan has been read and approved by the following committee:

Dr. Leslie Wo-Mei Fung, Director
Professor of Chemistry, Loyola

Dr. Michael E. Johnson
Professor of Medicinal Chemistry and Pharmacognosy,
University of Illinois at Chicago

Dr. Duarte Mota de Freitas
Assistant Professor of Chemistry, Loyola

Dr. Kenneth W. Olsen
Associate Professor of Chemistry, Loyola

Dr. Albert J. Rotermund
Associate Professor of Biology, Loyola

The final copies have been examined by the director of the dissertation and the signature which appears below verifies the fact that any necessary changes have been incorporated and that the dissertation is now given final approval by the Committee with reference to content and form.

The dissertation is therefore accepted in partial fulfillment of the requirements for the degree of Doctor of Philosophy.

November 25, 1986
Date

Leslie W. Fung
Director's Signature